

Fig. 1. Preparation route for PT powders.

Therefore, in this work, the effect of milling time on phase formation, and particle size of lead titanate powders was investigated in this connection. The potential of the vibro-milling technique as a simple and low-cost method to obtain usable quantities of single-phase lead titanate powders at low temperature and with nanosized particles was also examined.

2. Experimental procedure

Commercially available lead oxide, PbO (JCPDS file number 77-1971) and titanium oxide, TiO₂ (JCPDS file number 21-1272) (Fluka, >99% purity) were used in this study. The two oxide powders exhibited an average particle size in the range of 3 to 5 µm. PbTiO₃ powder was synthesized by the solid-state reaction of these raw materials. Powder-processing (Fig. 1) was carried out in a manner similar to that employed in the preparation of other materials, as described previously [12,13]. A vibratory laboratory mill (McCrone Micronizing Mill) powered by a 1/30 HP motor was employed for preparing the stoichiometric PbTiO₃ powders. The grinding vessel consists of a 125 ml capacity polypropylene jar fitted with a screw-capped, gasketless,

Table 1
Effect of milling time on the variation of particle size of PT powders measured by different techniques

Milling time (h)	Per. phase (%)	XRD		SEM		Laser scattering	
		A (nm)	c/a	D (nm)	P (nm)	D (nm)	P (nm)
0.5	89.20	40	1.056	145	40-250	1090	140-2560
1	100	20.8	1.062	107	71 - 143	660	270-1090
5	100	22.5	1.059	101	67-135	690	290-1140
10	100	21.9	1.059	95	63 - 128	690	290-1140
15	100	22.0	1.061	78	43-114	4640	1640-7790
20	100	21.3	1.056	68	28-109	4800	1710-8060
25	100	21.5	1.057	63	17-109	180	70-310
30	100	21.5	1.052	93	43-143	170	70-290
35	100	21.4	1.053	92	56-128	3030	560-6180

Per. phase=Perovskite phase.

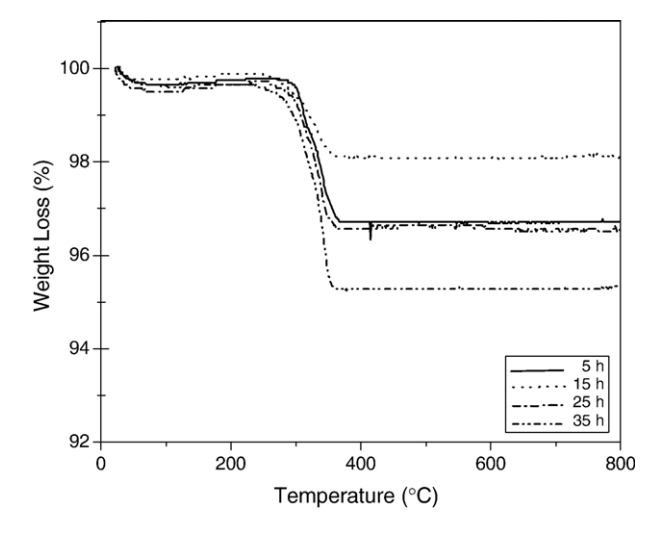


Fig. 2. TGA analysis of powder mixtures milled at different times.

polythene closure. The jar is packed with an ordered array of identical, cylindrical, grinding media of polycrystalline corundum. A total of 48 milling media cylinder with a powder weight of 20 g was kept constant in each batch. The milling operation was carried out in isopropanal inert to the polypropylene jar. Various milling times ranging from 0.5 to 35 h were selected in order to investigate the phase formation characteristic of lead titanate and the smallest particle size. After drying at 120 °C, the milled powders were calcined at 600 °C (inside a closed alumina crucible) for 1 h with heating/cooling rates of 20 °C min⁻¹ [11].

The reactions of the uncalcined PT powders taking place during heat treatment were investigated by a combination of thermogravimetric and differential thermal analysis techniques (TG-DTA, Shimadzu) at a heating rate of 10 °C min $^{-1}$ in air from room temperature up to 1000 °C. All powders were subsequently examined at room temperature by X-ray diffraction (XRD; Siemens-D500 diffractometer) using Ni-filtered CuK $_{\alpha}$ radiation to identify the phases formed and optimum milling time for the production of PbTiO $_{3}$ powders having the smallest particle size. The relative amount of perovskite and secondary phases was determined from XRD patterns of the samples by measuring the major characteristic peak intensities

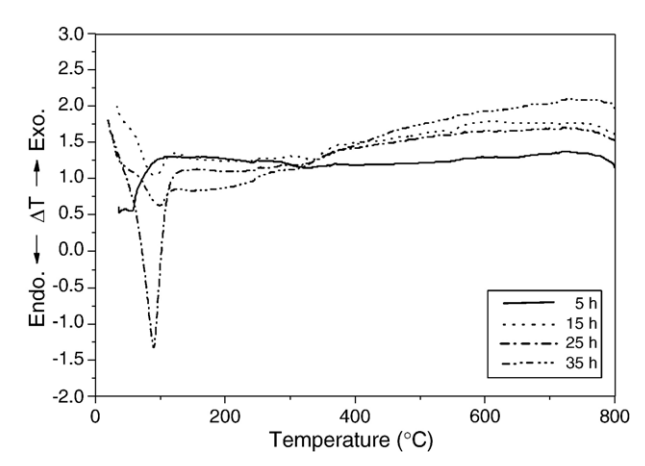


Fig. 3. DTA analysis of powder mixtures milled at different times.

A=Crystallite size.

c/a=Tetragonality factor.

D=Average particle size.

P=Particle size distribution or range.

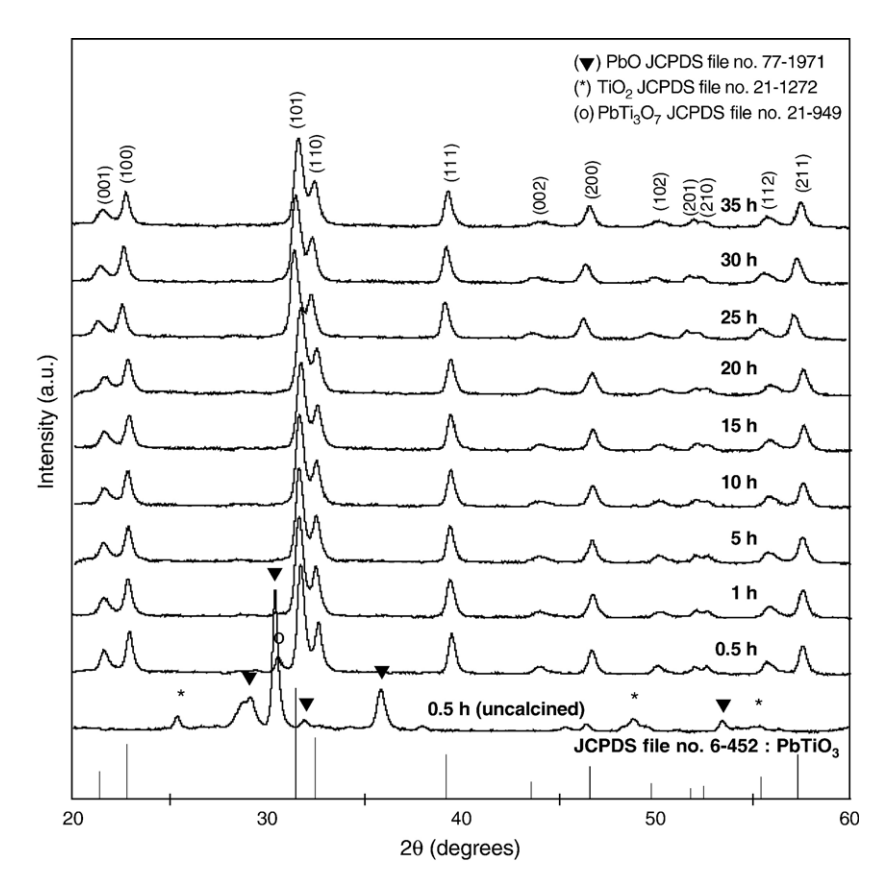


Fig. 4. XRD patterns of PT powders milled at different times (calcined at 600 °C for 1 h with heating/cooling rates of 20 °C min⁻¹).

for the perovskite (101) or I_P and secondary (o) phases or I_S . The following qualitative equation was used [14].

$$\text{perovskite phase(wt\%)} = \frac{I_{\text{P}}}{I_{\text{P}} + I_{\text{S}}} \times 100 \tag{1}$$

The crystalline lattice constants, lattice strain and average particle size were also estimated from XRD patterns [15]. The particle size distributions of the powders were determined by laser diffraction technique (DIAS 1640 laser diffraction

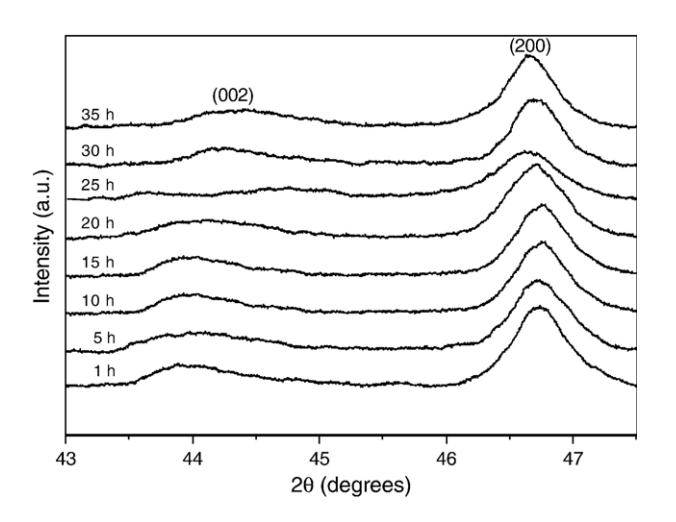


Fig. 5. Enlarged zone of XRD patterns showing (002) and (200) peaks broadening as a function of milling times.

spectrometer) with the particle sizes and morphologies of the powders observed by scanning electron microscopy (JEOL JSM-840 A SEM). The particle sizes of PT powders milled at different times obtained from different measuring techniques are provided in Table 1.

3. Results and discussion

TGA and DTA results for the powders milled at different times are compared and shown in Figs. 2 and 3, respectively. In general, similar thermal characteristics are observed in all cases. As shown in Fig. 2, all

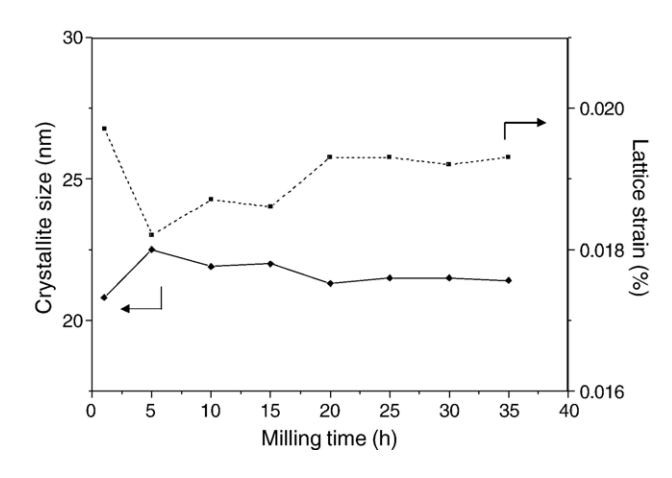


Fig. 6. Variation of crystalline size and lattice strain of PT powders as a function of milling times.

powders demonstrate two distinct weight losses below 400 °C. The first weight loss occurs below 100 °C and the second one above 200 °C. In the temperature range from room temperature to $\sim\!150$ °C, all samples show exothermic peaks in the DTA curves at 120 °C (Fig. 3), which are related to the first weight loss. These DTA peaks can be attributed to the decomposition of the organic species originating from the milling process [11,16]. Corresponding to the second fall in specimen weight, by increasing the temperature up to $\sim\!800$ °C, the solid-state reaction between lead oxide and titanium oxide occurs. The broad exothermic characteristic present in all the DTA curves represents that reaction, which has a maximum at $\sim\!600$ –750 °C. The slightly different temperature, intensities and shapes of the thermal peaks for the powders are probably related to the different sizes of the

powders subjected to different milling times and, consequently, caused by the removal of organic species and rearrangement of differently bonded species in the network [16]. No further significant weight loss was observed for temperatures above 500 $^{\rm o}{\rm C}$ in the TGA curves, indicating that the minimum firing temperature to form PbO–TiO₂ compounds is in good agreement with XRD results (Fig. 4) and those of previous authors [17,18].

To further study the effect of milling time on phase formation, each of the powders milled for different times were calcined at $600\,^{\circ}\text{C}$ for 2 h in air, followed by phase analysis using XRD. For the purpose of estimating the concentrations of the phase present, Eq. (1) has been applied to the powder XRD patterns obtained, as given in Table 1. As shown in Fig. 4, for the uncalcined powder subjected to $0.5\,\text{h}$ of vibro-

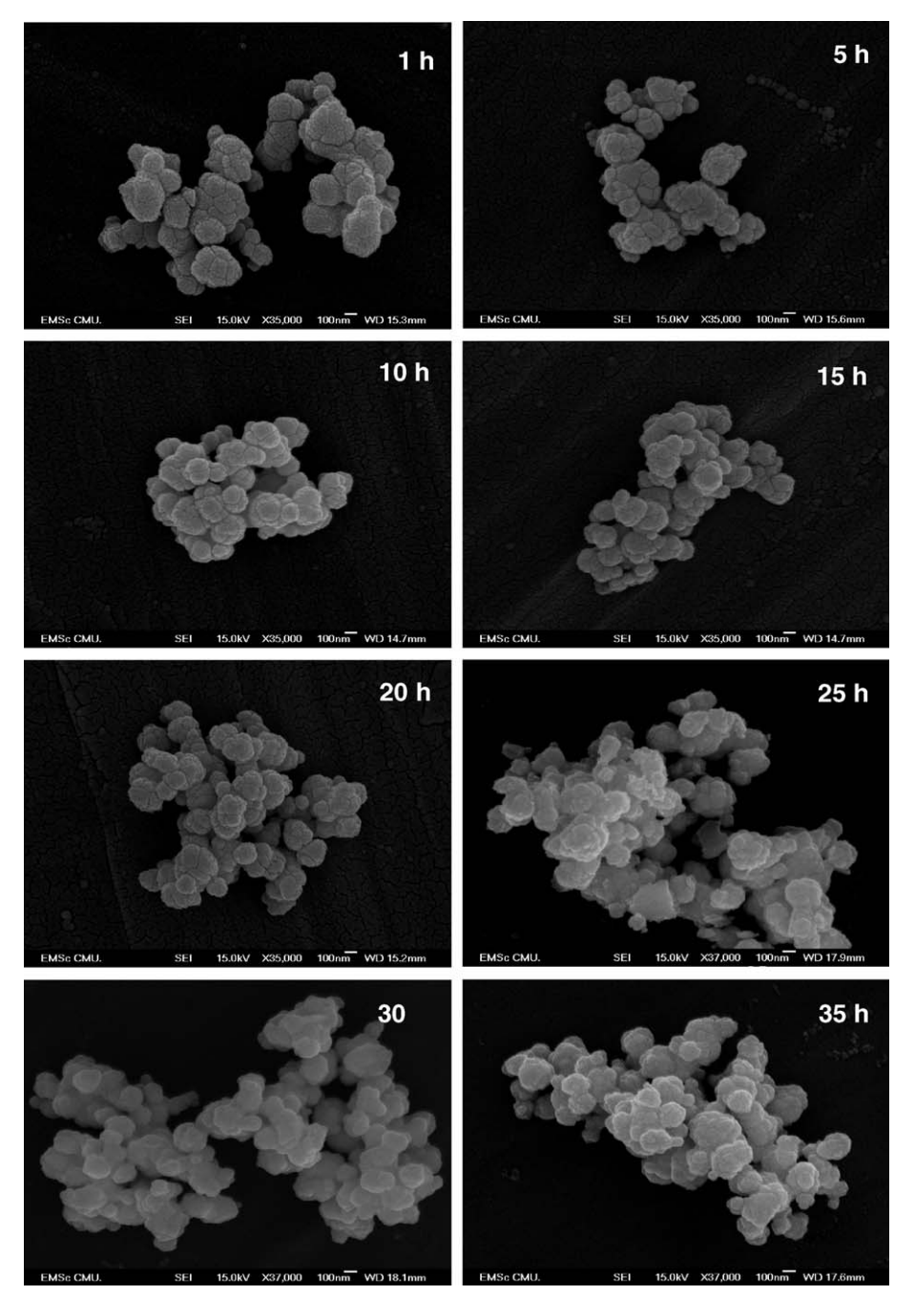


Fig. 7. SEM micrographs of PT powders milled at different times.

milling, only X-ray peaks of precursors PbO (∇) and TiO₂ (*) are present, indicating that no reaction had been initiated during the milling process. However, after calcinations at 600 °C, it is seen that the perovskite-type PbTiO₃ becomes the predominant phase in the powder milled for 0.5 h indicating that the reaction has occurred to a considerable extent. It is seen that ~11 wt.% of lead deficient phase, PbTi₃O₇ (o), reported by a number of workers [18,19] has been found only at a milling time of 0.5 h. This pyrochlore phase has a monoclinic structure with cell parameters a=107.32 pm, b=381.2 pm, c=657.8 pm and β =98.08° (JCPDS file number 21-949) [20]. This observation could be attributed mainly to the poor mixing capability under short milling time. With milling time of 1 h or more, it is apparent that a single phase perovskite PT (yield of 100% within the limitations of the XRD technique) was found to be possible after the same calcination process was applied.

In general, the strongest reflections found in the majority of these XRD patterns indicate the formation of the lead titanate, PbTiO₃. These can be matched with JCPDS file number 6-452 for the tetragonal phase, in space group P4/mmm with cell parameters a=389.93 pm and c=415.32 pm [21], in consistent with other works [10,11]. It should be

noted that no evidence for the introduction of impurity due to wear debris from the milling process was observed in any of the calcined powders (within the milling periods of 0.5–35 h), demonstrating the effectiveness of the vibro-milling technique for the production of high purity PT nanopowders.

Moreover, it has been observed that with increasing milling time, all diffraction lines broaden, e.g. (002) and (200) peaks, an indication of a continuous decrease in particle size and of the introduction of lattice strain, as shown in Fig. 5. These values indicate that the particle size affects the evolution of crystallinity of the phase formed by prolonged milling treatment (Fig. 6). For PT powders, the longer the milling time, the finer is the particle size, up to a certain level (Table 1). The results suggest that the steady state of the vibro-milling is attained at \sim 20 h of milling. Moreover, it is worthy to note that, in this condition, the mean crystalline size is close to \sim 21 nm. Also, the relative intensities of the Bragg peaks and the calculated tetragonality factor (c/a) for the powders tend to decrease with the increase of milling time. However, it is well documented that, as Scherer's analysis provides only a measurement of the extension of the coherently diffracting domains, the particle sizes estimated by this method can be significantly under

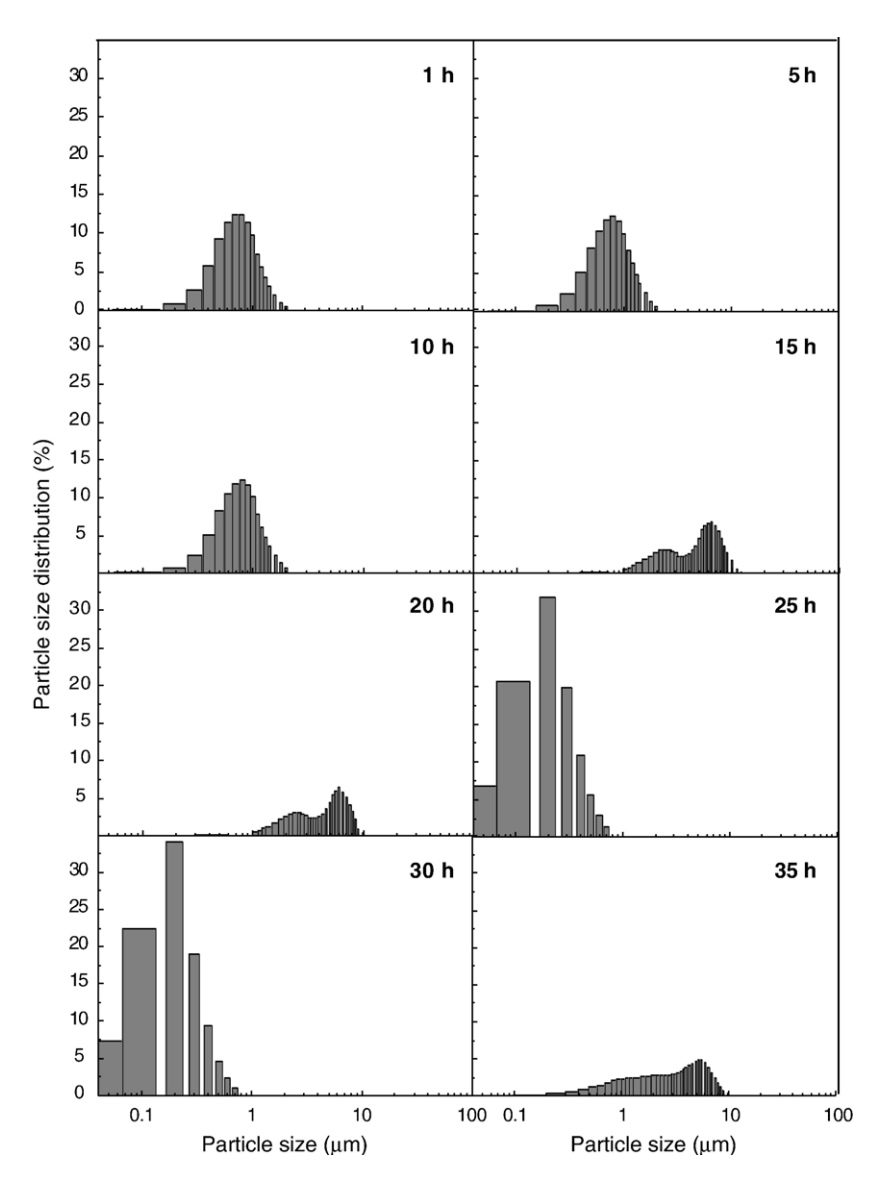


Fig. 8. Particle size distributions of PT powders milled at different times.

estimated [22]. In addition to strain, factors such as dislocations, stacking faults, heterogeneities in composition and instrumental broadening can contribute to peak broadening, making it almost impossible to extract a reliable particle size solely from XRD [15,23].

In this connection, scanning electron microcopy was also employed for particle size measurement (Table 1). The morphological evolution of the powders as a function of milling time was also revealed, as illustrated in the SEM micrographs (Fig. 7). At first sight, the morphological characteristic of PT powders with various milling times is similar for all cases. In general, the particles are agglomerated and basically irregular in shape, with a substantial variation in particle sizes. The powders consist of primary particles nanometers in size. Increasing the milling time over the range 0.5 to 35 h, the average size of the PT particle decreases significantly, until at 25 h, the smallest particle size (estimated from SEM micrographs to be \sim 17 nm) is obtained. However, it is also of interest to point out that a larger particle size was obtained for a milling time longer than 25 h. This may be attributed to the occurrence of hard agglomeration with strong inter-particle bonds within each aggregate resulting from dissipated heat energy of prolonged milling [24]. Fig. 7 also illustrates that vibro-milling has slightly changed the shape of the particles which become more equiaxed at long milling times. At the same time, the particle size is reduced. Fracture is considered to be the major mechanism at long milling times.

The effect of milling time on particle size distribution was found to be significant, as shown in Fig. 8. After milling times of 1, 5 and 10 h, the powders have a similar particle size distribution. They exhibit a single peak covering the size ranging from 0.2 to 1.1 µm. With increasing milling times to 15 and 20 h, the distribution curve of particle size separates into two groups. First is a monomodal distribution corresponding to the primary size of the PbTiO₃ particles. The second group (peak) is believed to arise mainly from particle agglomeration. By increasing the milling time to 25 and 30 h, a uniform particle size distribution with a much lower degree of particle agglomeration (<1 μm) is found. However, upon further increase of milling time up to 35 h, a bimodal distribution curve with peak broadening between 0.5 and 6.2 μm is observed again. Table 1 compares the results obtained for PT powders milled for different times via different techniques. Variations in these data may be attributed mainly to the formation of hard and large agglomerations found in the SEM results.

In this work, it is seen that the optimum milling time for the production of the smallest nanosized high purity PT powder was found to be at 25 h. The finding of this investigation indicates a strong relationship between the vibro-milling process and the yield of PT nanopowders. However, further investigation is required for the control and optimization of the PT formation. Studies on the effect of milling parameters and particle size distribution on phase formation kinetics would be useful for the particle size control. In case of the vibro-milling technique, other factors such as the milling speed, milling scale and type of milling media also need be taken into account.

4. Conclusion

The results infer that the milling time influences not only on the development of the solid-state reaction of lead titanate phase but also the particle size and morphology. The resulting PT powders have a range of particle size, depending on milling times. Production of a single-phase lead titanate nanopowder can be successfully achieved by employing a combination of 25 h milling time and calcination conditions of 600 °C for 2 h, with heating/cooling rates of 20 °C min⁻¹.

Acknowledgement

This work was supported by the Thailand Research Fund (TRF) and the Faculty of Science, Chiang Mai University. One of the authors (R.W.) wishes to acknowledge Maejo University for financial support during her study and also the Graduate School of Chiang Mai University.

References

- A.J. Moulson, J.M. Herbert, Electroceramics, 2nd ed.Wiley, Chichester, 2003
- [2] B. Jaffe, W.R. Cook, H. Jaffe, Piezoelectric Ceramics, Academic Press, New York, 1971.
- [3] O. Bouquin, M. Lejeune, J.P. Boilot, J. Am. Ceram. Soc 74 (1991) 1152.
- [4] T.R. Gururaja, A. Safari, A. Halliyal, Am. Ceram. Soc. Bull. 65 (1986) 1601.
- [5] J.S. Wright, L.F. Francis, J. Mater. Res. 8 (1993) 1712.
- [6] G.R. Fox, J.H. Adair, R.E. Newnham, J. Mater. Sci. 25 (1990) 3634.
- [7] A. Rujiwatra, J. Jongphiphan, S. Ananta, Mater. Lett. 59 (2005) 1871.
- [8] V.V. Dabhade, T.R. Rama Mohan, P. Ramakrishman, Appl. Surf. Sci. 182 (2001) 390.
- [9] S. Ananta, Mater. Lett. 58 (2004) 2781.
- [10] A. Udomporn, S. Ananta, Curr. Appl. Phys. 4 (2004) 186.
- [11] A. Udomporn, S. Ananta, Mater. Lett. 58 (2003) 1154.
- [12] S. Ananta, N.W. Thomas, J. Eur. Ceram. Soc. 19 (1999) 155.
- [13] S. Ananta, R. Brydson, N.W. Thomas, J. Eur. Ceram. Soc. 20 (2000) 2315.
- [14] S.L. Swartz, T.R. Shrout, Mater. Res. Bull. 17 (1982) 1245.
- [15] H. Klug, L. Alexander, X-Ray Diffraction Procedures for Polycrystalline and Amorphous Materials, 2nd ed.Wiley, New York, 1974.
- [16] S. Ananta, R. Tipakonitikul, T. Tunkasiri, Mater. Lett. 57 (2003) 2637.
- [17] C.G. Pillai, P.V. Ravindran, Thermochim. Acta 66 (1996) 109.
- [18] J. Tartaj, C. Moure, L. Lascano, P. Duran, Mater. Res. Bull. 36 (2001) 2301.
- [19] M.L. Calzada, M. Alguero, L. Pardo, J. Sol-Gel Sci. Technol. 13 (1998) 837.
- [20] Powder Diffraction File No. 21-949. International Centre for Diffraction Data, Newtown Square, PA, 2000.
- [21] Powder Diffraction File No. 6-452. International Centre for Diffraction Data, Newtown Square, PA, 2000.
- [22] C. Suryanarayana, Prog. Mater. Sci. 46 (2001) 1.
- [23] A. Revesz, T. Ungar, A. Borbely, J. Lendvai, Nanostruct. Mater. 7 (1996) 779.
- [24] P.C. Kang, Z.D. Yin, O. Celestine, Mater. Sci. Eng., A Struct. Mater.: Prop. Microstruct. Process. 395 (2005) 167.



Available online at www.sciencedirect.com



Materials Letters 60 (2006) 2666-2671

materials letters

www.elsevier.com/locate/matlet

Effects of milling time and calcination condition on phase formation and particle size of lead titanate nanopowders prepared by vibro-milling

R. Wongmaneerung, R. Yimnirun, S. Ananta*

Department of Physics, Faculty of Science, Chiang Mai University, Chiang Mai 50200, Thailand
Received 10 August 2005; accepted 22 January 2006
Available online 13 February 2006

Abstract

Effect of calcination conditions on phase formation and particle size of lead titanate (PbTiO₃) powders synthesized by a solid-state reaction with different vibro-milling times was investigated. Powder samples were characterized using XRD, SEM, TEM and EDX techniques. A combination of the milling time and calcination conditions was found to have a pronounced effect on the phase formation and particle size of the calcined PbTiO₃ powders. The calcination temperature for the formation of single-phase perovskite lead titanate was lower when longer milling times were applied. More importantly, by employing an appropriate choice of the milling time and calcination conditions, perovskite lead titanate (PbTiO₃) nanopowders have been successfully prepared with a simple solid-state reaction method.

© 2006 Elsevier B.V. All rights reserved.

Keywords: Lead titanate; Perovskite; Nanopowders; Calcination; Phase formation

1. Introduction

Lead titanate, PbTiO₃ (PT), is one of the perovskite-type ferroelectric materials having unique properties such as high transition temperature (~490 °C), excellent pyroelectric coefficient and large spontaneous polarization [1,2]. These characteristics make it an interesting candidate for many applications e.g. ultrasonic transducers, microactuators and multilayer capacitors [3,4]. To fabricate them, a fine powder of perovskite phase with the minimized degree of particle agglomeration is needed as starting material in order to achieve a dense and uniform microstructure at the sintering temperature [5,6].

Recently, the studies of nanoparticles are also a very attractive field. The evolution of a method to produce nanopowders of precise stoichiometry and desired properties is complex, depending on a number of variables such as starting materials, processing history, temperature, etc. The advantage of using a solid-state reaction method via mechanical milling for preparation of nanosized powders lies in its ability to produce mass quantities of powder in the solid state using simple

equipment and low cost starting precursors [7,8]. Although some research has been done in the preparation of PT powders via a vibro-milling technique [9,10], to our knowledge a detailed study considering the role of both milling times and firing conditions on the preparation of PT nanopowders has not been reported. Thus, in the present study, the primary attention was aimed towards the production of stoichiometric PbTiO₃ nanopowders by a mixed oxide method. The powder characteristics of the vibro-milling derived PbTiO₃ have also been thoroughly investigated.

2. Experimental procedure

The raw materials used were commercially available lead oxide, PbO and titanium oxide, TiO₂ (Fluka, >99% purity). The two oxide powders exhibited an average particle size in the range of 3.0 to 5.0 µm. PbTiO₃ powder was synthesized by the solid-state reaction of these raw materials. A McCrone Micronizing Mill was employed for preparing the stoichiometric PbTiO₃ powders as described in a previous work [11]. In order to improve the reactivity of the constituents, the milling process was carried out for various milling times ranging from 20 to 30 h (instead of 30 min [10]) with corundum media in

^{*} Corresponding author. Tel.: +66 53 943367; fax: +66 53 357512. E-mail address: supon@chiangmai.ac.th (S. Ananta).

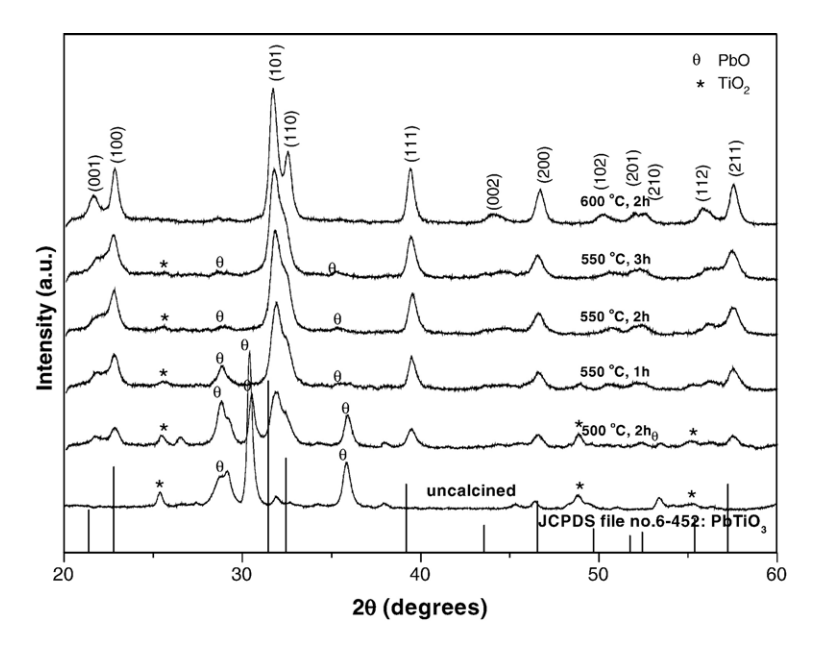


Fig. 1. XRD patterns of PT powders milled for 20 h and calcined at various conditions.

isopropyl alcohol (IPA). After drying at 120 °C for 2 h, various calcination conditions, i.e. temperature ranging from 500 to 600 °C, dwell times ranging from 1 to 4 h and heating/cooling rates ranging from 5 to 20 °C.min⁻¹, were applied (the powders were calcined inside a closed alumina crucible) in order to investigate the formation of PbTiO₃.

All powders were examined by room temperature X-ray diffraction (XRD; Siemens-D500 diffractometer) using Ni-filtered CuK_{α} radiation, to identify the phases formed, optimum milling time and firing conditions for the production of single-phase PbTiO₃ powders. The crystalline lattice constants, tetragonality factor (c/a), mean lattice strain and average particle size were also estimated from XRD patterns [12]. The particle size distributions of the powders were determined by

laser diffraction technique (DIAS 1640 laser diffraction spectrometer) with the particle sizes and morphologies of the powders observed by scanning electron microscopy (JEOL JSM-840A SEM). The structures and chemical compositions of the phases formed were elucidated by transmission electron microscopy (CM 20 TEM/STEM operated at 200 keV) and an energy-dispersive X-ray (EDX) analyzer with an ultra-thin window.

3. Results and discussion

Powder XRD patterns of the calcined powders after different milling times are given in Figs. 1–3, with the corresponding JCPDS patterns. As shown in Fig. 1, for the uncalcined powder subjected to 20

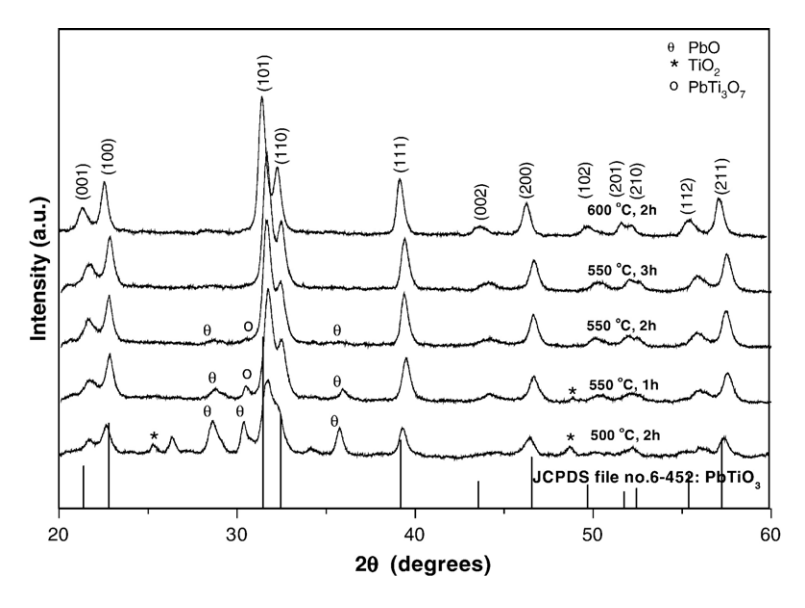


Fig. 2. XRD patterns of PT powders milled for 25 h and calcined at various conditions.

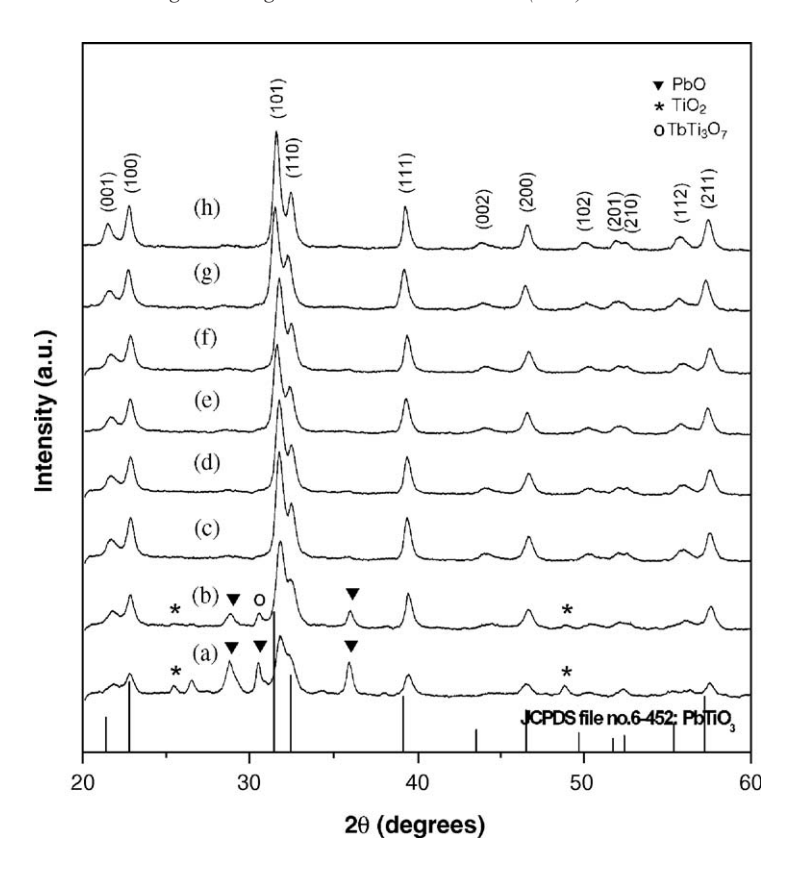


Fig. 3. XRD patterns of PT powders milled for 30 h and calcined at (a) 500 °C for 2 h, (b) 550 °C for 1 h, (c) 550 °C for 2 h, (d) 550 °C for 3 h, (e) 600 °C for 2 h, with heating/cooling rates of 5 °C/min and 550 °C for 3 h with heating/cooling rates of (f) 10 °C/min, (g) 20 °C/min and (h) 30 °C/min.

h of vibro-milling, only X-ray peaks of precursors PbO (∇) and TiO₂ (*) are present, indicating that no reaction was yet triggered during the vibro-milling process. However, after calcination at 500 and 550 °C, it is seen that the perovskite-type PbTiO₃ becomes the predominant phase indicating that the reaction has occurred to a considerable extent. Further calcination at 550 °C with dwell time of 1 h or more does not result in a very much increase in the amount of PbTiO₃ whereas the traces of unreacted PbO and TiO₂ could not be completely eliminated. This could be attributed to the poor reactivity of lead and titanium species [9,10]. However, it should be noted that after calcination at 600 °C for 2 h, the single phase of perovskite PT (yield of 100% within the limitations of the XRD technique) was obtained.

In general, the strongest reflections apparent in the majority of these XRD patterns indicate the formation of PbTiO₃. These can be matched with JCPDS file number 6–452 for the tetragonal phase, in space group P4/mmm with cell parameters a=389.93 pm and c=415.32 pm [13], consistent with other works [9,10]. For 20 h of milling, the optimum calcination temperature for the formation of a high purity PbTiO₃ phase was found to be about 600 °C.

To further study the phase development with increasing milling times, an attempt was also made to calcine mixed powders milled at 25 h and 30 h under various conditions as shown in Figs. 2 and 3, respectively. In this connection, it is seen that by varying the calcination temperature, the minimum firing temperature for the single phase formation of each milling batch is gradually decreased with increasing milling time (Figs. 1–3). The main reason for this behavior is that a complete solid-state reaction probably takes place more easily when the particle size is milled down to accelerate an atomic diffusion mechanism resulting in the suitable level of homogeneous mixing. It is therefore believed that the solid-state

reaction to form perovskite PT phase occurs at lower temperatures with decreasing the particle size of the oxide powders.

However, there is evidence that, even for a wide range of calcination conditions, single-phase PbTiO₃ cannot be produced easily, in agreement with literature [10,14]. A noticeable difference is noted when employing the milling time longer than 20 h (Figs. 2 and 3), since they lead to a considerable formation of lead deficient phase, PbTi₃O₇ (o), earlier reported by a number of workers [15,16]. This pyrochlore phase has a monoclinic structure with cell parameters a = 107.32 pm, b = 381.2 pm, c = 657.8 pm and $\beta = 98.08^{\circ}$ (JCPDS file number 21–949) [17]. This observation could be attributed mainly to the poor reactivity of lead and titanium species [9,10] and also the limited mixing capability of the mechanical method [18].

From Figs. 2 and 3, it is clear that the intensity of the perovskite peaks was further enhanced when the dwell times of the calcinations process were extended up to 3 h at the expenses of PbO, TiO₂ and PbTi₃O₇ phases. An essentially monophasic PbTiO₃ of perovskite structure was obtained at 550 °C when the calcination time was increased to 3 h and 2 h for the milling time of 25 h and 30 h, respectively, as shown in Figs. 2 and 3(c). This was apparently a consequence of the enhancement in crystallinity of the perovskite phase with increasing degree of mixing and dwell time, in good agreement with other works [18,19].

In the present study, an attempt was also made to calcine the powders with 30 h of milling times under various heating/cooling rates (Fig. 3). In this connection, it is shown that the yield of PbTiO₃ phase did not vary significantly with different heating/cooling rates ranging from 5 to 30 °C min⁻¹, in good agreement with the early observation for the PbTiO₃ powders subjected to 0.5 h of vibro-milling times [10]. It should be noted that no evidence of the introduction of impurity due

Table 1 Effect of calcination conditions on the variation of crystalline size, tetragonality factor (c/a) and mean lattice strain of PT powders milled for different times

Calcination condition <i>T/D/R</i> (°C/h/°C min ⁻¹)	Crystallite size (nm)	Lattice strain (%)	Tetragonality factor (c/a)
500/2/30	21.8	0.0188	1.038
550/1/30	19.4	0.0212	1.055
550/2/30	21.6	0.0190	1.052
550/3/30	20.9	0.0197	1.054
600/2/30	21.5	0.0193	1.057

T= calcination temperature.

D=dwell time.

R=heating/cooling rates.

to wear debris from the selected milling process was observed in all calcined powders, indicating the effectiveness of the vibro-milling technique for the production of high purity PbTiO₃ nanopowders.

The variation of calculated crystallite size, tetragonality factor (c/a) and lattice strain of the powders milled for different times with the calcination conditions is given in Table 1. In general, it is seen that the crystallite size of lead titanate decreases slightly with increasing calcination temperature for all different milling times, while the calculated values of the tetragonality factor and mean lattice strain progressively increase. However, it should be noted that by increasing the calcination time from 1 to 3 h, these calculated values decrease to the minimum at 2 h and then grow up further after longer dwell time was applied. There is no obvious interpretation of these observations, although it is likely to correspond to the competition between the major mechanisms leading to crystallization and agglomeration [19].

In this connection, a combination of SEM and TEM techniques was also employed for the particle size measurement. The morphological evolution during various calcination conditions of PT powders milled with different times was investigated by SEM technique as shown in Fig. 4. It is seen that all powders seem to have similar morphology. In general, the particles are agglomerated and basically irregular in shape, with a substantial variation in particle sizes, particularly in powders subjected to prolong milling times or high firing temperatures (Fig. 4(c) and (d)). The powders consist of primary particles of nanometers in size. The primary particles have sizes of $\sim 17-57$ nm, and the agglomerates measured $\sim 109-157$ nm. It is also of interest to point out that averaged particle size tends to increase with calcination temperatures (Fig. 4 and Table 1), in good agreement with other works [8,18]. This observation may be attributed to the occurrence of hard agglomeration with strong inter-particle bond within each aggregates resulting from firing process. The experimental work carried out here suggests that the optimal combination of the milling time and calcination condition for the production of single-phase PbTiO₃ powders with smallest particle size (~17 nm) is 25 h and 600 °C for 2 h with heating/cooling rates of 30 °C min⁻¹, respectively. Moreover, the employed heating/cooling rates for PbTiO3 powders observed in this work are also faster than those reported earlier [9,10].

A TEM bright field image of an agglomerated or intergrown particle of the calcined PT powders derived from milling time of 25 h is shown in Fig. 5(a). By employing the selected area electron diffraction (SAED) technique, a perovskite-like phase of tetragonal P4/mmm PbTiO₃ is identified (Fig. 5(b)), in good agreement with the XRD analysis and the data in JCPDS file no. 6-452 [13]. The reciprocal lattice pattern of this PT phase was also simulated with the Carine Crytallography 3.0 software, as demonstrated in Fig. 5(c). In addition,

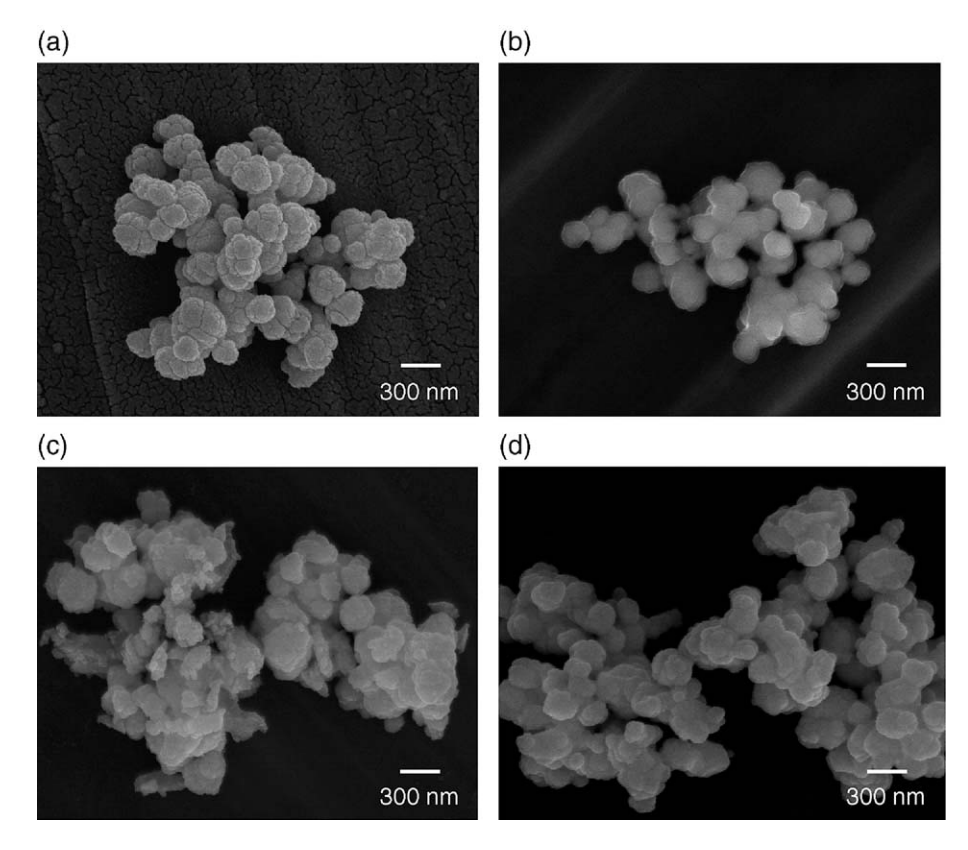


Fig. 4. SEM micrographs of PT powders milled for (a) 20 h and (b) 25 h, and calcined at 600 °C for 2h, (c) 25 h and (d) 30 h, and calcined at 550 °C for 3 h, with heating/cooling rates of 30 °C/min.

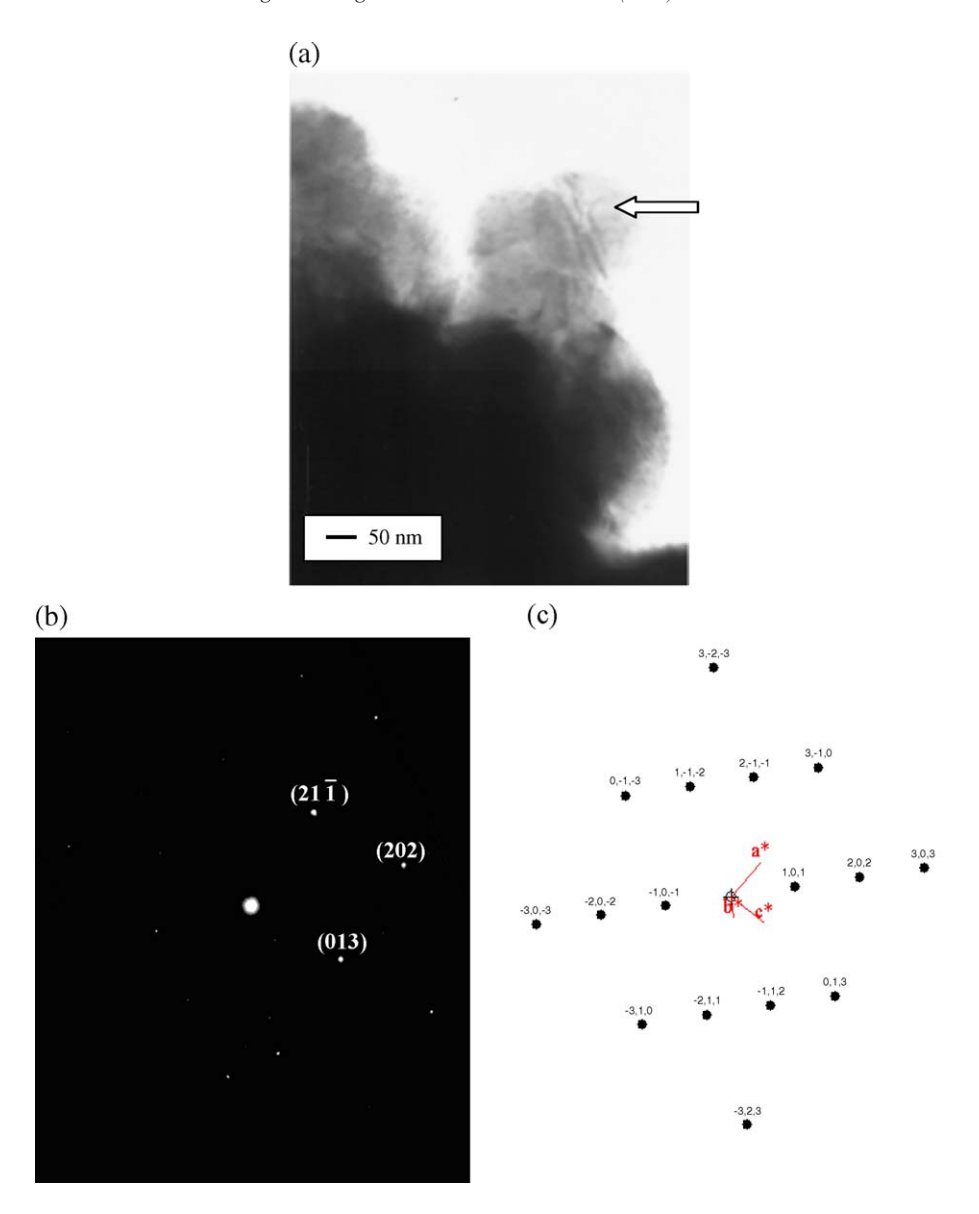


Fig. 5. (a) TEM micrograph, (b) SAED pattern ([13 $\overline{1}$] zone axis) and (c) reciprocal lattice pattern simulation of PT powders milled for 25 h and calcined at 600 °C for 2 h with heating/cooling rates of 30 °C/min.

EDX analysis using a 20 nm probe on a large number of particles of these calcined PbTiO₃ powders confirmed the existence of single phase perovskite, in good agreement with XRD results.

4. Conclusion

This work demonstrated that by applying an appropriate choice of the vibro-milling time, calcination temperature and dwell time, mass quantities of a high purity lead titanate nanopowders can be successfully produced by a simple solid-state mixed oxide synthetic route without the use of high purity starting precursors.

Acknowledgement

This work was supported by the Thailand Research Fund (TRF), the Faculty of Science and the Graduate School of Chiang Mai University.

References

- A.J. Moulson, J.M. Herbert, Electroceramics, 2nd ed., Wiley, Chichester, 2003.
- [2] B. Jaffe, W.R. Cook, H. Jaffe, Piezoelectric Ceramics, Academic Press, New York, 1971.
- [3] G.H. Haertling, J. Am. Ceram. Soc. 82 (1999) 797.
- [4] K. Uchino, Piezoelectrics and Ultrasonic Applications, Kluwer, Deventer, 1998.
- [5] J.S. Wright, L.F. Francis, J. Mater. Res. 8 (1993) 1712.
- [6] G.R. Fox, J.H. Adair, R.E. Newnham, J. Mater. Sci. 25 (1990) 3634.
- [7] V.V. Dabhade, T.R. Rama Mohan, P. Ramakrishman, Appl. Surf. Sci. 182 (2001) 390.
- [8] S. Ananta, Mater. Lett. 58 (2004) 2781.
- [9] A. Udomporn, S. Ananta, Curr. Appl. Phys. 4 (2004) 186.
- [10] A. Udomporn, S. Ananta, Mater. Lett. 58 (2003) 1154.
- [11] R. Wongmaneerung, R. Yimnirun, S. Ananta, Mater. Lett. (in press), doi:10.1016/j.matlet.2005.11.043.
- [12] H. Klug, L. Alexander, X-ray Diffraction Procedures for Polycrystalline and Amorphous Materials, 2nd ed., Wiley, New York, 1974.

- [13] JCPDS-ICDD Card no. 6-452, International Centre for Diffraction Data, Newtown Square, PA, 2000.
- [14] C.G. Pillai, P.V. Ravindron, Thermochim. Acta 66 (1996) 109.
- [15] J. Tartaj, C. Moure, L. Lascano, P. Duran, Mater. Res. Bull. 36 (2001) 2301.
- [16] M.L. Calzada, M. Alguero, L. Pardo, J. Sol-Gel Sci. Technol. 13 (1998) 837
- [17] JCPDS-ICDD Card no. 6-452, International Centre for Diffraction Data, Newtown Square, PA, 2000.
- [18] S. Ananta, R. Tipakontitikul, T. Tunkasiri, Mater. Lett. 57 (2003) 2637.
- [19] S. Ananta, R. Brydson, N.W. Thomas, Mater. J. Eur. Ceram. Soc. 20 (2000) 2315.





materials letters

Materials Letters 59 (2005) 1871-1875

www.elsevier.com/locate/matlet

Stoichiometric synthesis of tetragonal phase pure lead titanate under mild chemical conditions employing NaOH and KOH

Apinpus Rujiwatra^{a,b,*}, Jarunee Jongphiphan^{a,b}, Supon Ananta^b

^aInorganic Materials Research Unit, Department of Chemistry, Faculty of Science, Chiang Mai University, Chiang Mai 50200, Thailand ^bDepartment of Physics, Faculty of Science, Chiang Mai University, Chiang Mai 50200, Thailand

> Received 23 November 2004; received in revised form 8 February 2005; accepted 10 February 2005 Available online 10 March 2005

Abstract

Submicron- to nanometer-sized particles of single phase lead titanate have been prepared in stoichiometric proportion under mild hydrothermal conditions employing either potassium or sodium hydroxides as alkali mineralizers. In conjunction with reaction temperature and time, these variables played a crucial role in determining the habit of crystalline particles. The feasibility of using sodium hydroxide as an alternative for potassium hydroxide in the preparation of nanopowders of lead titanate was demonstrated. The influence of the preparative conditions, e.g. reaction temperature and time, on phase formation, morphology, the habit of crystalline particles, size and size distribution, was investigated.

© 2005 Elsevier B.V. All rights reserved.

Keywords: Lead titanate; Hydrothermal; Phase formation; Morphology; Powder technology

1. Introduction

As one of the most important ferroelectric base materials with high spontaneous polarization and coefficients, but low aging rate of the dielectric constant, lead titanate (PbTiO₃ or PT) can serve a variety of applications, including multilayer capacitors, infrared sensors, electro-optic devices and ultrasonic transducers [1]. The performance of these materials is often determined by the precursor powder characteristics and the microstructure of the sintered body. Since ceramics are usually formed by powder processing, their properties are inherited from the characteristics of the starting powders [2]. In this regard, both physical and chemical properties of the powders must be well defined and characterized with control of homogeneity, purity, particle size and shape, and chemical stoichiometry, being of importance. To this end, a variety of wet-chemical synthetic techniques have been developed as alternatives to

Table 1
The summary of synthetic conditions employed with water as the reaction media and the molar ratio of either PT:NaOH or PT:KOH of 1:4

Type of alkali	Reaction	Reaction	Particle size (µm)		
hydroxide	temperature (°C)	time (h)	Distribution	Mean diameter	
NaOH	150	6	0.04-1.00	0.20	
		12	0.04 - 10.00	1.95	
		24	0.04 - 2.00	0.54	
KOH	150	6	0.04 - 18.00	4.55	
		12	0.04 - 18.00	4.12	
		24	0.04 - 12.00	3.04	
	180	3	0.04-6.00	1.47	
		6	0.04-23.00	5.04	
		12	0.04-6.00	1.51	
	200	1.5	0.04-6.00	1.72	
		3	0.04-6.00	1.81	

^{*} Corresponding author. Tel.: +66 53 941906; fax: +66 53 892277. E-mail address: apinpus@chiangmai.ac.th (A. Rujiwatra).

the conventional solid state powder preparation [3–5]. In recent years, hydrothermal synthesis has been a major focus in the preparative investigations for a vast variety of ferroelectric powders due to the advantages over the other preparative techniques, e.g. lower temperature required,

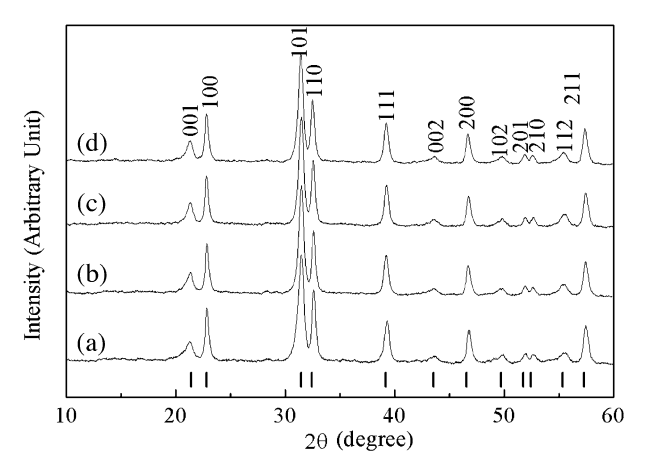


Fig. 1. The powder X-ray diffraction patterns of synthesized PT from the reactions with (a) NaOH at 150 $^{\circ}$ C for 6 h, (b) KOH at 150 $^{\circ}$ C for 6 h, (c) KOH at 180 $^{\circ}$ C for 6 h and (d) KOH at 180 $^{\circ}$ C for 3 h.

potential control over size and morphology of the crystals, and avoidance of high-temperature polymorphic phase transition [5]. The control of solution conditions is necessary for the formation of phase pure materials, particularly for the PT system [6-8]. Although a number of publications have reported on the hydrothermal synthesis of PT, a successful synthesis where both phase and morphology are controlled requires optimization of synthetic parameters, e.g. type and concentration of lead and titanium precursors, reaction temperature and time, and pH of reaction. Many authors agree that the major precursors, from which PT has been synthesized at temperatures lower than 250 °C, are the soluble forms of lead, either lead nitrate or lead acetate [5], and titanium with a complexing agent, e.g. tetramethylammonium hydroxide [6], isopropoxide [7] and water soluble titanium tetrachloride [8]. The reactions using hydrous titania (TiO2 · xH2O), though, necessitate high concentrations of alkali reagent, which in all of cases is potassium hydroxide (KOH). The disadvantage of the

contaminated alkali ions in the synthesized powder, in the case of lead zirconium titanate (PZT), has been reported.

Here we report on the preparation and characterization of submicron- to nano-sized PT powders with high perovskite phase purity and yield, and homogeneous morphology, via one-pot hydrothermal synthesis at relatively low temperatures. Attempts at substituting sodium hydroxide (NaOH) for the commonly used KOH have also been investigated and are reported here.

2. Experimental procedure

A mixture of titanium (IV) oxide (TiO2, Riedel-de Haën 99–100.5%) and lead (II) nitrate (Pb(NO₃)₂, Univar 99.0%) was prepared in a stoichiometric proportion of 1:1 in an aqueous media. Each solution had a final concentration of 1.32 mol dm⁻³. The alkali hydroxide pellets, in a molar ratio of four compared to that of the desired amount of PT to be synthesized, were gradually added to the mixture, which was then transferred to a hydrothermal autoclave with 70% filling factor. Two types of alkali hydroxide served as mineralizers in the reaction, i.e. sodium hydroxide (NaOH, Merck 99%) and potassium hydroxide (KOH, Merck 85%). The reaction was conducted under autogeneous pressure at temperatures ranging from 150 to 200 °C for 1.5-24 h. The solid products were recovered by filtration and washed with deionized water until the pH of the filtrate was about 7 in order to remove the remaining alkali on the surface of the powders. This was followed by rinsing with acetone. Powder X-ray diffractometry (XRD, Siemen D500/D501, CuK_{α} , Ni filter, $\lambda = 1.54$ Å) was used to characterize the crystalline solid products and a field emission scanning electron microscope (FESEM, JEOL JSM-6335F) equipped with the energy dispersive X-ray (EDX) analysis unit was employed in the investigation of morphology and elemental composition of the solids. The presence of lattice water and

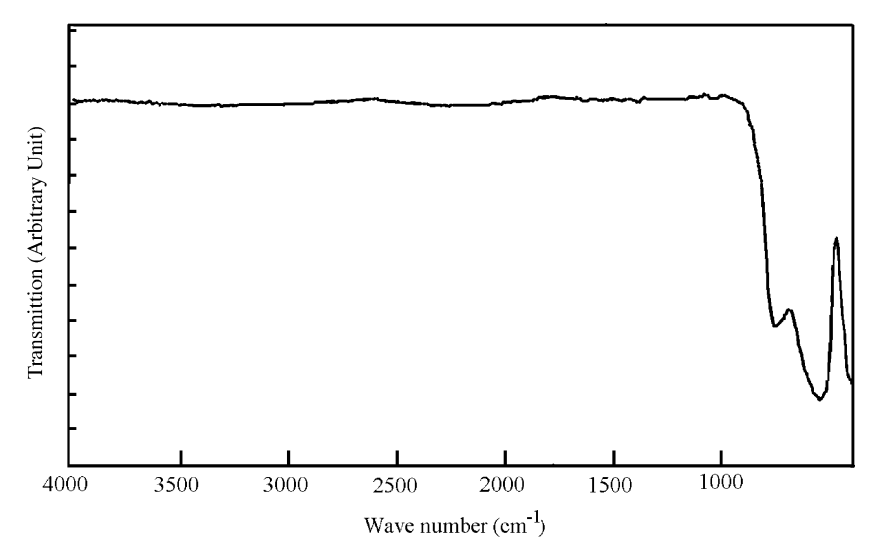


Fig. 2. The IR spectrum of PT powders obtained from the reaction with KOH as alkali reagent at 180 °C for 3 h.

also the incorporation of excess hydroxide species on the samples were investigated using infrared (IR) spectrophotometer (Nicolet magna 500, 4000–400 cm^{-1} , resolution of 0.5 cm^{-1}) measuring using a KBr disc. Moreover, the size distribution of the particles was also analyzed by particle size analyzer (CLAS 1064 ranging from 0.04–500.00 $\mu m/100$ classes).

3. Results and discussion

The synthesis procedure described above resulted in well crystallized yellow powders, which yielded more than 96 wt.% compared with the theoretical product mass. Since the pH of the reaction medium plays a critical role in the crystallization process, here the pH of the reaction

mixture was controlled by the amount of the alkali reagents, either KOH or NaOH, which was kept constant at 14, reported as the minimal pH required to yield well crystallized powder [9]. The formation of PT was examined as a function of type and amount of the alkali hydroxide, reaction temperature and time, as summarized in Table 1. Compared to the other methods used for synthesizing PT such as the wet-chemical route [10], the reaction conditions employed in this study are moderates. The reaction temperatures providing phase pure PT, as indicated by the powder XRD patterns, were also much lower than reported for the sol-gel technique [11]. The powder XRD patterns of every sample are alike and exemplified in Fig. 1, in which every peak could be indexed in the tetragonal PT phase, suggesting the occurrence of the tetragonal PT as the only phase in the

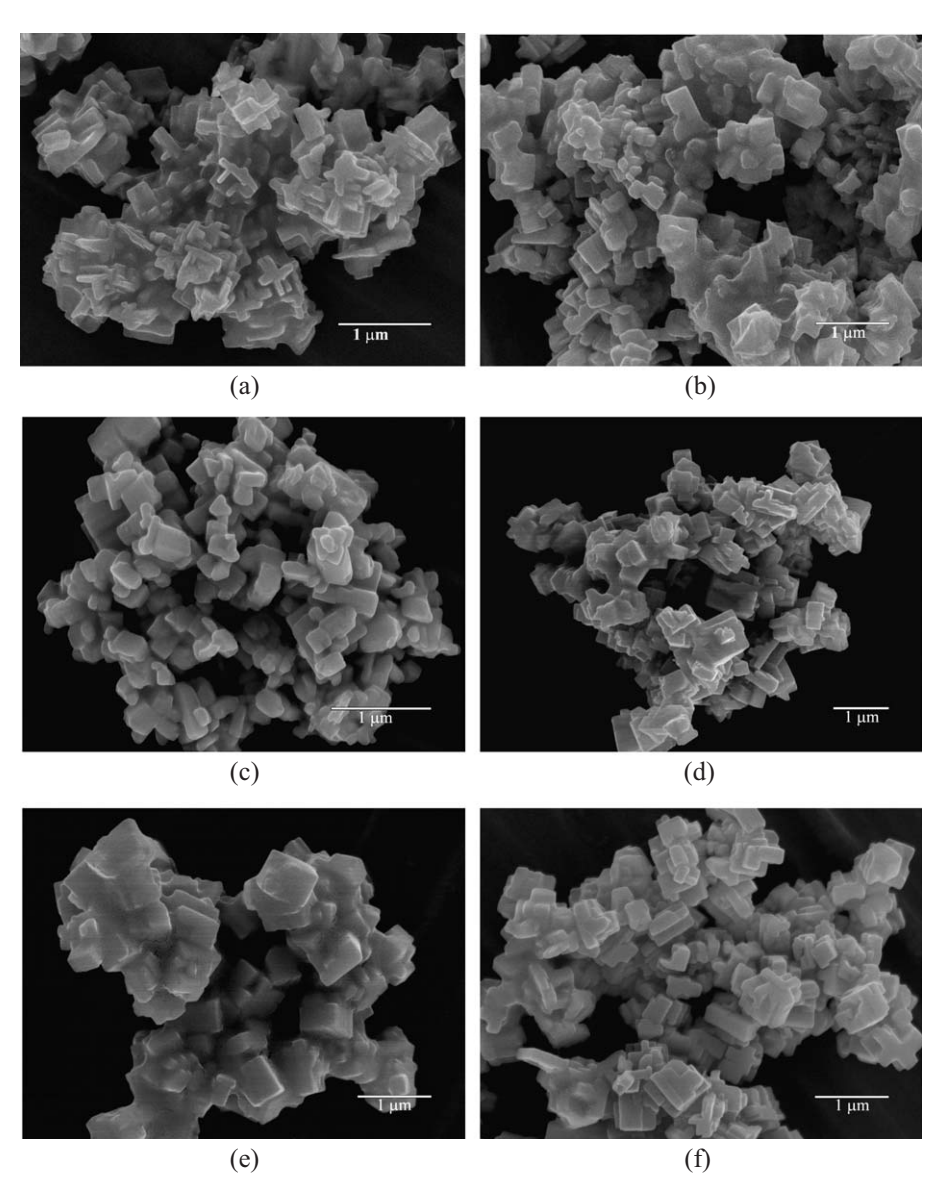
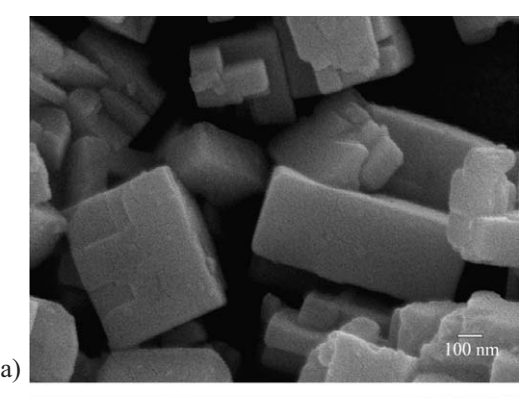
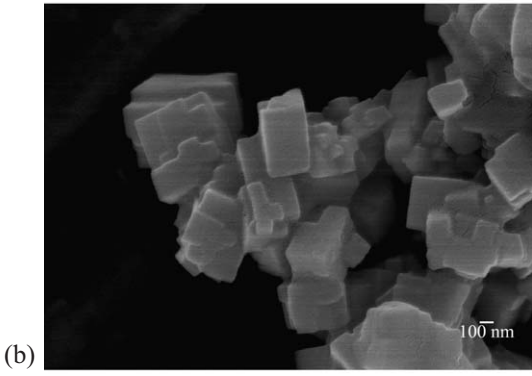


Fig. 3. Scanning electron micrographs of PT from the reactions with NaOH as alkali reagent at $150\,^{\circ}$ C for (a) 6, (b) 12 and (c) 24 h, compared with those using KOH at the same temperature for (d) 6, (e) 12 and (f) 24 h.

samples. The powder XRD patterns of the synthesized samples was successfully refined, based on every peak appearing in the powder patterns as having tetragonal P4/ mmm symmetry and refined cell parameters a and c of 3.8716(48)-3.8864(34) and 4.1317(46)-4.1507(25) Å, respectively. Both alkali reagents employed in the study, NaOH and KOH, led to the formation of tetragonal PT as the single phase with insignificant difference in refined cell parameters. The presence of different alkali cations, i.e. Na⁺and K⁺, in the reactions resulting from different alkali hydroxide had no influence on the type and phase of the synthesized PT powder. The elemental analysis of the PT powders are summarized in Table 1 with corresponding synthetic conditions revealing no remaining alkali cations, only lead and titanium in a Pb/Ti mole ratio of approximately one. The amount of oxygen measured on the surface of the samples slightly exceeded the calculated figures. The FTIR spectrum of the samples (Fig. 2) indicated neither lattice water nor hydroxide species due to the lack of characteristic absorption bands in the region 3550-3200 cm⁻¹ and 1630-1600 cm⁻¹ corresponding to antisymmetric and symmetric OH stretching and HOH bending, respectively [12]. The intense broad bands at 780 and 550 cm⁻¹ can be attributed to the presence of Ti-O bonds.

Regarding the influences of the alkali mineralizers, NaOH and KOH, employed in the reaction, the electron micrographs revealed no significant difference in morphologies of the powders, as shown in Fig. 3. The powders formed from the reactions with both NaOH and KOH as alkali mineralizer were either tabular or cubic in shape and occurring as conglomerate of the particles, which is consistent with those reported earlier [6]. It should be noted though that the degree of melting at grain boundaries, which has been reported as the principal disadvantages of the hydrothermal synthetic technique especially with TiO₂ starting materials, of these samples differed. The relation between degree of melting at grain boundaries and reaction temperature and time, however, could not be well established, although under the same synthetic conditions, the samples resulting from the reactions employing KOH apparently showed more disintegration and less melting at grain boundaries compared to those formed using NaOH. At the reaction temperature of 180 °C with KOH as alkali mineralizer, the degree of melting increased with increasing reaction time as shown by electron micrographs in Fig. 4. The powder with the best monodisperse particles, or the least melting at grain boundaries, was obtained when KOH was used as the alkali reagent, reacted at 180 °C for 3 h, when the particle size ranging from 40 to 6.00 µm with the average grain size of ca. $1.54 \, \mu m$ resulted. In contrast to the effect on morphology, the use of NaOH or KOH showed marked effect on grain size distribution and the average grain size (Table 1). The particles obtained from the reactions with NaOH showed a narrower size distribution and smaller average grain size of 0.20-1.95 µm compared to





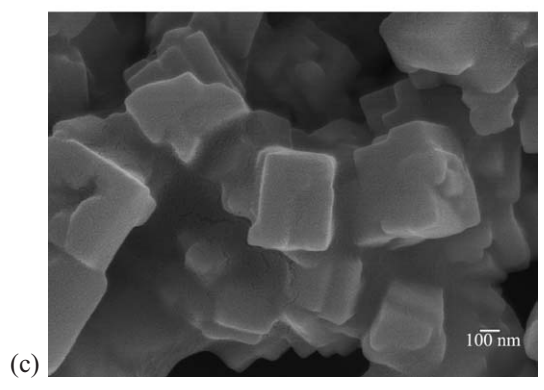


Fig. 4. Scanning electron micrographs of PT from the reactions with KOH as alkali reagent at $180\,^{\circ}\text{C}$ for (a) 3, (b) 6 and (c) 12 h.

the case of KOH when the average grain size of 3.04–4.55 μm resulted for the same synthesis conditions. The smallest mean grain size, 200 nm, was obtained when NaOH was used in the reaction at 150 °C for 6 h.

4. Conclusions

In the present study, tetragonal phase pure PT submicronto nano-sized particles with a Pb/Ti mole ratio of approximately one were prepared under hydrothermal conditions at low temperatures with more than 96 wt.% yield. No alkali mineralizer remained in the products after the reactions. The influence of NaOH, the scarcely used alkali, and KOH, which is the more widely known mineralizer, on chemical composition and particle morphologies was alike, although NaOH resulted in particles with a narrower size distribution

and smaller average grain size. KOH, on the other hand, showed an advantage over NaOH in giving better mono-disperse particles.

Acknowledgements

This work was supported by the Thailand Research Fund and the Commission on Higher Education for research funding under the project of Nanoscience and Nanotechnology Network.

References

 A.J. Moulson, J.M. Herbert, Electroceramics, 2nd ed., John Wiley & Sons, New York, 2003.

- [2] A. Udomporn, K. Pengpat, S. Ananta, J. Eur. Ceram. Soc. 24 (2004) 185
- [3] G. Haertlint, J. Am. Ceram. Soc. 82 (1999) 797.
- [4] G.R. Fox, J.H. Adair, R.E. Newnham, J. Mater. Sci. 25 (1990) 3634.
- [5] M.G. Gelabert, B.L. Gersten, R.E. Riman, J. Cryst. Growth 211 (2000) 497.
- [6] S.-B. Cho, J.-S. Noh, M.M. Lencka, R.E. Riman, J. Eur. Ceram. Soc. 23 (2003) 2323.
- [7] S.-K. Lee, G.-J. Choi, U.-Y. Hwang, K.-K. Koo, K.-K. Park, Mater. Lett. 57 (2003) 2201.
- [8] H. Cheng, J. Ma, Z. Zhao, L. Qi, J. Mater. Sci. Lett. 15 (1996) 1245.
- [9] E. Suvaci, J. Anderson, G.L. Messing, J.H. Adair, Key Eng. Mater. (2002) 206.
- [10] R.C. Emerson, E. Longoa, E.R. Leite, V.R. Mastelaro, J. Solid State Chem. 177 (2004) 1994.
- [11] Z. Xionghui, L. Yayan, W. Xiuyan, Y. Wenchun, W. Lan, G. Hongxia, Mater. Chem. Phys. 77 (2003) 209.
- [12] K. Nakamoto, Infrared and Raman Spectra of Inorganic and Coordination Compounds, 5th ed., Wiley-Interscience Publication, Toronto, 1997.



Available online at www.sciencedirect.com



JOURNAL OF CRYSTAL GROWTH

Journal of Crystal Growth 289 (2006) 224-230

www.elsevier.com/locate/jcrysgro

Influence of alkali reagents on phase formation and crystal morphology of hydrothermally derived lead titanate

Apinpus Rujiwatra^{a,*}, Nirawat Thammajak^a, Thapanee Sarakonsri^a, Rewadee Wongmaneerung^b, Supon Ananta^{a,b}

^aInorganic Materials Research Unit, Department of Chemistry, Faculty of Science, Chiang Mai University, Chiang Mai 50200, Thailand ^bDepartment of Physics, Faculty of Science, Chiang Mai University, Chiang Mai 50200, Thailand

> Received 29 July 2005; received in revised form 11 October 2005; accepted 14 October 2005 Available online 27 December 2005 Communicated by S. Uda

Abstract

The influence of three different alkali reagents, i.e. ammonium hydroxide, sodium hydroxide and potassium hydroxide, on phase formation and crystallite morphology of lead titanate prepared under mild hydrothermal conditions was investigated. The formation of three different phases of lead titanate including tetragonal perovskite, tetragonal body-centered and cubic phases, which showed preference to different types of bases, was discussed. The relation between phases and morphology of the hydrothermally derived lead titanate was illustrated. The formation mechanism of lead titanate when various mixtures of ammonium-alkali hydroxide were employed was also discussed. The transmission electron microscopic technique was also employed in the investigation of a typical hydrothermally derived sample revealing the presence of a pyrochlore phase, otherwise undetected by the XRD technique.

© 2005 Elsevier B.V. All rights reserved.

Keywords: A1. Crystal morphology; A1. Surface structure; A1. X-ray diffraction; A2. Growth from solutions; B1. Perovskite; B2. Piezoelectric materials

1. Introduction

Lead titanate (PbTiO₃ or PT) is an eminent ferroelectric material with high Curie temperature, high pyroelectric coefficient, low dielectric constant, and high spontaneous polarization, and therefore it has been employed extensively in electronic and electro-optic devices, such as capacitors, microactuators, ultrasonic transducers and infrared sensors [1–3]. Although various preparative routes are currently available for the preparation of PT fine powders, such as sol–gel [4], chemical coprecipitation [5], emulsion [6], and hydrothermal technique [7], only few routes offer reasonable controllability of size, morphology and degree of agglomeration. Hydrothermal technique allegedly has such capability, since it is an aqueous-based precipitation allowing the controlling ability over the nucleation, growth and aging processes [8]. Lead titanate

prepared by the hydrothermal technique exhibits different crystal structures and morphology including perovskite, pyrochlore, and tetragonal body-centered types, depending on various chemical preparative parameters, e.g. reaction temperature and pressure, starting precursor, feed stock concentration, pH, and ionic strength [9,10].

Although a number of publications have reported the hydrothermal prepartion of PT, a successful preparation where both phase and morphology are controlled requires optimization of synthetic parameters, such as type and concentration of lead and titanium precursors, reaction temperature, time, and pH. The common precursors, from which PT has been prepared at temperatures lower than 250 °C, are the soluble form of lead (either lead nitrate or lead acetate) [11], and titanium with complexing agent, e.g. tetramethylammonium hydroxide [12], isopropoxide [8] and water soluble titanium tetrachloride [13], all of which provide hydrous titania (TiO₂·xH₂O) as titanium source. The employment of these precursors, though, necessitates a high concentration of alkali reagent, which in all cases is

^{*}Corresponding author. Tel.: +66 53 941906; fax: +66 53 892277. E-mail address: apinpus@chiangmai.ac.th (A. Rujiwatra).

potassium hydroxide (KOH). Recently, our group reported the success of using sodium hydroxide (NaOH) instead of the commonly used KOH to yield phase-pure perovskite and stoichiometric PT with submicron- to nanometer-sizes, from lead nitrate and commercially available TiO₂ under very mild hydrothermal conditions [14].

During recent years, there have been reports on using other alkali reagents in the preparation of various ferroelectric materials e.g. PZT via sol-gel processing, PLZT via oxalate technique and also PT by polymeric precursor method [15–17]. The alkali reagent attracting our interest the most is ammonium hydroxide or the so-called ammonia solution. It has commonly been used both to adjust the pH of the reactions and to increase the solubility of solute. Although the ammonia solution with lower critical temperature and pressure than water is well-known to be a good pressure transmitting media under hydrothermal conditions and as the mild pH adjusting agent with the capability to control the morphology of the final solids [18], the employment of the ammonia solution in hydrothermal preparation of PT has not yet been reported. Furthermore, phase purity and morphology control of hydrothermally derived PT has been reported to be somewhat difficult to achieve, especially the latter one, which turns out to be a challenging problem for the future. Therefore, the purpose of the present work was to study the phase purity and controllability of the morphology of hydrothermally derived PT via the investigation of the influence of ammonium hydroxide, either with or without the presence of NaOH or the commonly used KOH, on phase formation and crystal morphology of the PT prepared from the reaction of lead nitrate and commercially available TiO₂ under mild hydrothermal conditions.

2. Experimental procedure

A stoichiometric mixture of lead (II) nitrate (Pb(NO₃)₂, Univar 99.0%) and commercially available titanium (IV) oxide (TiO₂, Riedel-de Haën 99-100.5%) was prepared with a final concentration of 1.32 mol dm⁻³ for each precursor. The reaction medium was either deionized water or 15–30% ammonia solution prepared from 30% solution (NH₃, Panreac Quimica SA 28.0-30.0%). The alkali hydroxide solution prepared from pellets with a concentration varied between 1.0 and 4.0 mol dm⁻³ was gradually added to the mixture, which was then transferred to a hydrothermal autoclave with 70% filling capacity. There were two types of alkali hydroxide employed in the reaction, i.e. sodium hydroxide (NaOH, Merck 99%) and potassium hydroxide (KOH, Merck 85%). The reaction was conducted under autogenous pressure at the temperature of 180 °C for 2-24 h. The solid products were recovered by filtration and washed with deionized water until the pH of the filtrate was 7 in order to remove the remaining hydroxide species on the surface of the powders. This was followed by rinsing with acetone. Powder X-ray diffractometer (XRD, Siemen D500/D501, CuK_α, Ni filter, $\lambda = 1.54 \,\text{Å}$) was used to characterize the crystalline solid products, and a field emission scanning electron microscope (FESEM, JEOL JSM-6335F) equipped with an energy dispersive X-ray (EDX) spectroscopic microanalyzer was employed in the investigation of morphology and elemental composition of the solids. The transmission electron microscope (TEM, JEOL JEM-2010) was used to confirm the crystallographic setting and to study the microstructure of the acicular PT. The powders were deposited on a copper-grid supported transparent carbon foil, so that the TEM investigations could be conducted. The presence of lattice water, ammonium cation and also the incorporation of excess hydroxide species on the samples were identified by infrared spectra (KBr disc) using a Fourier transform infrared (FTIR) spectrophotometer (Nicolet magna 500, 4000–400 cm⁻¹, resolution of $0.5\,\mathrm{cm}^{-1}$).

3. Results and discussion

The preparative procedure as described gave rise to well crystalline light-yellow powders, most of which possessed PT as either the only or major crystalline phase identified by the XRD patterns. The high concentration of 4.0 mol dm⁻³ of either KOH or NaOH, keeping the pH of the reaction mixture at 14, was crucial for the tetragonal phase-pure perovskite PT to form. Fig. 1 shows the XRD patterns of the phase-pure perovskite PT obtained from the reactions with either KOH or NaOH at the decisive concentration of 4.0 mol dm⁻³. The presence or absence of ammonium hydroxide in the reaction mixture showed insignificant effect on phase purity, particle size and shape of these phase-pure perovskite PT when the concentration of the added alkali hydroxide was sufficiently high, i.e. 4.0 mol dm⁻³ in this study. Every peak in each XRD pattern in Fig. 1 could be indexed and refined successfully

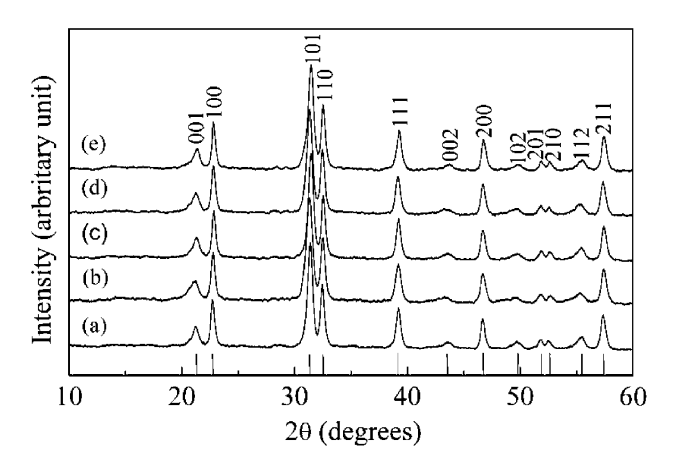


Fig. 1. Powder XRD patterns of tetragonal phase-pure perovskite PT synthesized under hydrothermal pressure at $180\,^{\circ}\text{C}$ using (a) only KOH [4 mol dm $^{-3}$] for 3 h compared to those using KOH [4 mol dm $^{-3}$] and 30% ammonia solution for (b) 3 h (c) 6 h, and (d) KOH [4 mol dm $^{-3}$] and 15% ammonia solution for 12 h, as well as (e) NaOH [4 mol dm $^{-3}$] and 30% ammonia solution for 6 h.

in the tetragonal P4mmm symmetry giving refined cell parameters a and c of 3.878(6)-3.885(2)4.152(6)–4.168(6) Å, respectively. It was noticeable that the well-crystalline phase-pure tetragonal PT with perovskite structure was formed under the studied hydrothermal conditions in only 3h (Figs. 1(a) and (b)). The electron micrographs, as shown in Fig. 2, revealed the morphology of these perovskite PT to be either cubic or tabular with similar aspect ratio ranging from 60 to 840 nm, which was in the same range as those reported earlier [12,15]. These crystallites commonly occurred as hard agglomerates of the primary particles, which is the common character of hydrothermally derived PT powders. The relation between reaction time and degree of melting at grain boundaries was also apparent from Fig. 2. The degree of melting at grain boundaries increased with reaction time, and this relation was independent of the alkali type and concentration.

As the concentration of the alkali hydroxide was reduced to less than 4 mol dm⁻³, i.e. 1 and 2 mol dm⁻³ providing the pH of 11–12, the influence of ammonium hydroxide on phase and morphology of the final solid products was

disclosed. The XRD patterns as shown in Fig. 3 showed the coexistence of the starting anatase TiO₂ and other oxide phases of titanium and lead with the desired PT indicating the incompleteness of the reaction. This may be accounted for by either the presence of ammonium hydroxide or the insufficiency of the added alkali hydroxide thus reducing the reaction pH to less than 14. The pH of 14 was acclaimed to be the optimal pH for the formation of phasepure perovskite PT in tetragonal P4mmm symmetry [19]. The presence of the desired PT was, however, more apparent in contrast to the other oxide phases of titanium and lead, as the reaction time was prolonged (Figs. 3(a) and (b)), suggesting that the longer reaction time may be required for the reaction to complete. It is intriguing that when ammonium hydroxide was present and the corresponding concentration was not outweighed by the concentration of either KOH or NaOH, the PT obtained from the reactions was the tetragonal body-centered PT in I4 symmetry with refined cell parameters a and c of 12.330(1)–12.34(6) and 14.42(2)–14.42(16) Å, respectively. The co-presence of ammonium hydroxide and either KOH or NaOH at low concentration, with the consequence of

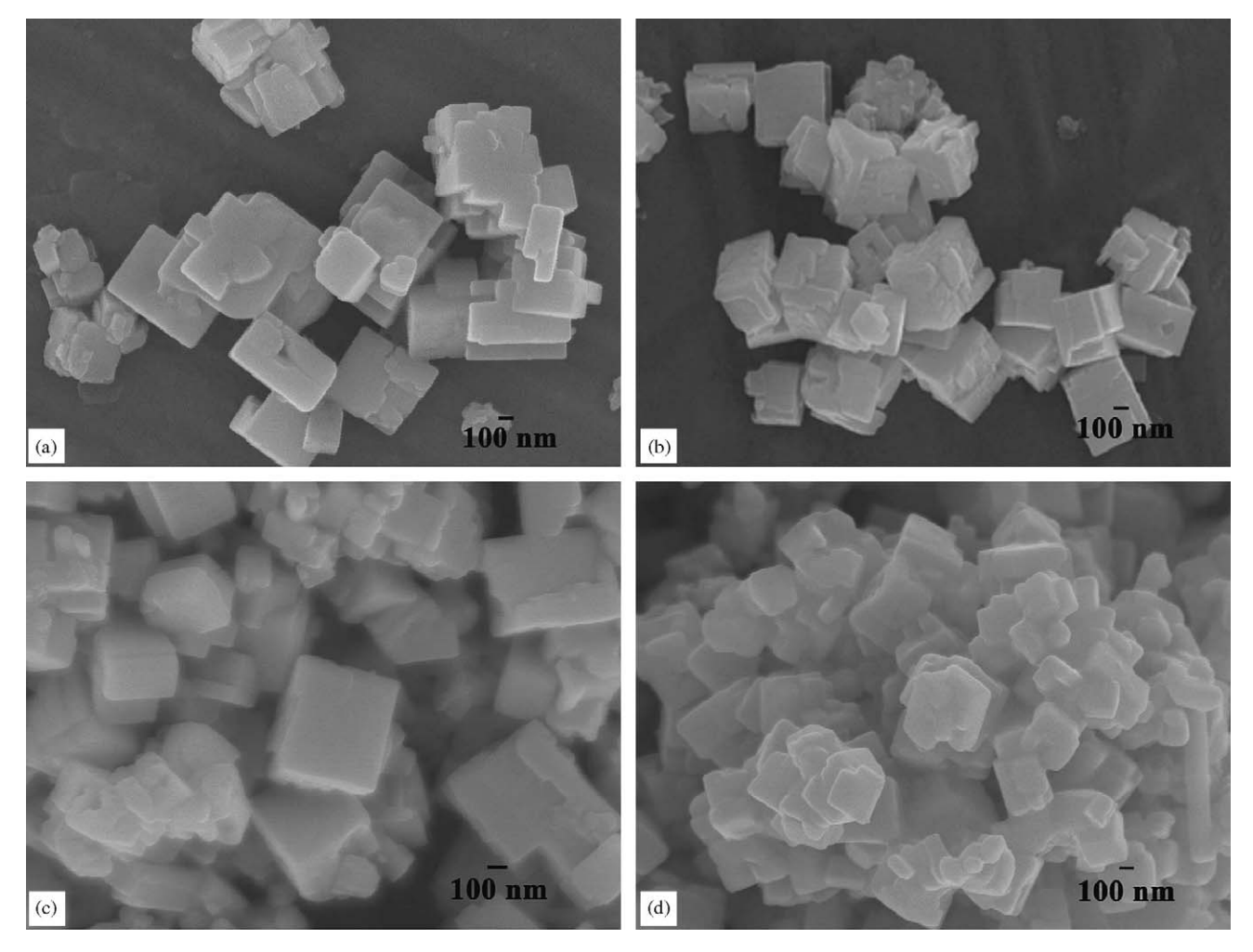


Fig. 2. The electron micrographs reveal the similar crystal habits of either cubic or tabular forms of the tetragonal phase-pure perovskite PT corresponding to the powder XRD patterns shown in Figs. 1(a)–(d) respectively.

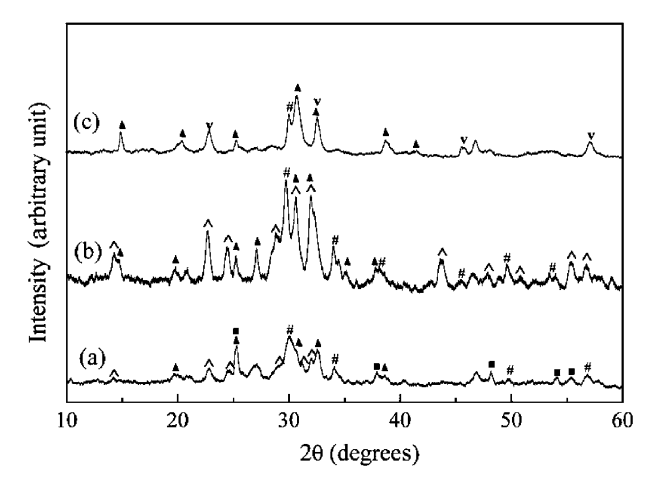


Fig. 3. XRD patterns of the powders obtained from the reactions conducted at $180\,^{\circ}\text{C}$ using 30% ammonia solution with the additive (a) KOH $[2\,\text{mol}\,\text{dm}^{-3}]$ for $6\,\text{h}$, (b) NaOH $[1\,\text{mol}\,\text{dm}^{-3}]$ for $12\,\text{h}$, and (c) without the addition of alkali hydroxide for $12\,\text{h}$; when \land and \lor indicate peaks corresponding to lead titanate in tetragonal I4 and cubic, respectively, whereas \blacktriangle , \blacksquare and # corresponding to Pb₃O₄, PbO and TiO₂.

the pH being lower than 14, therefore led to the formation of the tetragonal body-centered type of PT based on I4 symmetry, occurring as either the only PT phase or a mixture with the P4mmm perovskite phase.

When only 30% ammonia solution was employed without the addition of either KOH or NaOH, thus providing the reaction mixture the pH of 10, the formation of cubic PT in Fd3m symmetry with refined cell parameter a of 3.961 Å, co-present with lead oxide and titanium oxide phases, was clearly observed after 12 h (Fig. 3(c)). Formerly, the pH between 9 and 10 was reported to be suitable to produce stoichiometric PT with the perovskite structure [20]. The presence of lead oxide may be due to its partial solubility in the reaction medium as the pH range of 9–10 is near the limiting pH for the minimal solubility of lead oxide.

The influence of reaction time on the formation of tetragonal PT phases and hence the formation mechanism was also evident when the concentration of the ammonia solution was not outweighed by the alkali hydroxide. Fig. 4 shows the XRD patterns of the powders obtained from reactions conducted at 180 °C under hydrothermal pressure with varying reaction times. Ammonia solution (30%) was used as the solvent with added KOH to provide the final concentration of either 2 or 1 mol dm⁻³, both of which cases gave similar results. The XRD pattern of the powder, obtained from the reaction with the final KOH concentration of 1 mol dm⁻³ conducted under hydrothermal pressure at 180 °C for 2 h (Fig. 4(a)), indicated no formation of the desired PT, but only the remaining of the starting anatase TiO₂, coexisting with the other transformed titanium oxide phases, e.g. rutile TiO₂, Ti₄O₇ and K_xTi₈O₁₆. The incorporation of potassium(I) ion into the oxide framework of titanium should be noted. The presence of solid solution of Pb(NO₃) · 5Pb(OH)₂ and PbO was also revealed from the XRD patterns, suggesting the precipitation of

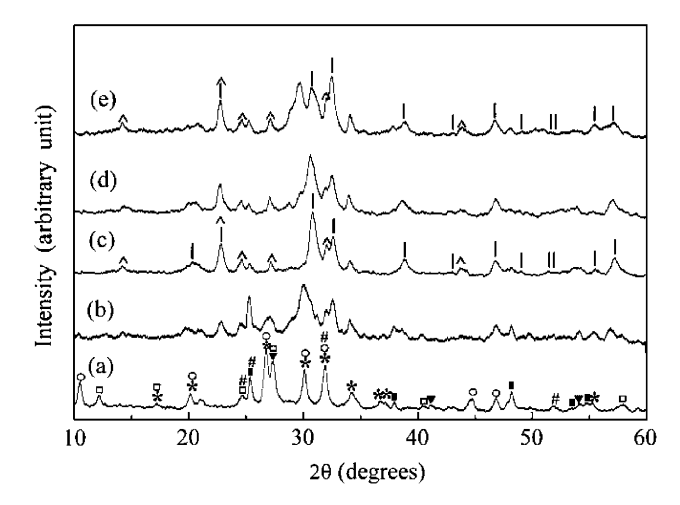


Fig. 4. The XRD patterns of the powders obtained from the reactions conducted at 180 °C using 30% ammonia solution with the additive KOH (a) $[1 \, \text{mol} \, \text{dm}^{-3}]$ for 2h, (b) $[2 \, \text{mol} \, \text{dm}^{-3}]$ for 6h, (c) $[2 \, \text{mol} \, \text{dm}^{-3}]$ for 12h, (d) $[1 \, \text{mol} \, \text{dm}^{-3}]$ for 12h, and (e) $[2 \, \text{mol} \, \text{dm}^{-3}]$ for 24h; when | and \land indicate peaks corresponding to PT in tetragonal P4mmm and I4, whereas *, \blacktriangleleft and \blacksquare corresponding to oxide phases of titanium, and #, \square and \bigcirc to the oxide phases of lead.

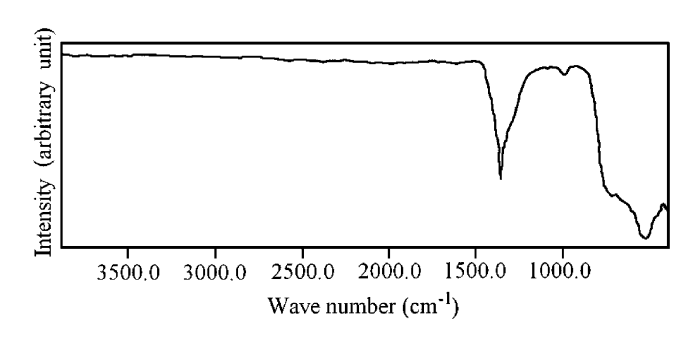


Fig. 5. Typical FTIR spectrum of the synthesized PT showing characteristic vibrational bands of neither water nor hydroxide species. The intense broad bands centering at 780 and 550 cm⁻¹ attribute to the Ti–O vibration.

lead(II) ion by the hydroxide residue and the formation of Pb(NO₃)·5Pb(OH)₂ solid solution intermediate. An ammonium residue, on the other hand, was not incorporated into the final crystalline powders. This was confirmed by the FTIR spectrum in which no characteristic bands of the amino group were observed (Fig. 5).

As the reaction time was prolonged, the characteristic XRD peaks of the starting materials and the solid solution intermediate lost intensities (Fig. 4(b)) and finally disappeared after 12 h, whereas those of both tetragonal perovskite and body-centered PT became visible as a mixture of these two tetragonal phases (Figs. 4(c) and (d)). The employment of different concentrations of the alkali hydroxide, i.e. 2 and 1 mol dm⁻³, showed insignificant influence on the formation of these PT phases, as shown by the powder XRD, if the other variables were alike. The higher concentration of 2 mol dm⁻³ resulted in slightly better crystallinity (Fig. 4(c)). The retaining of both tetragonal phases was evident after 24 h (Fig. 4(e)), although peak broadening was observed with additional

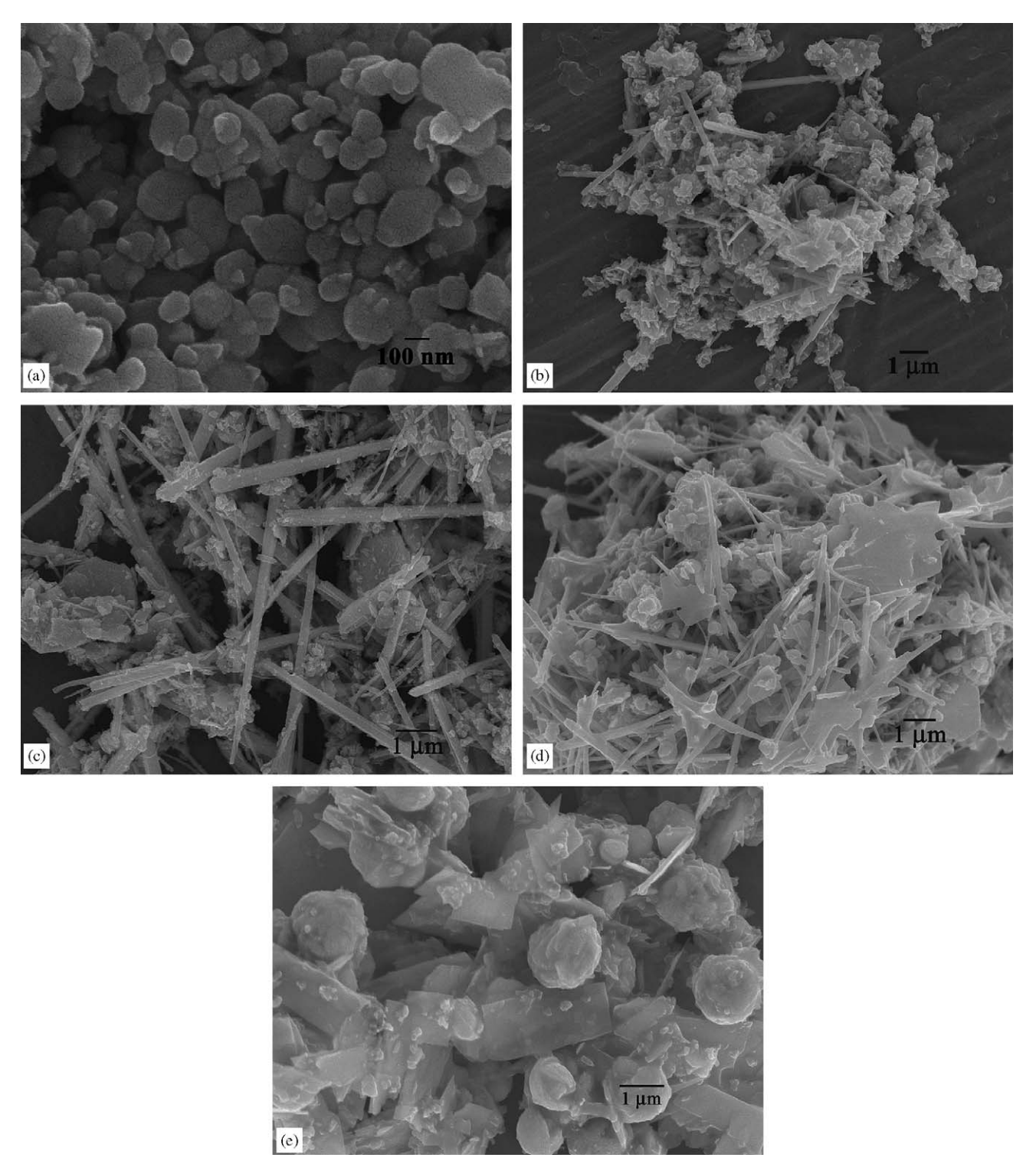


Fig. 6. The electron micrographs showing various types of morphologies of the powders obtained from the reactions using 30% ammonia with the addition of (a) KOH [1 mol dm $^{-3}$] for 2 h, (b) KOH [2 mol dm $^{-3}$] for 6 h, (c) NaOH [1 mol dm $^{-3}$] for 12 h, and (d) KOH [2 mol dm $^{-3}$] for 12 h, compared to (e) that without using any alkali hydroxide for 12 h.

unidentified peaks at 2θ ca. 29.7° and 34.1° , indicating the formation of other unidentified crystalline phases. The FTIR spectra of these samples are alike and exemplified in Fig. 5, indicating the remaining of neither lattice water nor hydroxide species due to the lack of characteristic

absorption bands in the region 3550–3200 cm⁻¹ and 1630–1600 cm⁻¹ corresponding to antisymmetric and symmetric OH stretching and HOH bending respectively [21]. There are two intense broad bands at 780 and 550 cm⁻¹, which are attributed to the Ti–O vibration.

According to the results described above, the formation of tetragonal PT phases under the studied hydrothermal conditions was assumed to occur through the phase transformation of the oxide framework of titanium with the diffusion of solvent soluble lead(II) ions into the framework, replacing the potassium(I) ions, formerly incorporated in the oxide framework. The added hydroxide residue would react with lead(II) ion leading to the Pb(OH)₂ precipitate, which would subsequently re-dissolve to provide lead(II) as the reaction was prolonged to form the final products. The concept of diffusion of lead(II) ion into the hydrated oxide framework of titanium under hydrothermal conditions was consistent with the formation mechanism proposed for PT in the other hydrothermal system, such as that using tetramethylammonium hydroxide [22].

The presence of the starting materials after 2h of reaction, as characterized by the XRD technique (Fig. 4(a)), was confirmed by the electron micrograph revealing the agglomeration of regular spherical shape particles (Fig. 6(a)) similar to the morphology of the starting precursors, with particle sizes ranging from 46 to 300 nm. The corresponding mole ratio of Pb:Ti was 3:1 determined by the EDX microanalyzer. As the reaction time was lengthened, both acicular and melt platelet crystallites appeared, with the former crystallite habit becoming more apparent with longer reaction time. The existence of acicular crystallites was very pronounced after 12h of reaction (Fig. 6(c)), which well agrees with the powder XRD results. Electron micrographs also revealed the

coexistence of acicular PT, with approximately equimolar ratio of Pb:Ti, and irregular platelet crystallites in every case where ammonium hydroxide was present and the reaction time was longer than 2h, as shown in Figs. 6(b)-(d). The lower concentration of added alkali hydroxide, either NaOH or KOH, was preferable for the formation of acicular crystallites with better defined shape and length, and of higher proportion compared to the bulk sample (Figs. 6(b)-(d)). The reaction of Pb(NO₃)₂ and TiO₂ in 30% ammonia solution with 1 mol dm⁻³ of NaOH under hydrothermal pressure at 180 °C for 12h provided the longest acicular crystallites of up to 14 µm in length with the cross-sectional diameter down to 50 nm (Fig. 6(c)). The electron micrograph of the powders consisting of cubic PT and other oxide phases of lead and titanium, on the other hand, showed neither acicular nor cubic crystallites as illustrated in Fig. 6(e), but only the agglomeration of irregular round shaped particles with approximately equimolar ratio of Pb:Ti, the determined platelet melt of which indicated a PbO-rich phase.

According to the SEM and XRD results as described, the exhibition of acicular morphology by the PT crystals well corresponds with the body-centered tetragonal PT in I4 symmetry. The correlation between the PT phase formation and the presence or absence of different types of the alkali reagents, and also the relation between phase formation and crystal morphology are therefore demonstrated here.

The typical sample obtained from the reaction of Pb(NO₃)₂ and TiO₂ in 30% ammonia solution with

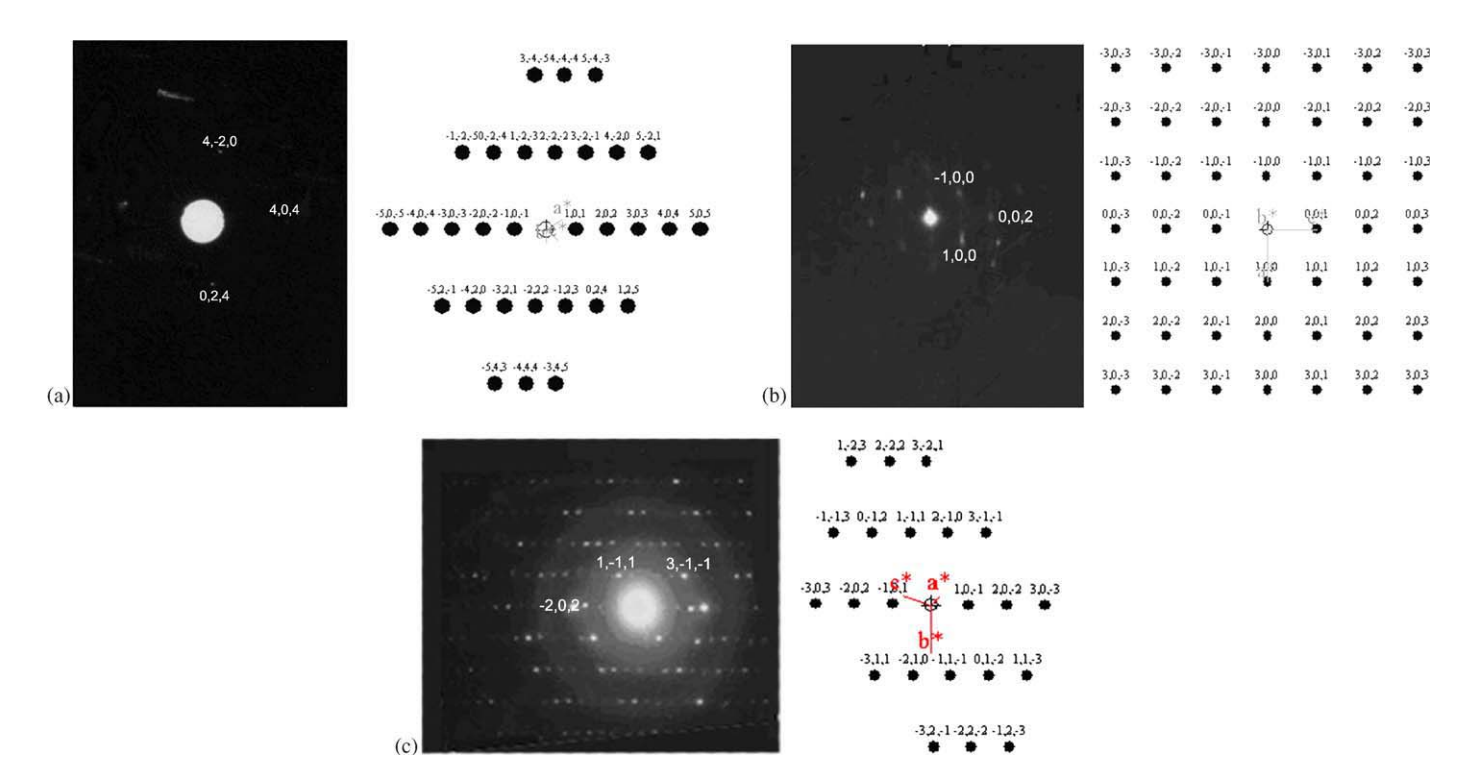


Fig. 7. The TEM images of (a) tetragonal body-centered PT (zone axis = $[\bar{1}\,\bar{2}\,1]$), (b) tetragonal pervoskite PT (zone axis = $[0\,\bar{2}\,0]$), and (c) the pyrochlore PbTi₃O₇ (zone axis = $[2\,\bar{4}\,\bar{2}]$) taken from hydrothermally derived typical sample compared with the correspondingly simulated diffraction patterns.

1 mol dm⁻³ of NaOH under hydrothermal pressure at 180 °C for 12 h, which provided the longest acicular crystallites (Fig. 6(c)) with corresponding XRD pattern shown in Fig. 3(b), was selected for TEM experiments. The TEM micrographs as shown in Fig. 7, showing the diffraction patterns compared to the simulated patterns of the corresponding phase, reveal the coexistence of three PT phases, i.e. tetragonal perovskite PT, tetragonal bodycentered PT and the pyrochlore PbTi₃O₇. By using selected area electron diffraction (SAED) method, the acicular phase was identified as the tetragonal body-centered PT, whereas the cubic phase as the tetragonal perovskite PT. This well agrees with the XRD and SEM results suggesting the coexistence of these two tetragonal phases of PT. The platelet phase deposited on the surface of the acicular phase was however identified as the monoclinic pyrochlore PbTi₃O₇, although the presence of this phase was not shown by the XRD technique. It is therefore intriguing to note the advantage of TEM, which lies in its ability to reveal microstructural features often missed by the XRD diffraction method which requires at least 5 wt% of the component [23].

4. Conclusion

Submicron to nano-sized PT powders were prepared from the reaction between Pb(NO₃)₂ and commercially available TiO₂ under hydrothermal conditions. The influence of different alkali reagents, i.e. ammonium hydroxide, NaOH and KOH, and their concentration on phase formation and crystallite morphology of the prepared PT was investigated. The excess of the alkali hydroxide over ammonium hydroxide in the reaction mixtures always led to the formation of tetragonal phase-pure perovskite PT in P4mmm symmetry, independently from the presence of ammonia. The presence of ammonia with a low concentration of alkali hydroxide led to the formation of tetragonal body-centered PT in I4 symmetry as a mixture with the P4mmm perovskite phase. The PT phase in I4 symmetry, however, could not be prepared as a single phase under the studied conditions. The acicular PT was exhibited by the tetragonal I4 phase, whereas the regular cubic or tabular PT well corresponded to the tetragonal P4mmm phase. The employment of only ammonia without the addition of the alkali hydroxide resulted though in the formation of cubic PT based on Fd3m symmetry. The TEM was also employed to study the microstructures of the synthesized PT and showed results agreeing with those by the XRD, indicating the coexistence of two tetragonal phases. The presence of the pyrochlore phase of PbTi₃O₇, though was not shown by the XRD technique, was disclosed by the TEM technique. The influence of reaction time on phase

formation, and therefore on the formation mechanism, in the cases where both the alkali hydroxide and ammonia were used in the reactions, were also discussed.

Acknowledgments

The authors would like to thank the Thailand Research Fund, Faculty of Science and the Development and Promotion of Students with Talents in Science and Technology Project for the financial support, Professor Jumras Limtrakul for providing hydrothermal reactors, and Assoc. Prof. Duang Buddhasukh for help in language improvment.

References

- A.J. Moulson, J.M. Herbert, Electroceramics, Second ed, Wiley, New York, 2003.
- [2] Y. Xu, Ferroelectric Materials and Their Applications, North-Holland, New York, 1991.
- [3] F. Jona, G. Shirane, Ferroelectric Crystals, Dover Publications, New York, 1993.
- [4] A. Udomporn, K. Pengpat, S. Ananta, J. Eur. Ceram. Soc. 24 (2004) 206.
- [5] J. Tartaj, J.F. Fernandez, F. Villafuerte-Castrejon, Mater. Res. Bull. 36 (2001) 479.
- [6] J. Fang, J. Wang, L.M. Gan, S.C. Ng, Mater. Lett. 52 (2002) 304.
- [7] J. Fang, J. Wang, S.C. Ng, C.H. Chew, L.M. Gan, J. Mater. Sci. 34 (1999) 1943.
- [8] S.-B. Cho, J.-S. Noh, M.M. Lencka, R.E. Riman, J. Eur. Ceram. Soc. 23 (2003) 2323.
- [9] H. Cheng, J. Ma, Z. Zhao, D. Qiang, J. Am. Ceram. Soc. 75 (1992) 1123
- [10] M.M. Lencka, R.E. Riman, J. Am. Ceram. Soc. 76 (1993) 2649.
- [11] M.C. Gelabert, B.L. Gersten, R.E. Riman, J. Crystal Growth 211 (2000) 497.
- [12] X. Zeng, Y. Liu, X. Wang, W. Yin, L. Wang, H. Guo, Mater. Chem. Phys. 77 (2002) 209.
- [13] S.-K. Lee, G.-J. Choi, U.-Y. Hwang, K.-K. Koo, K.-K. Park, Mater. Lett. 57 (2003) 2201.
- [14] H. Cheng, J. Ma, Z. Zhao, L. Qi, J. Mater. Sci. Lett. 15 (1996) 1245.
- [15] A. Rujiwatra, J. Jongphiphan, S. Ananta, Mater. Lett. 59 (2005)
- [16] Y.-J. Oh, I.-W. Hwang, I.-B. Shim, Y.-R. Kim, Bull. Korean Chem. Soc. 18 (1997) 588.
- [17] M. Pereira, P.Q. Mantas, J. Eur. Ceram. Soc. 18 (1998) 565.
- [18] F.M. Pontes, J.H.G. Rangel, E.R. Leite, E. Longo, J.A. Varela, E.B. Araujo, J.A. Eiras, Thin Solid Film 366 (2000) 232.
- [19] H.Y. Xu, H. Wang, Y.C. Zhang, W.L. He, M.K. Zhu, B. Wang, H. Yan, Ceram. Int. 30 (2004) 93.
- [20] E. Suvaci, J. Anderson, G.L. Messing, J.H. Adair, Key Eng. Mater. (2002) 206.
- [21] K. Nakamoto, Infrared and Raman Spectra of Inorganic and Coordination Compounds, Fifth ed, A WILEY-INTERSCIENCE PUBLICATION, Toronto, 1997.
- [22] G.A. Rossetti Jr., D.J. Watson, R.E. Newnham, J.H. Adair, J. Crystal Growth 116 (1992) 251.
- [23] H.P. Klug, L.E. Alexander, X-ray Diffraction Procedures, Second ed, Wiley, New York, 1974.



Available online at www.sciencedirect.com

Materials Letters 58 (2004) 449-454



A modified two-stage mixed oxide synthetic route to lead zirconate titanate powders

R. Tipakontitikul, S. Ananta*

Department of Physics, Faculty of Science, Chiang Mai University, Chiang Mai 50200, Thailand Received 19 August 2002; received in revised form 2 June 2003; accepted 6 June 2003

Abstract

An approach to synthesis lead zirconate titanate $[Pb(Zr_{1-x}Ti_x)O_3; PZT]$ powders with a modified two-stage mixed oxide synthetic route has been developed. To ensure a single-phase perovskite formation, an intermediate phase of zirconium titanate $(ZrTiO_4)$ was employed as starting precursor. The formation of perovskite phase in the calcined PZT powder has been investigated as a function of calcination temperature, soaking time and heating/cooling rates by differential thermal analysis (DTA) and X-ray diffraction (XRD) techniques. The morphology evolution was determined by scanning electron microscopy (SEM) technique. It has been found that the unreacted PbO and $ZrTiO_4$ phases tend to form together with PZT, with the latter appearing in both tetragonal and rhombohedral phases, depending on calcination conditions. It is seen that optimisation of calcination conditions can lead to a 100% yield of PZT in a tetragonal phase. © 2003 Elsevier B.V. All rights reserved.

Keywords: Lead zirconate titanate; PZT powder; Perovskites; Piezoelectric materials; Phase formation; X-ray techniques

1. Introduction

Lead zirconate titanate, $Pb(Zr_{1-x}Ti_x)O_3$ or PZT, is one of the most widely used piezoelectric materials with a perovskite structure. The compositions close to the morphotropic phase boundary (MPB) have been extensively exploited in commercial [1,2]. The excellent piezoelectric and electrostrictive properties make it a promising material for ferroelectric memory, optoelectronic, electrostrictive actuator, and electromechanical transducer applications [3,4].

There has been a great deal of interest in the preparation of single-phase PZT powders as well as in the sintering and piezoelectric properties of PZT-based ceramics. The mixed oxide synthetic route is probably one of the most fundamental, practical routine methods which has been used, and it has been developed and modified in both scientific research and industrial mass production for many years [5,6]. In general, PZT powders prepared by a mixed oxide route have spatial fluctuations in their compositions. The extent of the fluctuation depends on the characteristics of the

starting powders as well as on the processing schedule. The reaction sequence through which PZT are formed by solid state reactions has been investigated by many workers but with varying conclusions [7-12]. Mori et al. [7] were the first to study the mechanisms of a two-step reaction, initiated by the constituent oxides reacting to form a solid solution of lead titanate (PbTiO₃) and zirconium oxide (ZrO₂), which later homogenized to form the PZT phase. On the other hand, Speri [8] proposed a three-step reaction sequence, which was further substantiated by Hanky and Biggers [9]. The formation of PZT via a homogenisation process, commencing at 700 °C, by interdiffusion of Zr⁴⁺ and Ti⁴⁺ within and between the PZT phases formed at the original PbO/ZrO2 and PbTiO3/ZrO2 interfaces was proposed by Chandratreya et al. [10]. However, this sequence does not agree with the two-stage process proposed by Mori et al. [7]. Similar problem of pyrochlore formation has been encountered in the preparation of lead magnesium niobate (PMN) powders, where the use of the B-site precursor MgNb₂O₆ has been proposed by Swart and Shrout [11] as an effective way of producing PMN powder in high yield. More recently, Babushkin et al. [12] subsequently combined the approach of Swart and Shrout with that of Mori et al. by investigating a two-stage synthesis with Zr_{0.52}Ti_{0.48}O₂ as a precursor. The essentially pyrochlore-free powders obtained

^{*} Corresponding author. Tel.: +66-53-943-376; fax: +66-53-357-512. *E-mail address:* supon@chiangmai.ac.th (S. Ananta).

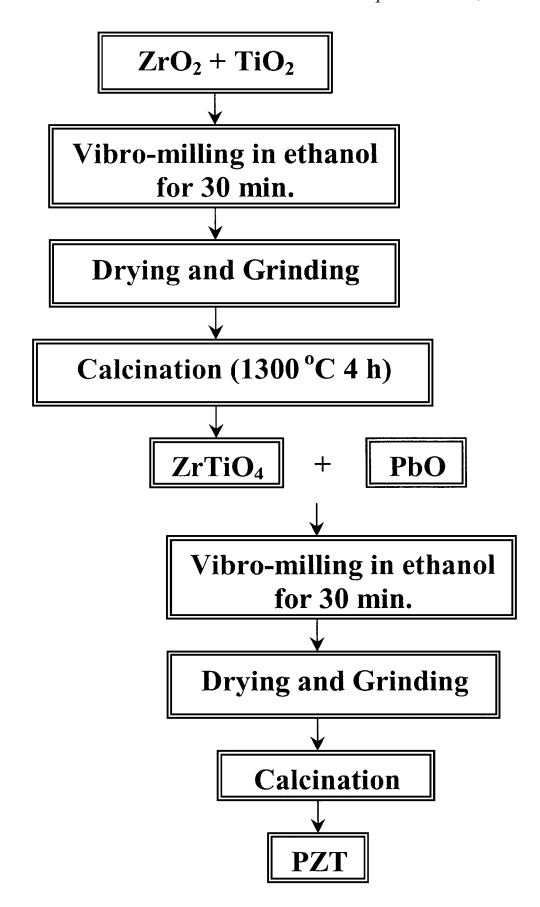


Fig. 1. Preparation route for the PZT powder.

could be attributed to its high reactivity with PbO. Whereas some workers have been prompted to investigate synthetic route different from the mixed oxide approach, e.g. sol-gel [13], hydrothermal [14], co-precipitation [15], and combustion [16], the overall aim of the work described here is to refine the two-stage mixed oxide method further. An attempt has been made to synthesis and investigate the PZT powders by employing an intermediate phase of zirconium titanate (ZrTiO₄) as a key precursor. The following elements are investigated in this connection: (a) development of a mod-

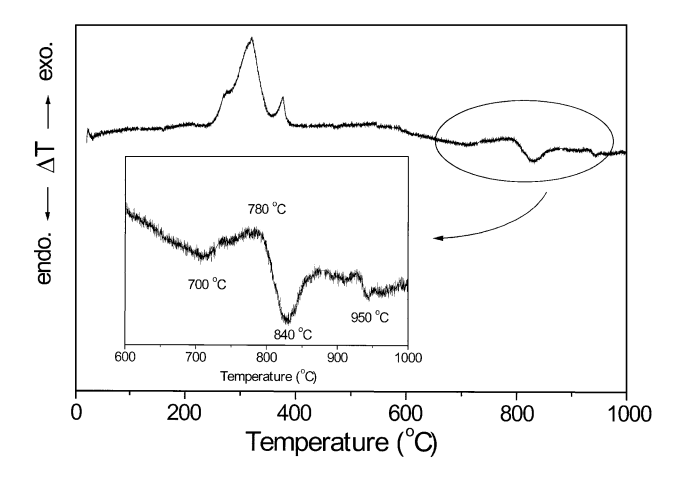


Fig. 2. A DTA curve for the mixture of PbO-ZrTiO₄ powder.

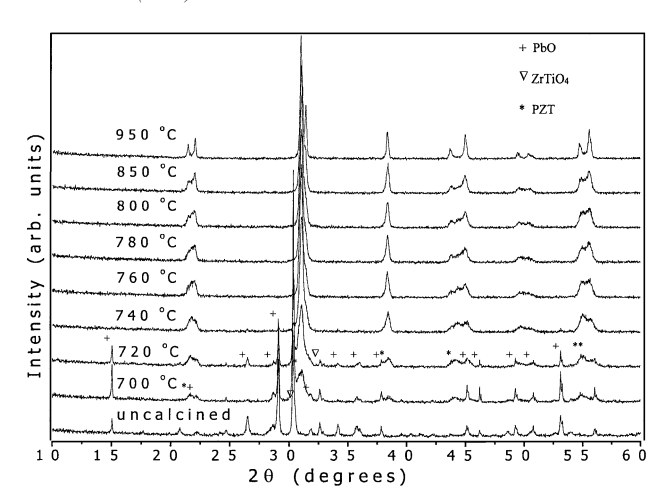


Fig. 3. Powder XRD patterns of the calcined powders at various calcinations temperatures for 2 h with heating/cooling rates of 20 $^{\circ}\mathrm{C}$ $\mathrm{min}^{-1}.$

ified mixed oxide synthetic route; (b) reproducibility of the method and (c) the ability to use laboratory grade chemical.

2. Experimental procedure

Pb($Zr_{0.5}Ti_{0.5}$)O₃ was synthesised by the solid state reaction of appropriate amounts of relatively inexpensive laboratory grade lead oxide, PbO, zirconium oxide, ZrO_2 and titanium oxide, TiO_2 (Fluka, >99% purity). The three oxide powders exhibited an average particle size in the range of 5.0-10.0 µm. The following reaction sequences are proposed for the formation of PZT:

$$ZrO_2(s) + TiO_2(s) \rightarrow ZrTiO_4(s)$$
 (1)

$$2PbO(s) + ZrTiO_4(s) \rightarrow 2Pb(Zr_{0.5}Ti_{0.5})O_3(s)$$
 (2)

Powder processing was carried out as shown schematically in Fig. 1. The methods of mixing, drying, grinding, firing

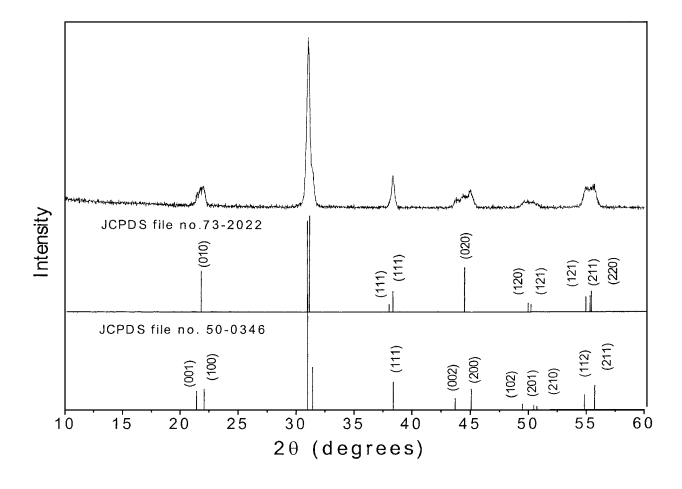


Fig. 4. Computerised JCPDS data-matching confirms the formation of both tetragonal and rhombohedral PZT phases in the calcined powder.

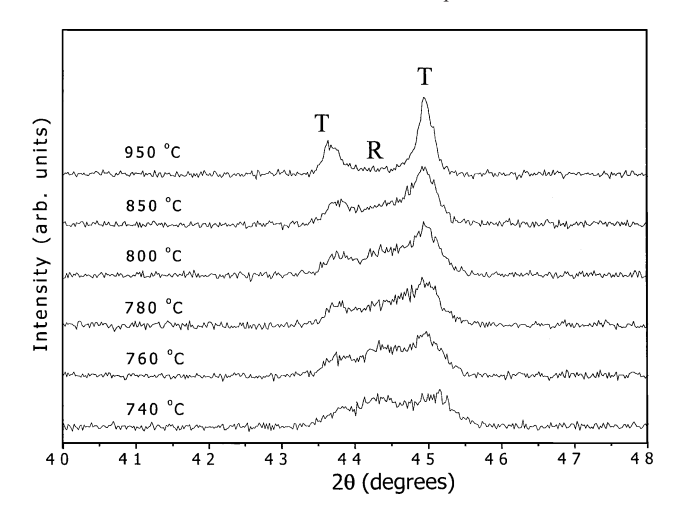


Fig. 5. Enlarged XRD peaks for the tetragonal (T) and rhombohedral (R) phases as a function of calcinations temperatures.

and sieving of the products were similar to those employed in the preparation of the perovskite-like PMN, PFN and LMN powders as described previously [17,18]. Various calcination conditions, i.e. temperatures ranging from 700 to 950 °C, soaking times ranging from 0.5 to 2 h and heating/cooling rates ranging from 5 to 20 °C min⁻¹, were selected, in order to investigate the formation of lead zirconate titanate. The reactions of the uncalcined PZT powders taking place during heat treatment were investigated by differential thermal analysis (DTA) (NETZSCH-Gerätebau Thermal Analysis STA 409) using a heating rate of 10 $^{\circ}\text{C min}^{-1}$ in air from room temperature up to 1000 °C. Calcined powders were subsequently examined by room temperature X-ray diffraction (XRD; Philips PW 1729 diffractometer) using CuK_{α} radiation, to identify the phases formed and optimum calcination conditions for the manufacture of perovskite PZT powder. Powder morphol-

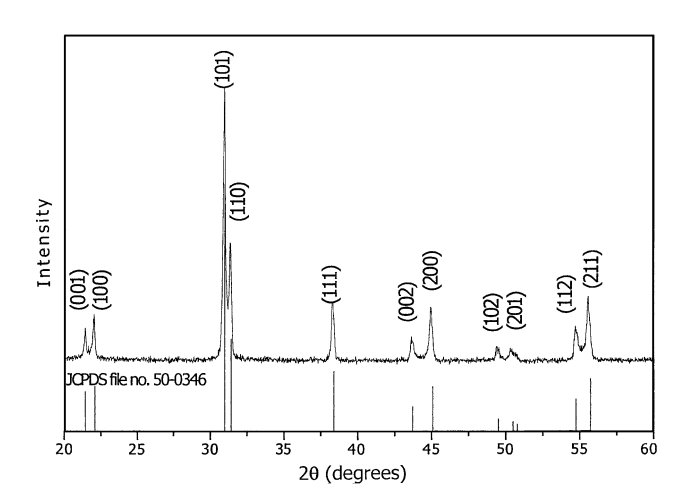


Fig. 6. Computerised JCPDS data-matching confirms the formation of the single-phase tetragonal PZT.

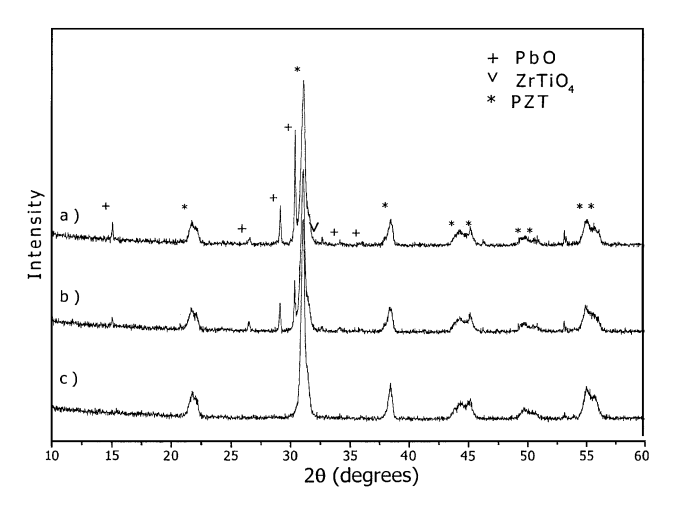


Fig. 7. Powder XRD patterns of the calcined powders at 760 $^{\circ}$ C with heating/cooling rates of 20 $^{\circ}$ C min⁻¹ for (a) 0.5 h, (b) 1 h and (c) 2 h.

ogies and grain sizes were directly imaged using scanning electron microscopy (SEM; JEOL JSM-840A).

3. Results and discussion

A DTA curve obtained for a powder mixed in the stoichiometric proportions of $Pb(Zr_{0.5}Ti_{0.5})O_3$ is shown in Fig. 2. In the temperature range $200-400\,^{\circ}C$, the sample shows several large exothermic peaks in the DTA curve. These DTA peaks can be attribute to the decomposition of the organic species from the milling process. The different temperature, intensities, and shapes of the thermal peaks probably are related to the different natures of the organic species and consequently, caused by the removal of species differently bounded in the network. In the temperature

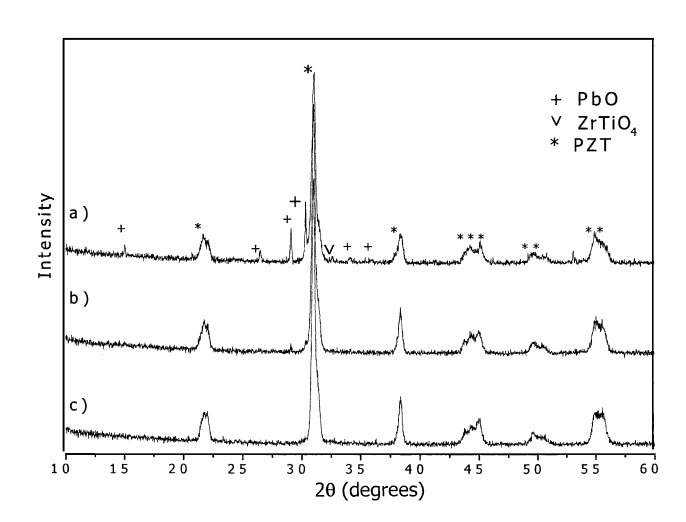


Fig. 8. Powder XRD patterns of the calcined powders at 760 °C for 2 h with heating/cooling rates of (a) 5 °C \min^{-1} , (b) 10 °C \min^{-1} and (c) 20 °C \min^{-1} .

Table 1
Calculated PZT phases as a function of calcination conditions

Calcination conditions			Qualitative concentrations of PZT phase		
Temperature (°C)	Time (h)	Rates (°C min ⁻¹)	Tetragonal (wt.%)	Rhombohedral (wt.%)	
700	2	20	*	*	
720	2	20	*	*	
740	2	20	*	*	
760	0.5	20	*	*	
760	1	20	*	*	
760	2	5	*	*	
760	2	10	*	*	
760	2	20	60	40	
780	2	20	64	36	
800	2	20	72	28	
850	2	20	79	21	
900	2	20	87	13	
950	2	20	100	0	

The estimated precision of the concentrations for the two phases is \pm 0.1%. *PZT, PbO and ZrTiO₄ phases were found and Eq. (3) is not valid.

range 700–1000 °C, both exothermic and endothermic peaks are observed in the DTA curve. The enlarge zone of this DTA curve showed that the exothermic peak centered at \sim 780 °C may result from perovskite phase crystallization, and the last endothermic peak centered at \sim 840 °C may be caused by the decomposition of lead oxide. These temperatures have been obtained from the

calibration of the sample thermocouple and were used to define the ranges of temperatures (700–950 $^{\circ}$ C), soaking time (0.5 to 2 h) and heating/cooling rates (5 to 20 $^{\circ}$ C min⁻¹) for the XRD investigation.

Powder XRD patterns of the calcined powders are given in Figs. 3-8, with the corresponding JCPDS patterns also shown. The optimum calcination temperature for the formation of a high purity PZT phase was found to be about 760 °C, i.e. slightly lower than the exothermic temperature in Fig. 2. In general, the strongest reflections apparent in the majority of the XRD patterns indicate the formation of two lead zirconate titanate phases. These can be matched with JCPDS file numbers 50-0346 and 73-2022 for the tetragonal $Pb(Zr_{0.44}Ti_{0.56})O_3$ and rhombohedral $Pb(Zr_{0.52}Ti_{0.48})O_3$ (Fig. 4), respectively. As is well known, the variations in composition may lead to a diffuse MPB between the tetragonal and rhombohedral PZT phases [19]. The most obvious different between the patterns for tetragonal and rhombohedral PZT phases concerns the presence of a splitting of (002)/(200) peak at two-theta $\sim 45^{\circ}$ for the former phase (Fig. 5).

It is seen that, with the exception of powder calcined at 950 °C, the rhombohedral PZT phase is always present in the product. Moreover, some additional weak reflections are found in the XRD patterns (marked by + and ∇), which correlate with the precursors PbO and ZrTiO₄, respectively. The relative amounts of the two majority PZT phases, i.e. tetragonal (T) and rhombohedral (R),

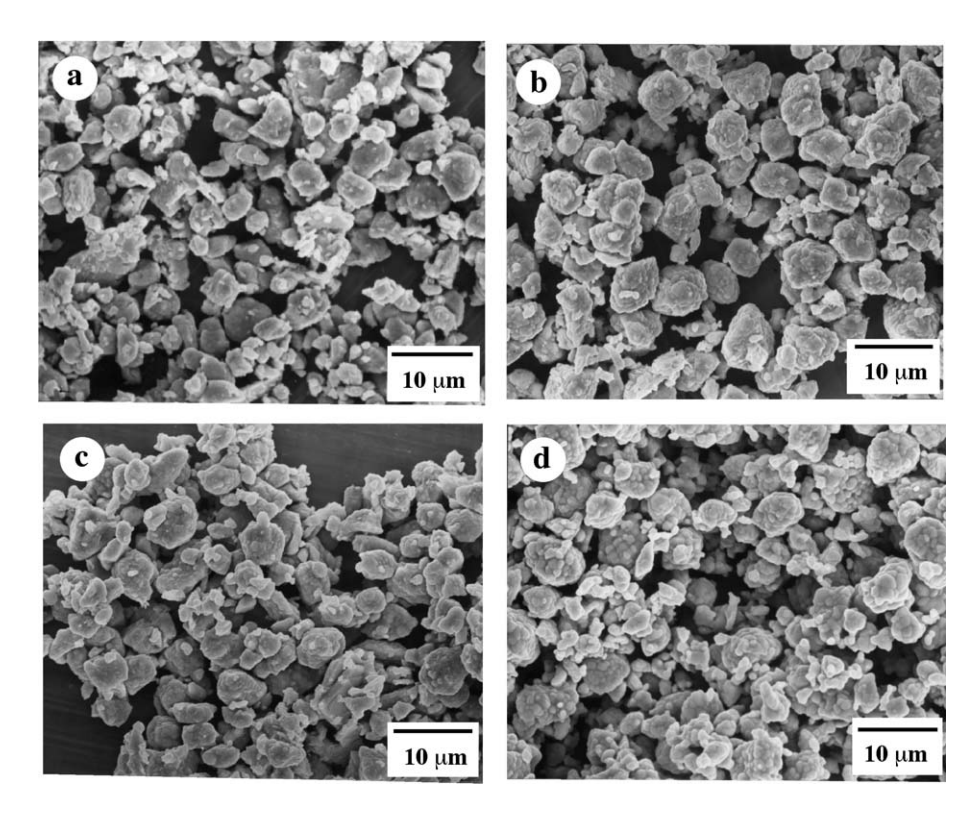


Fig. 9. SEM micrographs of the PZT powders calcined at (a) 700 $^{\circ}$ C, (b) 760 $^{\circ}$ C, (c) 850 $^{\circ}$ C and (d) 950 $^{\circ}$ C.

which are present in each calcined powder, may in principle, be calculated from the intensities of the most intense X-ray reflections:

wt.% tetragonal phase =
$$\left(\frac{I_{\rm T}}{I_{\rm T}+I_{\rm R}}\right) \times 100$$
 (3)

This equation is analogous to the well-known equation [11,16] widely employed in connection with the fabrication of complex perovskite materials. It should be seen as a first approximation since its applicability requires comparable maximum intensities of the peaks of tetragonal and rhombohedral phases. Here I_T and I_R refer to the intensities of the {200} tetragonal and {020} rhombohedral peaks. For the purpose of estimating the concentrations of the phases present, Eq. (3) has been applied to the powder XRD patterns obtained as given in Table 1. This study shows that minor amount of the unreacted PbO and ZrTiO₄ phases tends to co-exist along with the PZT phase, after scanning calcinations in the temperature range 700-740 °C. Upon calcination at 760°, the phases of PbO and ZrTiO₄ have been found completely disappear, and crystalline PZT of both tetragonal and rhombohedral is the only detectable phases in the powder. By increasing the calcination temperature from 760 to 950 °C, the yield of the tetragonal PZT phase increases significantly until at 950 °C, a single phase of tetragonal PZT is formed (Fig. 6). Neither lead titanate (PbTiO₃) or lead zirconate (PbZrO₃) earlier reported by Chakrabarti and Maiti [20] has been found in this study. It is also of interest to point out that no evidence has been obtained for the existence of pyrochlore phase Pb₂Ti₂O₇ reported by Babushkin et al. [21]. The effect of soaking time and heating/cooling rates on phase formation was found to be quite significant (Figs. 7 and 8). In this work, it is seen that the optimum soaking time and heating/cooling rates for the formation of a high purity PZT phase were found to be at 2 h and 20 °C min⁻¹, respectively. Therefore, XRD results clearly show that, in general, the methodology presented in this work provides a simple method for preparing perovskite PZT powders via a modified solidstate mixed oxide synthetic route without the addition of PbO in excess [22,23]. It is interesting to note that the use of zirconium titanate precursor together with the vibro-milling technique can effectively enhance the yield of the PZT phase.

The morphological changes in the PZT powders formed by a modified two-stage mixed oxide are illustrated in Fig. 9(a-d) as a function of formation temperature. After calcinations at 700 to 950 °C, the powders have similar morphology. They had spherical secondary particles composed of submicrometer-sized primary particulates. This structure is similar to that of BaTiO₃ powders synthesised by previous researchers [24]. The primary particles have sizes of $\sim 0.05-0.20~\mu m$, and the agglomerates measure $\sim 1.0-8.0~\mu m$. At 700 °C, three phases (PbO, ZrTiO₄ and

PZT) were observed in X-ray diffraction analysis (Fig. 3), but from the SEM micrograph (Fig. 9(a)), it was difficult to distinguish these three phases because of the lumpy particle morphology, indicating significant growth interaction in the multiphase composition. By increasing the calcination temperature from 700 to 850 °C, the mixture of both tetragonal and rhombohedral PZT phases with various sizes of irregular shaped particles (clusters) was observed (Fig. 9(b and c)). Upon further increases of temperature up to 950 °C, the tetragonal PZT phase with similar clusters was found (Fig. 9(d)). In general, this granule characteristic will offer an apparent advantage towards achieving a high sintered density and homogeneous microstructure for PZT ceramic at a reduced sintering temperature.

4. Conclusions

A modified, two-stage mixed oxide synthetic route for preparing high purity PZT powders has been developed, which show a high level of reproducibility. It represents significant time-savings compared to synthetic procedures currently advocated, and require only relatively impure and inexpensive laboratory-grade precursors, as long as the purity is higher than 99%. Evidence has been gained from XRD that a single phase of perovskite PZT powder has been obtained in this study by using a combination of zirconium titanate precursor, the vibro-milling technique together with a careful calcinations treatment.

Acknowledgements

This work was supported by the Thailand Research Fund (TRF). Thanks are also due to Dr. A. Niyompan and Mr. W. Prachamon, Department of Physics, Ubon Ratchatanee University for the helpful discussion on experimental technique.

References

- B. Jaffe, W.R. Cook, H. Jaffe, Piezoelectric Ceramics, Academic Press, New York, 1971.
- [2] A.J. Moulson, J.M. Herbert, Electroceramics, Chapman & Hall, New York, 1990.
- [3] R.C. Buchanan, Ceramic Materials for Electronics, Marcel Dekker, New York, 1991.
- [4] G.H. Haertling, J. Am. Ceram. Soc. 82 (1999) 797.
- [5] T.R. Shrout, P. Papet, S. Kim, G.S. Lee, J. Am. Ceram. Soc. 73 (1990) 1862.
- [6] B.V. Hiremath, A.I. Kingon, J.V. Biggers, J. Am. Ceram. Soc. 66 (1983) 790.
- [7] S. Mori, H. Mitsuda, K. Date, H. Hioki, T. Miyazawa, Natl. Tech. Rept. 10 (1964) 32.
- [8] W.M. Speri, PhD Thesis, Rutgers University NJ, 1969.
- [9] D.L. Hanky, J.V. Biggers, J. Am. Ceram. Soc. 12 (1981) 172.
- [10] S.S. Chandratreya, R.M. Fulrath, J.A. Pask, J. Am. Ceram. Soc. 64 (1981) 422.

- [11] S.L. Swartz, T.R. Shrout, Mat. Res. Bull. 17 (1982) 1245.
- [12] O. Babushkin, T. Lindback, J.C. Lue, J.Y.M. Leblais, J. Eur. Ceram. Soc. 16 (1996) 1293.
- [13] K. Yao, L. Zhang, X. Yao, J. Am. Ceram. Soc. 81 (1998) 1571.
- [14] J.Y. Choi, C.H. Kim, D.K. Kim, J. Am. Ceram. Soc. 81 (1998) 1353.
- [15] J.H. Choy, Y.S. Han, S.J. Kim, J. Mater. Chem. 7 (1997) 1807.
- [16] M. Maria, A. Sekar, K.C. Patil, J. Mater. Chem. 2 (1992) 739.
- [17] S. Ananta, N.W. Thomas, J. Eur. Ceram. Soc. 19 (1999) 155.
- [18] S. Ananta, R. Brydson, N.W. Thomas, J. Eur. Ceram. Soc. 20 (2000) 2315.
- [19] A.K. Arora, R.P. Tandon, A. Mansingh, Ferroelectrics 132 (1992) 9.
- [20] N. Chakrabarti, H.S. Maiti, Mater. Lett. 30 (1997) 169.
- [21] O. Babushkin, T. Lindback, K. Brooks, N. Setter, J. Eur. Ceram. Soc. 17 (1997) 813.
- [22] H.C. Wang, W.A. Schulze, J. Am. Ceram. Soc. 73 (1990) 825.
- [23] J. Chen, M.P. Harmer, D.M. Smyth, J. Appl. Phys. 76 (1994) 5394.
- [24] H. Chazono, H. Kishi, J. Am. Ceram. Soc. 83 (2000) 101.



Available online at www.sciencedirect.com



Current Applied Physics 6 (2006) 307-311



www.elsevier.com/locate/cap www.kps.or.kr

Phase formation and transitions in the lead magnesium niobate—lead zirconate titanate system

R. Tipakontitikul, S. Ananta *, R. Yimnirun

Department of Physics, Faculty of Science, Chiang Mai University, Chiang Mai 50200, Thailand

Available online 22 December 2005

Abstract

The phase formation and transition mechanism of perovskite ceramics in the $(1-x)Pb(Mg_{0.33}Nb_{0.66})O_3$ — $xPb(Zr_{0.52}Ti_{0.48})O_3$, (1-x)PMN—xPZT system prepared by a modified mixed-oxide synthetic route have been investigated for various chemical compositions and firing temperatures. Lattice parameter changes were examined as a function of composition. It is seen that perovskite phases undergo the transitions (pseudo)cubic to tetragonal in the x value range 0.0–1.0. The degree of tetragonality and average lattice parameters were found to increase with PZT content across the whole solid solution range. © 2005 Elsevier B.V. All rights reserved.

PACS: 77.84.-S; 61.10.Nz; 77.80.Bh

Keywords: Ferroelectric materials; X-ray diffraction; Phase transition

1. Introduction

Lead magnesium niobate, Pb(Mg_{0.33}Nb_{0.67})O₃ or PMN, is one of the perovskite-type relaxor ferroelectrics which have been investigated extensively as potential candidates for electroceramic components such as multilayer ceramic capacitors and electrostrictive actuators [1–3]. It exhibits diffuse phase transition phenomena at room temperature with low loss and non-hysteretic characteristics [4,5]. PMN has been studied extensively from the late 80's in solid solutions with PbTiO₃ (PT) which are of interest because of their high dielectric constant, range of Curie temperatures and superior electrostrictive response [1–3]. By contrast, the normal ferroelectric compound lead zirconate titanate, Pb(Zr, Ti)O₃ or PZT, is a representative perovskite ferroelectric and piezoelectric prototype because of its sharp phase transition mode with excellent pyroelectric and piezoelectric properties [6,7]. Therefore, it is one of the most widely studied piezoelectric compounds for ferroelectric memories, optoelectronics, electrostrictive actuators, and electromechanical transducers [3,8]. However, despite the many previous studies of the synthesis and characterization of these perovskite ferroelectric materials [5–8], the synthesis and phase formation of the whole series of the solid solutions in the PMN–PZT system has rarely been studied. Systematic investigation of these materials is required for a better understanding of phase development in (1-x)PMN–xPZT solid solutions. In the present work, therefore, the phase formation and transition mechanisms in the (1-x)PMN–xPZT system (x=0.0-1.0) are examined as a function of chemical composition and firing temperature. The relationships between these experimental results are discussed.

2. Experimental

The B-site precursor method [4,9] was used to prepare powders of composition $(1-x)Pb(Mg_{0.33}Nb_{0.67})O_3-xPb(Zr_{0.52}Ti_{0.48})O_3$ or (1-x)PMN-xPZT, where x=0.0, 0.1, 0.3, 0.5, 0.7, 0.9 and 1.0. The raw materials were the reagent grade oxides PbO, MgO, Nb₂O₅, ZrO₂, and TiO₂

^{*} Corresponding author. Tel.: +66 53 943367; fax: +66 53 357512. E-mail address: supon@chiangmai.ac.th (S. Ananta).

(Fluka, >99% purity). These oxide powders exhibited an average particle size in the range 3.0–5.0 μm. Ceramic-processing was carried out via the B-site precursor method shown schematically in Fig. 1. For the preparation of the lead magnesium niobate end member, the columbite precursor MgNb₂O₆ [10] was synthesized and calcined at 1050 °C for 2 h, then ball-milled with PbO for 24 h, dried, calcined at 750 °C for 2 h in air and sieved into fine powder. The PZT powder was then prepared by employing zirconium titanate (ZrTiO₄) precursor [11] in order to minimise the formation of undesired pyrochlore phases. The intermediate B-site precursor phases of ZrTiO₄ were first prepared by employing a procedure outline earlier

(calcined at $1300\,^{\circ}\text{C}$ for 4 h) [9]. PbO was then added to the calcined ZrTiO₄ precursor, wet-milled, dried and calcined at $900\,^{\circ}\text{C}$ for 2 h to form another end component, PZT [9]. The (1-x)PMN-xPZT powders were then formulated from PMN and PZT components by employing the similar mixed-oxide procedure. Each composition was mixed with an aqueous solution (3 wt.%) of polyvinyl alcohol, pressed isostatically into pellets at 100 MPa and sintered at $1100-1320\,^{\circ}\text{C}$ in air for 4 h in a closed alumina cricible. In order to maintain a lead atmosphere during the firing process, samples were embedded in powders of identical composition. X-ray diffraction (XRD; Philips PW 1729 diffractometer) using CuK α radiation was used

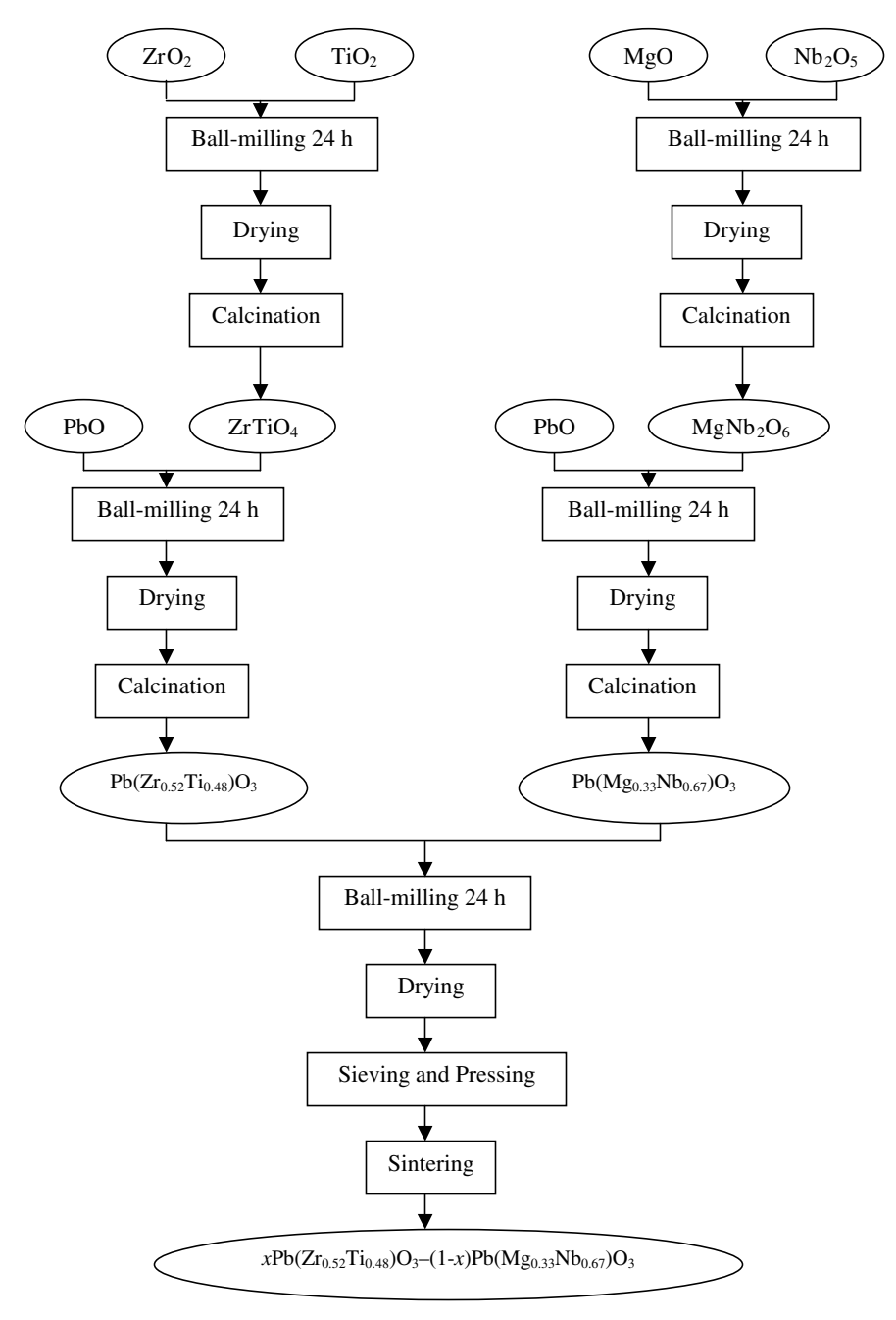


Fig. 1. Preparation route for the (1 - x)PMN-xPZT ceramics.

to determine the phases formed and optimum firing temperatures for the formation of desired phase. Lattice parameters of the perovskite phases were determined by Cohen's method in conjunction with the least squares method [12].

3. Results and discussion

X-ray diffraction patterns of (1 - x)PMN-xPZT ceramics sintered at various temperatures are given in Fig. 2, indicating the formation of both perovskite and pyrochlore phases in each composition. In this study, it is evident that except at x = 0.1, complete crystalline solid solution of the perovskite structure occurred throughout the whole compositional range of the (1 - x)PMN-xPZT system. Although the effectiveness of the B-site precursor method in suppressing pyrochlore formation during perovskite development in lead-based perovskite systems has been reported by several researchers [1–6], in the work reported here, small amounts of a second phase (*) correlating with a pyrochlore phase of Pb_{1.83}Mg_{0.29}Nb_{1.71}O_{6.39} (JCPDS file no. 33-769) [4] could be detected by XRD in the composition x = 0.1. This can be attributed to poor homogeneity due to the limitations of mixed-oxide processing especially with respect to the ball-milling and the volatility of PbO at high firing temperatures. For x = 0.0 (pure PMN), the Xray diffraction pattern shows only a single (200) peak, confirming its (pseudo)cubic symmetry at room temperature, in good agreement with reports of other workers [5,13]. When the x value increases to 0.3, the broadened peaks especially at $2\theta \sim 44.5^{\circ}-45^{\circ}$ show that the distortion of the (pseudo)cubic lattice is enlarged. At x = 0.5, the structure transforms to the tetragonal phase because of lattice deformation, which is characterized by splitting of the (002)/(200) peaks at about 44°-45° 2θ (Fig. 3). On increasing the PZT content, the intensity ratio of the (002)/(200) peaks tends to increase until at x = 1.0, where the peaks match that of piezoelectric PZT. The variation of these doublet-diffraction lines as a function of PZT content can be explained by microscopic compositional fluctuations occurring in these perovskite materials, which cannot provide real homogeneity in the solid solutions, and also by the different stresses induced in the particles, which determine the existence of tetragonal ferroelectric phases [14].

The lattice parameters of the perovskite phase calculated from the XRD data are plotted as a function of PZT content (Fig. 4), together with the tetragonality factor (or axial ratio of c/a) and average lattice parameters of $(a^2c)^{1/3}$. The parameters of (pseudo)cubic PMN (x=0.0) and tetragonal PZT (x=1.0) are 0.4046 nm, and a=0.4033 and

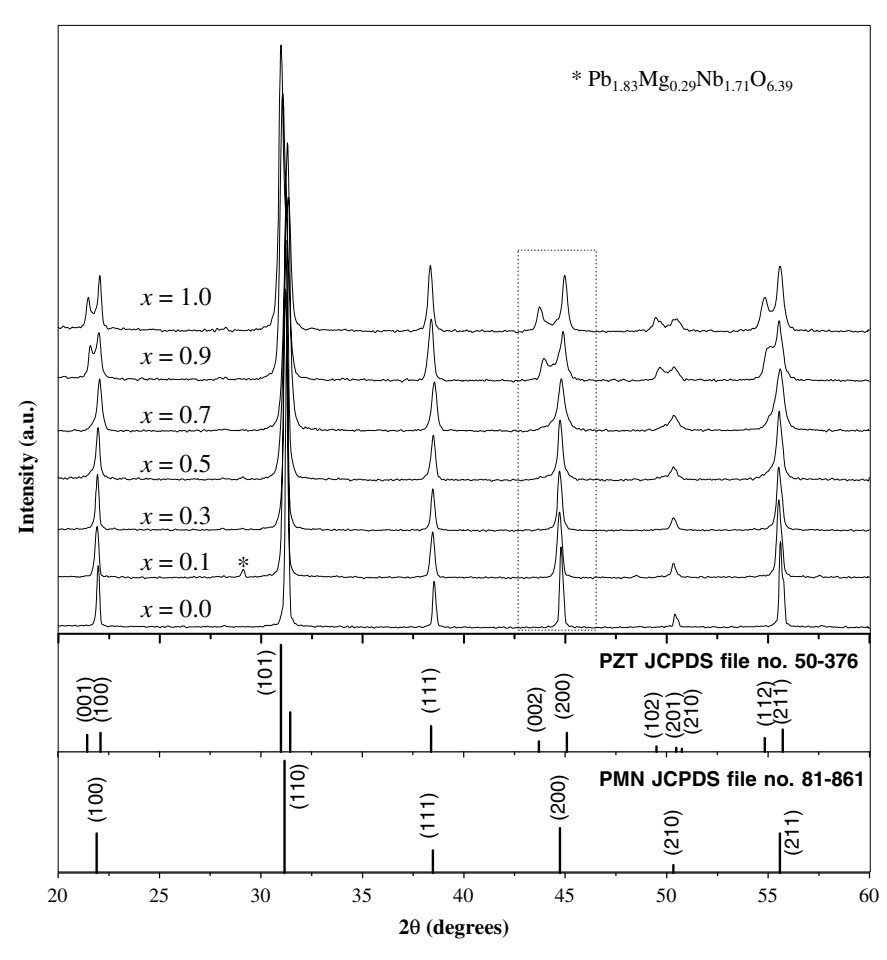


Fig. 2. XRD pattern of the (1 - x)PMN–xPZT ceramics after sintering at the optimum conditions.

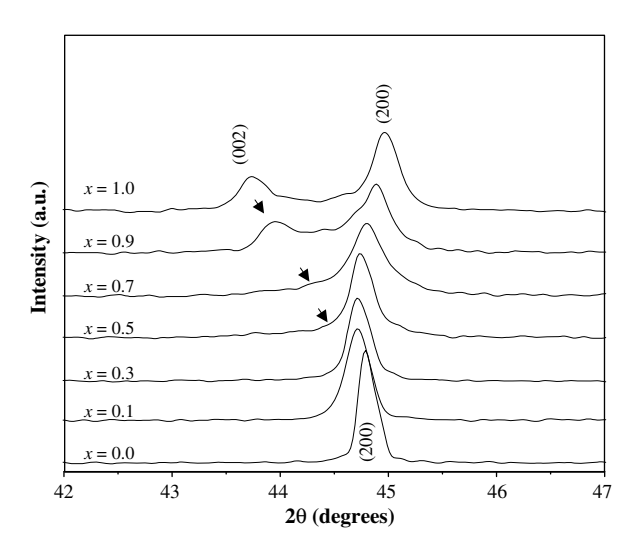


Fig. 3. XRD pattern of the (1 - x)PMN–xPZT ceramics, showing doublets (002)T and (200)T.

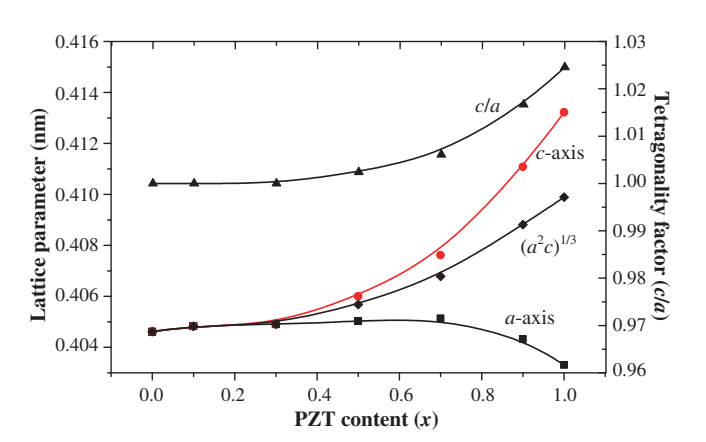


Fig. 4. Variation of cell parameters in the (1 - x)PMN-xPZT system.

c = 0.4132 nm, respectively, consistent with reported data (JCPDS file nos. 81-861 and 50-376) [15,16]. The results of the cell refinement show that all the PMN-PZT compositions with PZT contents in the range between x = 0.0 and x = 0.4 have single phase (pseudo)cubic symmetry, with cell parameters depending on the PZT content. At x = 0.5, however, peak splitting is detected (Fig. 3), with a = 0.4050 and c = 0.4060 nm, and c/a = 1.0024. From the crystallographic analyses, therefore, the phase boundary between the (pseudo)cubic and tetragonal symmetries seems to be located at x = 0.4–0.5. However, this real composition boundary could not be determined under the present experimental limit of accuracy. The possible range of compositions for further studies is $0.4 \le x \le 0.5$. High resolution XRD analysis is necessary to detect the possible superposition of phases and to restrict the range of compositions for a better characterization of the PMN-PZT compositions in the range of structural change.

With further increases in x, the a-axis shrinks while the c-axis expands continuously at approximately similar rates. Consequently, the values of $(a^2c)^{1/3}$ increase slowly, while the axial ratios of c/a increase rapidly to 1.0245. By com-

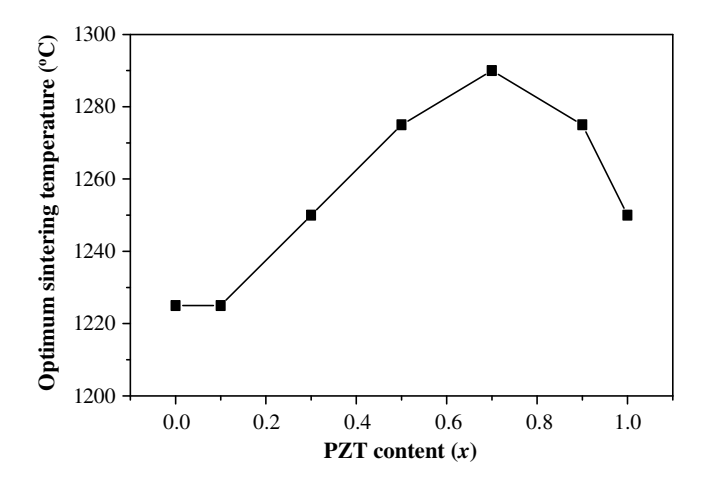


Fig. 5. Variation of the optimum sintering temperature as a function of PZT content

paring the B-site cation sizes of PMN and PZT [1], the continuous increase in the average lattice parameter (from 0.4046 nm at x=0.0–0.4098 nm at x=1.0) can be well understood, in terms of the formation of complete crystalline solid solutions of a perovskite structure. In our experiments, the lattice parameters calculated from the diffraction data indicate that the c/a axial ratio increases as the PZT content (x) increases. Fig. 5 shows the variation of the optimum firing temperature (where maximum yields of perovskite phase and density were obtained) as a function of PZT content. Relative densities of the sintered samples were \sim 95–98% of the theoretical values.

4. Conclusions

The phase formation and transition mechanism of perovskite PMN–PZT ceramics has been investigated for various chemical compositions and firing temperatures. X-ray diffraction has indicated that except at x=0.1, complete solid solutions occur across the entire compositional range of the (1-x)Pb(Mg_{0.33}Nb_{0.67})O₃–xPb(Zr_{0.52}Ti_{0.48})O₃ system. Lattice parameters of the (pseudo)cubic phase and of the tetragonal phase were found to vary with chemical composition. The degree of tetragonality and average lattice parameters increased continuously with increasing PZT content.

Acknowledgements

This work was supported by the Thailand Reseach Fund (TRF). One of the authors (R.T.) wishes to thank Ubon Ratjatanee University, the Ministry of University Affair and the Graduate School, Chiang Mai University for the support.

References

- [1] A.J. Moulson, J.M. Herbert, Electroceramics, second ed., Wiley, Chichester, 2003.
- [2] G.H. Haertling, J. Am. Ceram. Soc. 82 (1999) 797.

- [3] K. Uchino, Acta Mater. 46 (1998) 3745.
- [4] S. Ananta, N.W. Thomas, J. Eur. Ceram. Soc. 19 (1999) 629.
- [5] Y.C. Liou, J.H. Chen, Ceram. Int. 30 (2004) 17.
- [6] R. Yimnirun, S. Ananta, E. Meechoowas, S. Wongsaenmai, J. Phys. D: Appl. Phys. 36 (2003) 1615.
- [7] C.H. Wang, Ceram. Int. 30 (2004) 605.
- [8] R. Yimnirun, S. Ananta, P. Laoratanakul, Mater. Sci. Eng. B 112 (2004) 79.
- [9] R. Tipakontitikul, S. Ananta, Mater. Lett. 58 (2004) 449.
- [10] S. Ananta, Mater. Lett. 58 (2004) 2781.

- [11] S. Ananta, R. Tipakontitikul, T. Tunkasiri, Mater. Lett. 57 (2003) 2637.
- [12] B.D. Cullity, Elements of X-ray diffraction, Addison-Wesley, New York, 1978, pp. 363–367.
- [13] C. Lei, K. Chen, X. Zhang, Mater. Sci. Eng. B 111 (2004) 107.
- [14] A. Boutarfaia, S.E. Bouaoud, Ceram. Int. 22 (1996) 281.
- [15] Powder diffraction file no. 81-861. International Centre for Diffraction Data, Newton Square, PA, 2000.
- [16] Powder diffraction file no. 50-376. International Centre for Diffraction Data, Newton Square, PA, 2000.

ARTICLE IN PRESS



Available online at www.sciencedirect.com



materials letters

Materials Letters xx (2006) xxx-xxx

www.elsevier.com/locate/matlet

One-pot hydrothermal synthesis of highly dispersed, phase-pure and stoichiometric lead zirconate

Apinpus Rujiwatra ^{a,*}, Saowalak Tapala ^a, Sanchai Luachan ^a, Orawan Khamman ^b, Supon Ananta ^b

^a Inorganic Materials Research Unit, Department of Chemistry, Faculty of Science, Chiang Mai University, Chiang Mai 50200, Thailand
^b Department of Physics, Faculty of Science, Chiang Mai University, Chiang Mai 50200, Thailand

Received 7 January 2006; accepted 3 February 2006

Abstract

Phase-pure and stoichiometric lead zirconate powders consisting of submicro- to micrometer-sized particles were successfully synthesized via a simple, one-pot hydrothermal technique at moderate temperatures and short reaction times. High concentration of potassium hydroxide mineralizer was necessary in the formation of well-crystalline lead zirconate. The type of zirconium precursor, reaction temperature and time showed apparent influences over particle shape, size and distribution. Transmission electron microscope was used to confirm the crystallographic setting of the prepared lead zirconate.

© 2006 Elsevier B.V. All rights reserved.

Keywords: Lead zirconate; Perovskite; Hydrothermal synthesis; Piezoelectric materials

1. Introduction

Lead zirconate, (PbZrO₃, PZ) is an important material used in both energy storage application for DC field, and in making a series of solid solutions e.g. Pb(Zr,Ti)O₃, PbZrO₃-Pb(Mg_{1/3} $Nb_{2/3}O_3$ and $PbZrO_3-PbTiO_3-Pb(Fe_{1/5}Nb_{1/5}Sb_{3/5})O_3$, all of which found tremendous applications in electroceramic industries e.g. piezoelectric sensors, transducers, actuators, pyroelectric detectors, resonators and electro-optic devices [1-3]. The double hysteresis behavior observed for PZ has also made this material a potential candidate for microelectronic and microelectromechanical systems (MEMS) [4-6]. In all of these applications, phase purity and stoichiometry of the material are known to be of importance to ensure the performance of the devices [7]. The study on the preparation of phase-pure and stoichiometric PZ therefore has been of immense interest. The preparation of highly dispersed, homogeneous and well-defined crystals of PZ has been known to be even more challenging. Beside the conventional solid state reaction, there are various chemical techniques employed for the preparation of PZ powder, such as sol-gel, co-precipitation, citrate combustion, and the

most widely used molecular precursors, all of which have certain limitations e.g. costly starting reagents, multiphasic products and inability in shape and size control [8–10]. Hydrothermal synthesis although has been proved to be the most

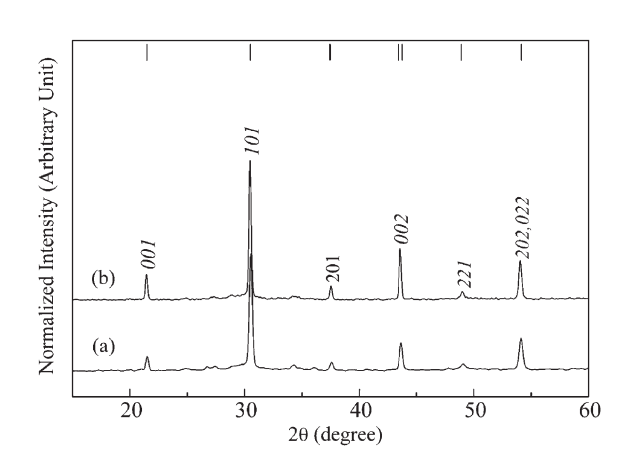


Fig. 1. Powder X-ray diffraction pattern of PZ powders obtained from the reactions between (A) $Pb(NO_3)_2$ and $Zr(NO_3)_2 \cdot 6H_2O$, and (B) $Pb(NO_3)_2$ and $ZrO(NO_3)_2 \cdot H_2O$ in 6 mol dm⁻³ KOH(aq) solution at 180 °C for 24 h. The solid lines indicating theoretical peak positions in orthorhombic *Pbma* with corresponding hkl indices are also shown.

^{*} Corresponding author. Tel.: +66 53 941906; fax: +66 53 892277. E-mail address: apinpus@chiangmai.ac.th (A. Rujiwatra).

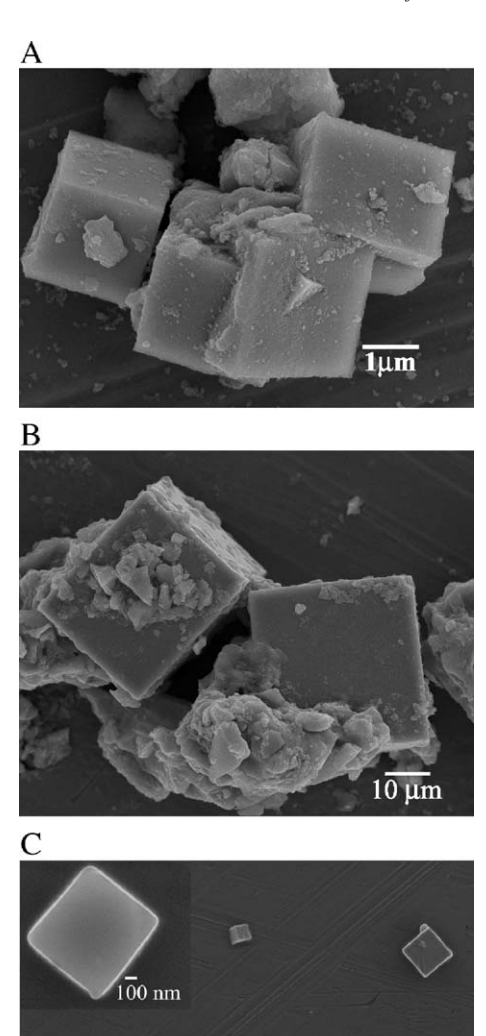


Fig. 2. Scanning electron micrographs of PZ particles obtained from the reactions using (A) $Zr(NO_3)_4\cdot 6H_2O$ at $180\,^{\circ}C$ for 24h, (B) $ZrO(NO_3)_2\cdot 6H_2O$ at $200\,^{\circ}C$ for 24h and (C) $ZrO(NO_3)_2\cdot 6H_2O$ at $200\,^{\circ}C$ for 72h.

10 μm

simplest and cost-effective chemical technique in the preparation of the relevant materials, such as lead titanate (PT) [11], lead titanate zirconate (PZT) [12] and lanthanum-modified PZT (PLZT) [13,14], there is no earlier report on the successful application of this preparative technique in the case of PZ. Here the hydrothermal technique was successfully applied for the preparation of highly dispersed, phase-pure and stoichiometric PZ in a high yield at low temperatures and short reaction times.

2. Experimental procedure

Stoichiometric mixtures of lead(II) nitrate $\{Pb(NO_3)_2, 99.0\%$ Univar $\}$ and either zirconium(IV) nitrate hydrate $\{Zr(NO_3)_4\cdot 6H_2O, 99.0\%$ PROLABO $\}$ or zirconyl nitrate hydrate $\{ZrO(NO_3)_2\cdot 6H_2O, 99.0\%$ Aldrich $\}$ were prepared in aqueous medium. The potassium hydroxide pellets (KOH, 85% Merck)

were then added to the mixtures making up to 6 mol dm⁻³, and thereby the pH of 14. The reaction mixtures were stirred at ambient temperature for 2 h before transferred to a hydrothermal autoclave with 70% filling factor. The hydrothermal reactions were performed under autogenous pressure at the temperatures between 180–200 °C for varied reaction times ranging from 24 to 72 h. The solid products were recovered by filtration and washed with deionized water until the pH of the filtrate was 7 in order to

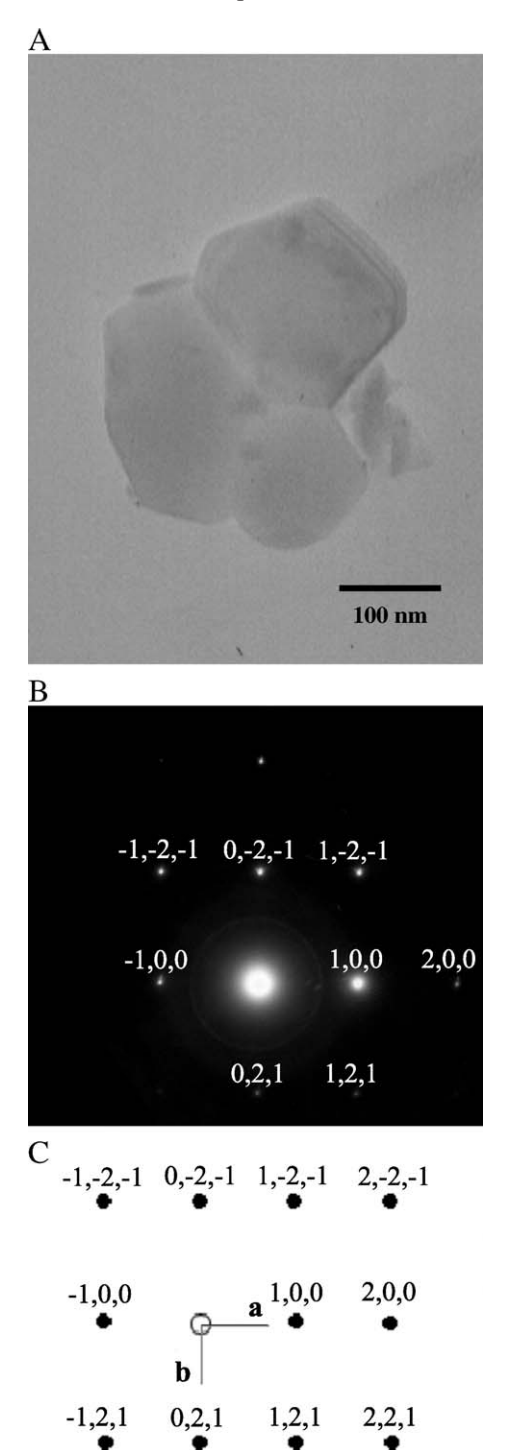


Fig. 3. (A) A TEM image taken from selected PZ nanoparticles and (B) a corresponding SAED pattern (sai[[0-12] zone axis) compared with (C) a reciprocal lattice pattern simulated based on the orthorhombic Pbma.

remove any remaining hydroxide species on the surface of the powders. Powder X-ray diffractometer (Bruker D8 Advance, CuK_{α} , Ni filter, $\lambda = 1.540598\,\text{Å}$, $40\,\text{kV}$, $30\,\text{mA}$) was used to characterize the crystalline solid products, and a field emission scanning electron microscope (JEOL JSM-6335F) equipped with an energy dispersive X-ray spectroscopic microanalyzer was employed in the investigation of morphology and elemental composition of the solids. The transmission electron microscope (TEM, JEOL JEM-2010) was used to confirm the crystallographic setting of the powder samples, which were dispersed in a solvent before deposited onto 3 mm copper-grids supported transparent carbon foil. The particle size of the powders was determined by particle sizer (CILAS 1064 Liquid, 0.04–500.00 μ m/100 Classes) using water as a liquid medium.

3. Results and discussion

Every reaction between Pb(NO₃)₂ and either Zr(NO₃)₄·6H₂O or ZrO(NO₃)₂·6H₂O with equimolar ratio of Pb: Zr in an aqueous medium with KOH as a mineralizer at temperatures as low as 180-200 °C under the investigated hydrothermal conditions provided the off-white powder products. The weight percentages of the synthesized powders were higher than 90%, in relative to the theoretical mass, in every case. They were identified by powder X-ray diffraction to be well-crystalline and phase-pure PZ, suggesting no further heat treatment was necessary. Fig. 1 shows typical powder X-ray diffraction patterns of the synthesized PZ powders. Every peak in Fig. 1 could be indexed in orthorhombic *Pbma* [15] with refined cell parameters a=b=5.88(6) Å and c=4.27(3)Å, indicating the absence of multiphasic problem, commonly encountered by the other preparative techniques [16]. Due to structural studies reported earlier [17], orthorhombic is the most stable phase for PZ at ambient conditions, although the unit cells can be indexed in different space groups. It is noticeable that PZ yielded from the hydrothermal reactions reported here was formed in a different space group than the commonly reported P2cb [18] and Pba2 [19]. The presence of KOH at high concentration, i.e. 6 mold m⁻³ in this study, was apparently necessary in all cases for the formation of well crystalline PZ, which was shown to form only after a short reaction time of 24h at 200°C. White gel, which was amorphous to powder X-ray diffraction, was observed when the KOH(aq) solution concentration was less than $6 \mod m^{-3}$.

Scanning electron micrographs revealed well-defined cubic morphology of the synthesized PZ particles in submicron to micron sizes as exemplified in Fig. 2. These particles were present as either the agglomerates or well-dispersed single particles depending on the zirconium sources as well as the synthetic conditions, i.e. reaction temperature and time. This is an intrigued result due to the well-known fact that to obtain ceramic powders consisting of mostly monodispersed particles is hardly achieved [20]. Although less reaction time was required for the well-crystalline PZ with well-defined cubic morphology to form if ZrO(NO₃)₄·6H₂O was used as zirconium source at 180 °C, the reaction of Pb(NO₃)₂ with ZrO(NO₃)₂·6H₂O at 200 °C for 72h provided the best cubic particles of PZ which mostly dispersed as single particles rather than as the agglomerates (Fig. 2(C)). The PZ particle sizes were determined to be well distributed in a narrow range, between ca. 5–15 μm with an average diameter of ca. 7.5 μm, although small particles of nanometer scale were also occasionally observed from the scanning electron micrographs.

The difficulties in achieving the PZ powders with equimolar Pb:Zr stoichiometry has been pronounced by other preparative techniques

[18]. The hydrothermally synthesized PZ powders were however revealed by energy dispersive X-ray microanalyzer to possess equimolar ratio of Pb:Zr, indicating the potential of this preparative technique in controlling the reaction stoichiometry.

Bright field TEM images of typical nanoparticles of the PZ powders were taken and shown in Fig. 3(A). By using selected area electron diffraction (SAED) method, the crystallographic setting of the PZ was analyzed and confirmed to be *Pbma*, which was well agreed with the powder XRD results. It is also intriguing to note the advantage of TEM in identifying the presence of nanoparticles in the bulk samples, which were otherwise hardly observed due to the limitation of both the particle sizer and the SEM experiments. The presence of both microand nanoparticles suggests the potential of this technique in the preparation of PZ nanoparticles.

4. Conclusion

In the present study, the successful preparation of phase-pure and stoichiometric PZ under moderate hydrothermal conditions at short reaction times was reported. The optimal hydrothermal conditions under the investigation afforded the PZ particles with discrete shape and size in a highly dispersed fashion, suggesting the potential controllability of the synthetic technique over the powders' intrinsic characteristics, and thereby the performance of the ceramic products.

Acknowledgements

The authors thank the Thailand Research Fund (TRF) and Nanoscience and Nanotechnology Center, Chiang Mai University, for financial supports.

References

- K. Uchino, Piezoelectrics and Ultrasonic Applications, Kluwer, Deventer, 1998
- [2] B. Jaffe, W.R. Cook Jr., H. Jaffe, Piezoelectric Ceramics, Academic Press, London, 1971.
- [3] D.M. Ibrahim, H.W. Hennike, Trans. J. Br. Ceram. Soc. 80 (1981) 18.
- [4] K. Singh, Ferroelectrics 94 (1989) 433.
- [5] B.P. Pokharel, D. Pandey, J. Appl. Phys. 86 (1999) 3327.
- [6] G.H. Haertling, J. Am. Ceram. Soc. 82 (1999) 797.
- [7] A.J. Moulson, J.M. Herbert, Electroceramics, 2nd ed.Wiley, New York, 2003.
- [8] E.E. Oren, E. Taspinar, A.C. Tas, J. Am. Ceram. Soc. 80 (1997) 2714.
- [9] Y.S. Rao, C.S. Sunandana, J. Mater. Sci. Lett. 11 (1992) 595.
- [10] V.B. Reddy, P.N. Mehrotra, J. Anal. Appl. Pyrolysis 2 (1980) 225.
- [11] A. Rujiwatra, J. Jongphiphan, S. Ananta, Mater. Lett. 59 (2005) 1871.
- [12] Y. Deng, L. Liu, Y. Cheng, C. Nan, S. Zhao, Mater. Lett. 11 (2003) 1675.
- [13] S. Cho, M. Oledzka, R.E. Riman, J. Cryst. Growth 226 (2001) 313.
- [14] M. Traianidis, C. Courtois, A. Leriche, J. Eur. Ceram. Soc. 20 (2000) 2713.
 [15] V.A. Shuvaeva, M.Y. Antipin, O.E. Fesenko, V.G. Smotrakov, T.U. Struchkov, Kristallografiya 37 (1992) 1033.
- [16] K.K. Li, F. Wang, G.H. Haertling, J. Mater. Sci. 30 (1995) 1386.
- [17] I.M. Reaney, A. Glazounov, F. Chu, A. Bell, N. Setter, British Cream. Trans. 96 (1997) 217.
- [18] S.D. Pradhan, S.D. Sathaye, K.R. Patil, A. Mitra, Mater. Lett. 48 (2001) 351.
- [19] Y. Kobayashi, S. Endo, L.C. Ming, K. Deguchi, T. Ashida, H. Fujishita, J. Phys. Chem. Solids 60 (1999) 57.
- [20] R.M. Piticescu, A.M. Moisin, D. Taloia, V. Badilit, I. Soare, J. Eur. Ceram. Soc. 24 (2004) 931.

Elsevier Editorial System(tm) for Materials Letters
Manuscript Draft
Manuscript Number:
Title: Effect of Vibro-Milling Time on Phase Formation and Particle Size of Lead Zirconate Nanopowders
Article Type: Letter
Section/Category:
Keywords:
Corresponding Author: Dr. Supon Ananta, PhD
Corresponding Author's Institution: Chiang Mai University
First Author: Orawan Khamman, MS
Order of Authors: Orawan Khamman, MS; Wanwilai Chaisan, MS; Rattikorn Yimnirun, PhD; Supon Ananta,

Manuscript Region of Origin:

PhD

Abstract: A perovskite phase of lead zirconate, PbZrO3, nanopowder was synthesized by a solid-state reaction via a rapid vibro-milling technique. The effect of milling time on the phase formation and particle size of PbZrO3 powder was investigated. Powder samples were characterized using TG-DTA, XRD, SEM and laser diffraction techniques. It was found that an average particle size of 50 nm was achieved at 25 h of vibro-milling after which a higher degree of particle agglomeration was observed on continuation of milling to 35 h. In addition, by employing an appropriate choice of the milling time, a narrow particle size distribution curve was also observed.

Manuscript: Text only

Corresponding author:

Dr. S. Ananta

Department of Physics

Faculty of Science

Chiang Mai University

Chiang Mai 50200 Thailand

Tel: (00) 53 943367; fax: (00) 53 943445

E-mail: suponananta@yahoo.com

Effect of Vibro-Milling Time on Phase Formation and Particle Size

of Lead Zirconate Nanopowders

O. Khamman, W. Chaisan, R. Yimnirun and S. Ananta*

Department of Physics, Faculty of Science, Chiang Mai University, Chiang Mai

50200, Thailand

Abstract

A perovskite phase of lead zirconate, PbZrO₃, nanopowder was

synthesized by a solid-state reaction via a rapid vibro-milling technique. The

effect of milling time on the phase formation and particle size of PbZrO3

powder was investigated. Powder samples were characterized using TG-DTA,

XRD, SEM and laser diffraction techniques. It was found that an average

particle size of 50 nm was achieved at 25 h of vibro-milling after which a

higher degree of particle agglomeration was observed on continuation of

milling to 35 h. In addition, by employing an appropriate choice of the milling

time, a narrow particle size distribution curve was also observed.

Keywords: Lead zirconate; Milling; Nanopowders; Phase formation; Particle size

1. Introduction

Lead zirconate, PbZrO₃ (PZ), is one of the antiferroelectric materials which exhibit a perovskite structure. It shows antiferroelectric phase with cubic symmetry at high temperature and undergoes two phase transitions which are close in temperature (~ 230 °C and 220 °C) on cooling [1]. The low temperature phase has orthorhombic symmetry with antiparallel shift of Pb ions along the pseudocubic <110>, which results in antiferroelectricity [2]. When combined with other oxides, lead zirconate can form a series of solid solutions $Pb(Zr_{1-x},Ti_x)O_3$ (PZT), $(Pb,La)(Zr,Ti)O_3$ such as (PLZT), Pb(Fe_{1/3}W_{2/3})O₃-PbZrO₃ (PFW-PZ) and Pb(Zn_{1/3}Nb_{2/3})O₃-PbZrO₃ (PZN-PZ) [2-4]. These compositions are widely used in ultrasonic transducers, electrooptic devices, nonvolatile memories, microactuators and multilayer capacitors [1-4]. To fabricate them, a fine powder of perovskite phase with a minimal degree of particle agglomeration is needed as the starting material in order to achieve a dense and uniform microstructure at a given sintering temperature. Thus, a crucial focus of powder synthesis in recent years has been the formation of uniform-sized, single morphology particulates ranging in size from nanometer to micrometers [5-8].

The development of a method to produce nanopowders of precise stoichiometry and desired properties is complex, depending on a number of variables such as nature and purity of starting materials, processing history, temperature, etc. To obtain nanosized PZ powders, many investigations have focused on several chemistry-based preparation routes, such as sol-gel [5], homogeneous precipitation [6], hydrothermal reaction [7], oxidant-peroxo method [8], besides the more conventional solid-state reaction of mixed

oxides [9]. All these techniques are aimed at reducing the particle size and temperature of preparation of the compound even though they are more involved and complicated in approach than the solid-state reaction. Moreover, high-purity PZ nanopowders are still not available in bulk quantity. The advantage of using mechanical milling for preparation of nanosized powders lies in its ability to produce mass quantities of powders in the solid state using simple equipment and low cost starting precursors [10]. Although some research has been done in the preparation of PZ powders via a vibro-milling technique [9], to our knowledge a systematic study regarding the influence of milling time on the preparation of PZ powders has not yet been reported.

Thus, in the present study, the effect of milling time on phase formation, and particle size of lead zirconate powders was investigated in this connection. The potential of the vibro-milling technique as a simple and low-cost method to obtain usable quantities of single-phase lead zirconate powders at low temperature and with nanosized particles was also examined.

2. Experimental procedure

The starting materials were commercially available lead oxide, PbO (JCPDS file number 77-1971) and zirconium oxide, ZrO₂ (JCPDS file number 37-1484) (Fluka, >99% purity). The two oxide powders exhibited an average particle size in the range of 3 to 5 µm. PbZrO₃ powder was synthesized by the solid-state reaction of these raw materials. Powder-processing was carried out in a manner similar to that employed in the preparation of other materials, as described previously [10,11]. A vibratory laboratory mill (McCrone Micronizing Mill) powered by a 1/30 HP motor was employed for preparing the

stoichiometric PbZrO₃ powders. The grinding vessel consists of a 125 ml capacity polypropylene jar fitted with a screw-capped, gasketless, polythene closure. The jar is packed with an ordered array of identical, cylindrical, grinding media of polycrystalline corundum (instead of employing zirconia media under alcohol for 8 h [9]). A total of 48 milling media cylinder with a powder weight of 20 g was kept constant in each batch. The milling operation was carried out in isopropanal inert to the polypropylene jar. Various milling times ranging from 0.5 to 35 h were selected in order to investigate the phase formation characteristic of lead zirconate and the smallest particle size. After drying at 120 °C for 2 h, the reaction of the uncalcined powders taking place during heat treatment was investigated by thermogravimetric and differential thermal analysis techniques (TG-DTA, Shimadzu) at a heating rate of 10 °C/min in air from room temperature up to 1000 °C. Based on the TG-DTA results and literature [9,12], the mixture was calcined at 800 °C (in closed alumina crucible) for 2 h with heating/cooling rates of 10 °C/min.

All powders were subsequently examined by room temperature X-ray diffraction (XRD; Siemens-D500 diffractometer), using Ni-filtered CuK $_{\alpha}$ radiation to identify the phases formed and optimum milling time for the production of PbZrO $_{3}$ powders having the smallest particle size. The relative amount of perovskite and secondary phases was determined from XRD patterns of the samples by measuring the major characteristic peak intensities for the perovskite (221) or I_{P} and secondary (o) phases or I_{S} . The following qualitative equation was used [10].

perovskite phase (wt %) =
$$\frac{I_P}{I_P + I_S} \times 100$$
 (1)

The crystalline lattice constants, lattice strain and average particle size were also estimated from XRD patterns [13]. The particle size distributions of the powders were determined by laser diffraction technique (DIAS 1640 laser diffraction spectrometer) with the particle sizes and morphologies of the powders observed by scanning electron microscopy (JEOL JSM-840A SEM). The particle sizes of PZ powders milled at different times obtained from different measuring techniques are provided in Table 1.

3. Results and discussion

The TGA and DTA results for the powders milled at different times are compared and displayed in Fig. 1(a) and (b), respectively. In general, similar thermal characteristics are observed in all cases. In the temperature range from room temperature to ~ 150 °C, all samples show both exothermic and endothermic peaks in the DTA curves (Fig. 1(b)), which are related to a slight drop in weight loss at the same temperature range. These observations can be attributed to the decomposition of the organic species originating from the milling process [10,11]. Corresponding to the large fall in specimen weight, (~ 8-9%), the other DTA peaks are detected within ~ 300 to 450 °C temperature range. However, it is to be noted that there is no obvious interpretation of these peaks, although it is likely to correspond to a phase transformation of ZrO₂ precursor alloyed with PbO precursor suggested by Aoyama *et al.* [14]. Increasing the temperature up to ~ 800 °C, the solid-state reaction between lead oxide and zirconium oxide occurs. The broad exothermic characteristic

from ~ 500-700 °C in all DTA curves represent that reaction, which is supported by a gradual decrease in sample weight over the same temperature range. The slightly different temperature, intensities and shapes of the thermal peaks for the powders are probably related to the different sizes of the powders subjected to different milling times and, consequently, caused by the removal of organic species and rearrangement of differently bonded species in the network [2,15].

To further study the effect of milling time on phase formation, each of the powders milled for different times were calcined at 800 °C for 2 h in air, followed by phase analysis using XRD. For the purpose of estimating the concentrations of the phase present, Eq. (1) has been applied to the powder XRD patterns obtained, as given in Table 1. As shown in Fig. 2, for the uncalcined powder subjected to 0.5 h of vibro-milling, only X-ray peaks of precursors PbO (•) and ZrO2 (°) are present, indicating that no reaction had been initiated during the milling process. However, after calcination, it is seen that the perovskite-type PbZrO₃ becomes the predominant phase in the powder milled for 0.5 h, indicating that the reaction has occurred to a considerable extent. It is seen that only traces of unreacted PbO and ZrO2 precursors have been found along with the PZ parent phase at a milling time of 1.5 h or less. This observation could be attributed mainly to the poor mixing capability under short milling time, similar with other work [10]. With milling time of 2 h or more, it is apparent that a single-phase perovskite PZ (yield of 100% within the limitations of the XRD technique) was found to be possible after the same calcination process was applied.

In general, the strongest reflections found in the majority of these XRD patterns indicate the formation of the lead zirconate, PbZrO₃. These can be matched with JCPDS file number 35-0739 for the orthorhombic phase, in space group P2cb (no. 32) with cell parameters a = 823.1 pm, b = 1177.0 pm and c = 588.1 pm [16], consistent with other works [6,7]. It should be noted that no evidence for the introduction of impurity due to wear debris from the milling process was observed in any of the calcined powders (within the milling periods of 0.5-35 h), demonstrating the effectiveness of the vibro-milling technique for the production of high purity PZ nanopowders, without any introduction of excess ZrO_2 [9].

Moreover, it has been observed that with increasing milling time, all diffraction lines broaden, e.g. (261) and (402) peaks, as shown in Fig. 2, an indication of a continuous decrease in particle size and of the introduction of lattice strain. These observations indicate that the prolonged milling treatment affects the particle size and evolution of crystallinity of the phase formed (Table 1), in good agreement with other similar system [10]. For PZ powders, the longer is the milling time, the finer is the particle size, up to a certain level. The results suggest that the steady state of the vibro-milling is attained at \sim 25 h of milling. Moreover, it is worthy to note that, in this condition, the mean crystalline size is close to \sim 50 nm. Also, the relative intensities of the Bragg peaks and the calculated lattice parameters (b and c) for the powders tend to decrease with the increase of milling time. However, it is well documented that, as Scherer's analysis provides only a measurement of the extension of the coherently diffracting domains, the particle sizes estimated by this method can be significantly under estimated [17]. In addition to strain, factors such as

dislocations, stacking faults, heterogeneities in composition and instrumental broadening can contribute to peak broadening, making it almost impossible to extract a reliable particle size solely from XRD [12,18].

In this connection, scanning electron microcopy was also employed for particle size measurement (Table 1). The morphological evolution of the powders and their corresponding particle size distributions as a function of milling time were also revealed, as illustrated in Fig. 3. At first sight, the morphological characteristic of PZ powders with various milling times is similar for all cases. In general, the particles are agglomerated and basically irregular in shape, with a substantial variation in particle sizes. The powders consist of primary particles nanometers in size. Increasing the milling time over the range 5 to 35 h, the average size of the PZ particles decreases significantly, until at 25 h, the smallest particle size (estimated from SEM micrographs to be ~ 50 nm) is obtained. However, it is also of interest to point out that larger particle size was obtained for a milling time longer than 25 h. This may be attributed to the occurrence of hard agglomeration with strong inter-particle bonds within each aggregate resulting from dissipated heat energy of prolong milling [19]. Fig. 3 also illustrates that vibro-milling has slightly changed the shape of the particles which become more rounded at long milling times. At the same time, the particle size is reduced. Fracture is considered to be the major mechanism at long milling times.

As shown in Fig. 3, after milling times of 5 and 15 h, the powders have a similar particle size distribution. They exhibit a single peak covering the size ranging from 0.29-3.00 μ m. With increasing milling times to 25 h, a uniform particle size distribution with a much lower degree of particle agglomeration (<

1 μ m) is found. However, upon further increase of milling time up to 35 h, a bimodal distribution curve with peak broadening between 0.24 and 6.20 μ m is observed. First is a monomodal distribution corresponding to the primary size of the PbZrO₃ particles. The second group (peak) is believed to arise mainly from particle agglomeration. Table 1 compares the results obtained for PZ powders milled for different times via different techniques. Variations in these data may be attributed mainly to the formation of hard and large agglomerations found in the SEM results.

In this work, it is seen that the optimum milling time for the production of the smallest nanosized high purity PZ powder was found to be at 25 h. The finding of this investigation indicates a strong relationship between the vibro-milling process and the yield of PZ nanopowders. However, in case of the vibro-milling technique, other factors such as the milling speed, milling scale and type of milling media also need to be taken into account.

4. Conclusion

The results infer that the milling time influences not only the development of the solid-state reaction of lead zirconate phase but also the particle size and morphology. The resulting PZ powders have a range of particle size, depending on milling times. Production of a single-phase lead zirconate nanopowder can be successfully achieved by employing a combination of 25 h milling time and calcination condition of 800 °C for 2 h, with heating/cooling rates of 10 °C.min⁻¹.

Acknowledgement

This work was supported by the Thailand Research Fund (TRF), the Royal Golden Jubilee Ph.D. Program, the Faculty of Science and the Graduate School of Chiang Mai University.

References

- [1] B. Jaffe, W.R. Cook, H. Jaffe, Piezoelectric Ceramics, Academic Press, New York, 1971.
- [2] F. Jona, G. Shirane, F. Mazzi, R. Pepinsky, Phys. Rev. 105 (1957) 849.
- [3] T.R. Shrout, A. Halliyal, Am. Ceram. Soc. Bull. 66 (1987) 704.
- [4] A.J. Moulson, J.M. Herbert, Electroceramics, 2nd ed., Wiley, Chichester, 2003.
- [5] D.M. Ibrahim, H.W. Hennicke, Trans. J. Br. Ceram. Soc. 80 (1981) 18.
- [6] E.E. Oren, E. Taspinar, A.C. Tas, J. Am. Ceram. Soc. 80 (1997) 2714.
- [7] A. Rujiwatra, S. Tapala, S. Luachan, O. Khamman, S. Ananta, Mater. Lett. (2006) *in press*.
- [8] E.R. Camargo, M. Popa, J. Frantti, M. Kakihana, Chem. Mater. 13 (2001) 3943.
- [9] M.T. Lanagan, J.H. Kim, S. Jang, R.E. Newnham, J. Am. Ceram. Soc. 71 (1988) 311.
- [10] R. Wongmaneerung, R. Yimnirun, S. Ananta, Mater. Lett. 60 (2006) 1447-1452.
- [11] A. Udomporn, S. Ananta, Mater. Lett. 58 (2004) 1154.
- [12] C. Puchmark, G. Rujijanagul, S. Jiansirisomboon, T. Tunkasiri, Ferroelectric Lett. 31 (2004) 1.

- [13] H. Klug, L. Alexander. X-Ray Diffraction Procedures for Polycrystalline and Amorphous Materials, 2nd ed., Wiley, New York, 1974.
- [14] T. Aoyama, N. Kurata, K. Hiroto, O. Yamaguchi, J. Am. Ceram. Soc. 78(1995) 3163.
- [15] M.D. Johannes, D.J. Singh, Phys. Rev. B 71 (2005) 212101.
- [16] Powder Diffraction File No. 35-0739. International Centre for Diffraction Data, Newtown Square, PA, 2000.
- [17] C. Suryanarayana, Prog. Mater. Sci. 46 (2001) 1.
- [18] A. Revesz, T. Ungar, A. Borbely, J. Lendvai, Nanostruct. Mater. 7 (1996) 779.
- [19] P. C. Kang, Z. D. Yin, O. Celestine, Mater. Sci. Eng. A. 395 (2005) 167.

Table Caption

Table 1 Effect of milling time on the particle size of PZ powders measured by different techniques.

Figure Caption

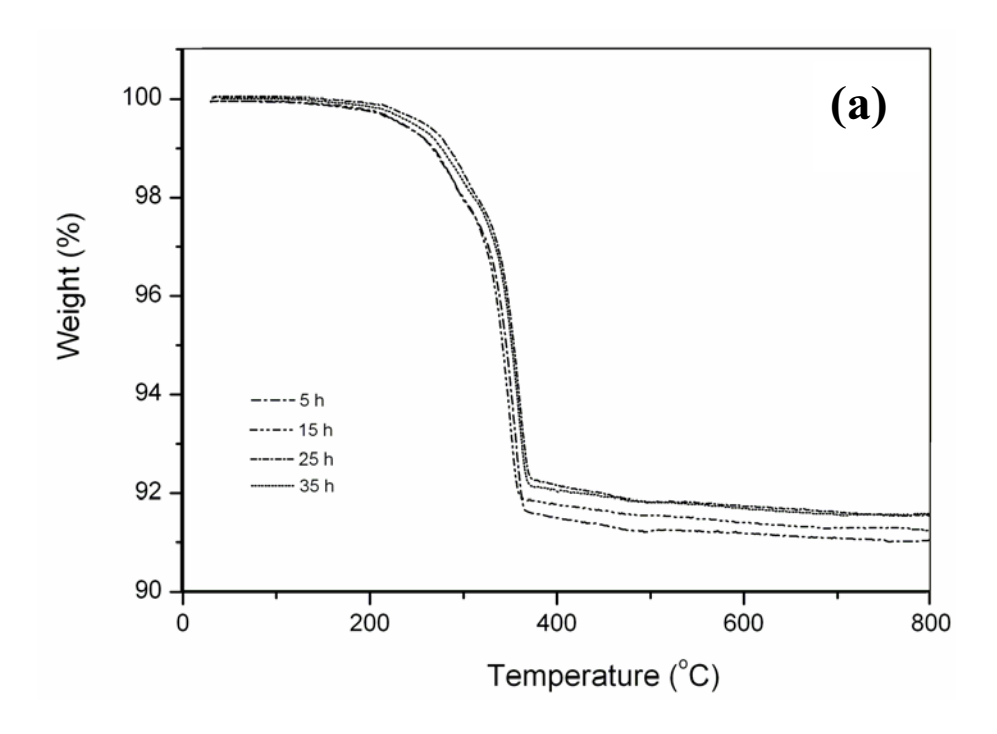
- Fig. 1 (a) TGA and (b) DTA analysis of powder mixtures milled at different times.
- Fig. 2 XRD patterns of PZ powders milled at different times (calcined at 800 °C for 2 h with heating/cooling rates of 10 °C/min).
- Fig. 3 SEM micrographs and particle size distribution of PZ powders milled at different times.

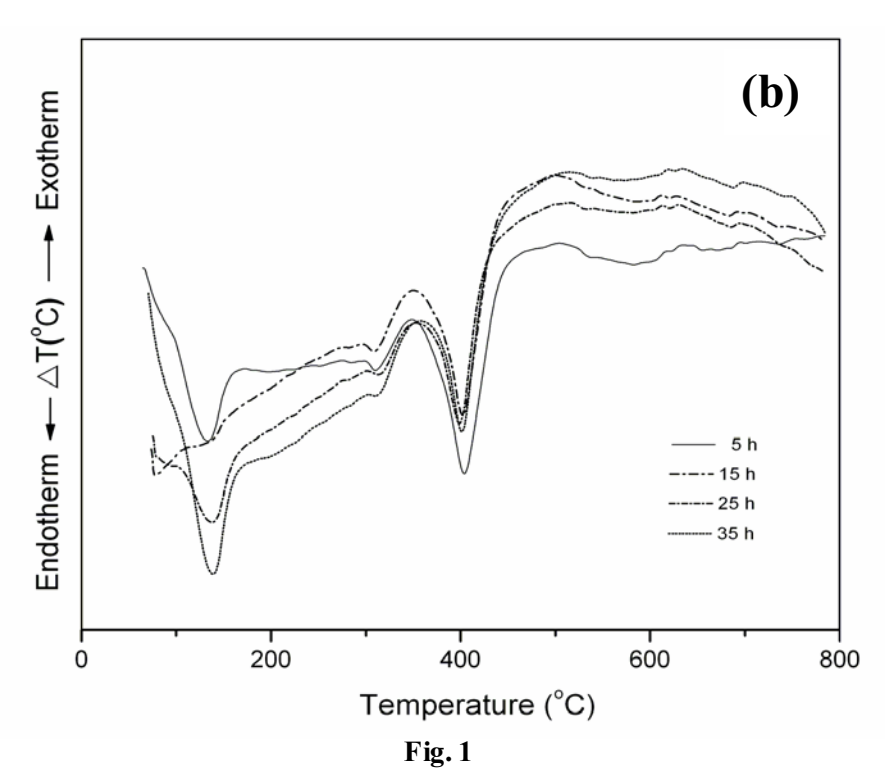
Table 1

		XRD				SEM		Laser scattering	
Milling time	Pero vskite	A	а	b	С	D	P	D	P
(h)	phase (%)	(nm)	(nm)	(nm)	(nm)	(nm)	(nm)	(nm)	(nm)
0.5	93.34	57.39	0.8162	1.1624	0.5814	3800	2410-5000	5280	2840-7650
2	100	42.51	0.8161	1.1611	0.5816	1800	970-2520	1380	1340-5600
5	100	30.73	0.8184	1.1679	0.5846	880	740-950	1380	580-3000
15	100	18.17	0.8238	1.1712	0.5872	300	70-700	720	290-2210
25	100	18.19	0.8241	1.1720	0.5879	180	50-400	180	35-750
35	100	19.34	0.8238	1.1712	0.5872	250	50-420	1540	240-6200

A =Crystallite size a, b, c =Lattice parameters

D =A verage particle size P =Particle size distribution or range





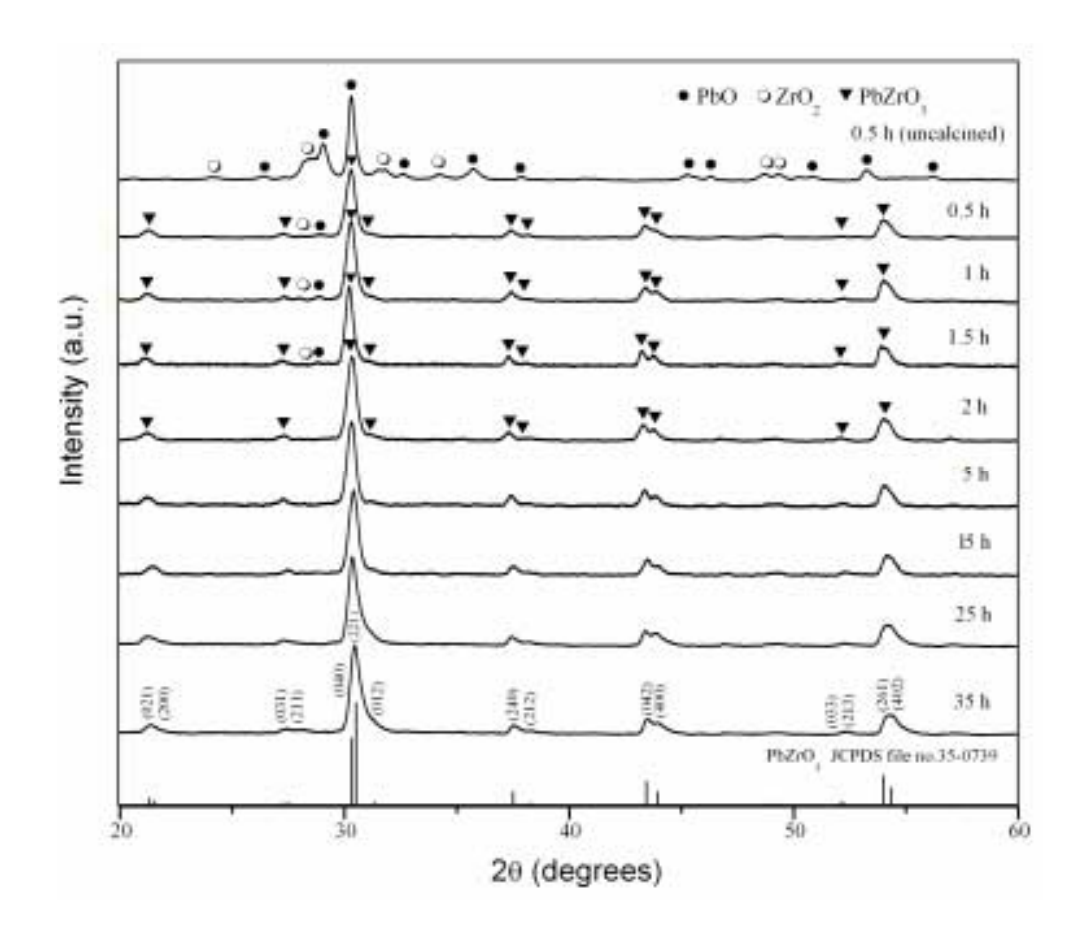
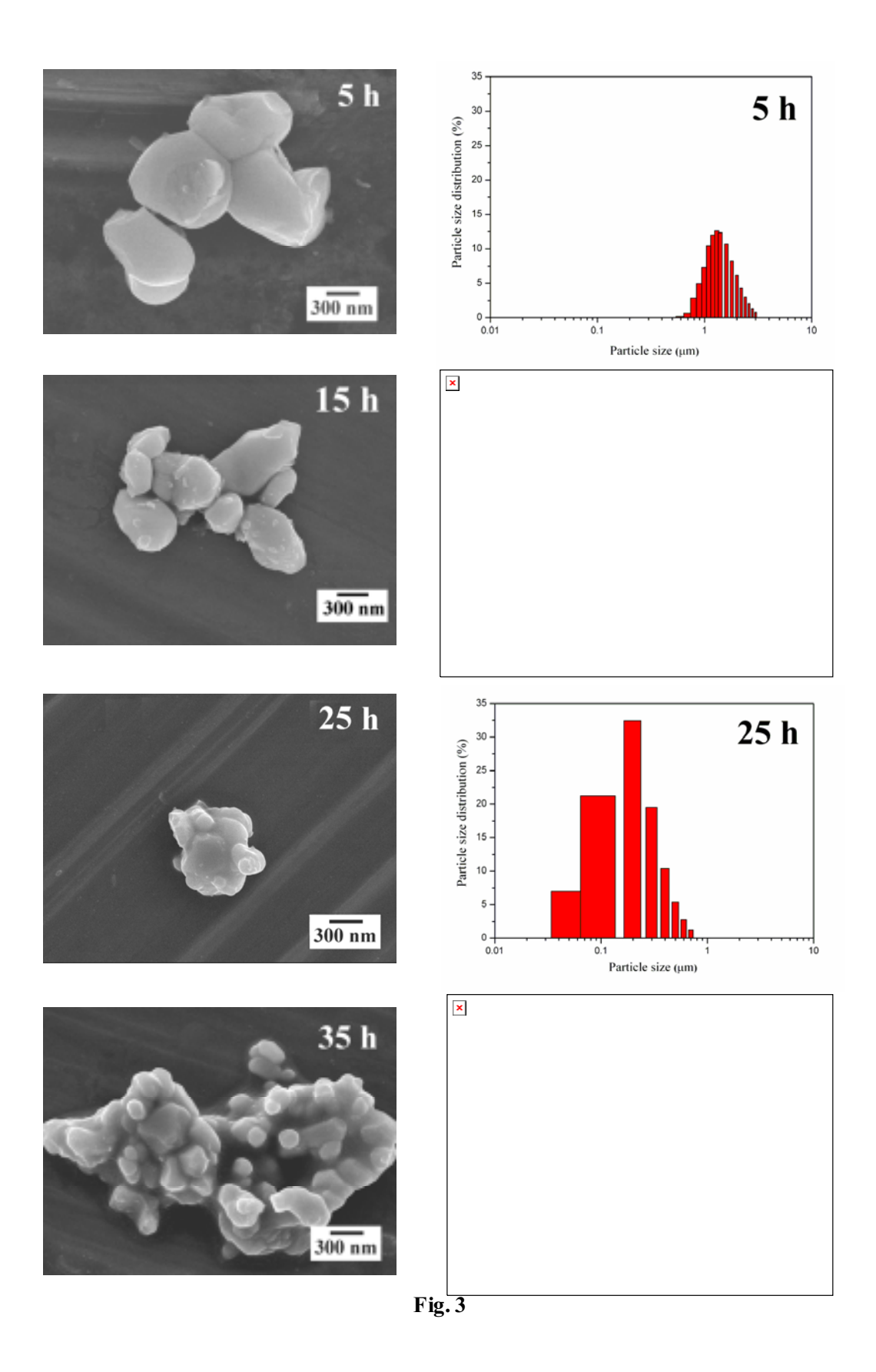


Fig. 2



1

*Corresponding author Dr. Supon Ananta

Department of Physics Faculty of Science Chiang Mai University

Chiang Mai 50200

Thailand

Tel: +66-53-943367; fax: +66-53-943445

E-mail: Supon@chiangmai.ac.th (S. Ananta)

Effects of Calcination Conditions on Phase and Morphology Evolution of Lead

Zirconate Powders Synthesized by Solid-State Reaction

W. Chaisan, O. Khamman, R. Yimnirun and S. Ananta

Department of Physics, Faculty of Science, Chiang Mai University,

Chiang Mai 50200, Thailand

ABSTRACT

Lead zirconate (PbZrO₃) powder has been synthesized by a solid-state reaction

via a rapid vibro-milling technique. The effects of calcination temperature, dwell time

and heating/cooling rates on phase formation, morphology, particle size and chemical

composition of the powders have been investigated by TG-DTA, XRD, SEM and EDX

techniques. The results indicated that at calcination temperature lower than 800 °C

minor phases of unreacted PbO and ZrO2 were found to form together with the

perovskite PbZrO₃ phase. However, single-phase PbZrO₃ powders were successfully

obtained at calcination conditions of 800 °C for 3 h or 850 °C for 1 h, with

heating/cooling rates of 20 °C/min. Higher temperatures and longer dwell times clearly

favored the particle growth and formation of large and hard agglomerates.

Keywords: Lead Zirconate; PbZrO₃; Perovskite; Calcination; Phase formation;

Powders-Solid state reaction

1. Introduction

Lead zirconate, PbZrO₃ (PZ), which is a typical antiferroelectric (AFE) material at room temperature with a Curie temperature of ~ 230 °C, has an orthorhombic symmetry with a structure similar to that of classical ferroelectric of orthorhombic barium titanate (BaTiO₃) [1-3]. The dipoles due to a displacement of the Zr⁴⁺ ions from the geometric centre of the surrounding six O²⁻ ions in the material are alternately directed in opposite senses so that the spontaneous polarization is zero [3,4]. It is reported that the antiferroelectric to ferroelectric transition can be induced when subjected to a strong electric field [5]. In addition, the ferroelectric (FE) phase of PZ is only stable over a relatively narrow temperature interval [6,7]. This interval is reported extendable with application of an electric field or with chemical substitutions [8-10]. More importantly, a size of the interval depends largely on the impurity concentration [11]. Therefore, the stoichiometry of the sample is of particular important in detailed studies on AFE-FE phase transition of PZ-based materials. Practically, this material is a potential candidate for energy storage applications for DC fields and low loss linear capacitor, owing to its AFE nature [1,12]. Recently, the double hysteresis behavior of this material makes it attractive for the microelectronic, microelectromechanical systems (MEMs) as well as for actuator applications [12-14].

Lead zirconate when combined with other oxides can form a series of solid solution materials such as $Pb(Zr_x,Ti_{1-x})O_3$, $PbZrO_3-Pb(Mg_{1/3}Nb_{2/3})O_3$, $PbZrO_3-PbTiO_3-Pb(Fe_{1/5}Nb_{1/5}Sb_{3/5})O_3$, and $PbZrO_3-Pb(Mg_{1/3}Nb_{2/3})O_3$, which find tremendous applications in the electroceramic industries [13-15]. In all these applications, the stoichiometry and homogeneity of materials are known to be the important factor for ensuring the